**OPEN REPORT**
SCK•CEN-BLG-1065

# "Magnetic Susceptibilities" as they appeared to me An Amperian approach

Van den Bosch, A

**April,** 2008

SCK•CEN
Boeretang 200
BE-2400 Mol
Belgium

OPEN REPORT OF THE BELGIAN NUCLEAR RESEARCH CENTRE
SCK•CEN-BLG-1065

# "Magnetic Susceptibilities" as they appeared to me An Amperian approach

Van den Bosch, A

April, 2008
Status: Unclassified
ISSN 1379-2407

SCK•CEN
Boeretang 200
BE-2400 Mol
Belgium

© SCK•CEN
Studiecentrum voor Kernenergie
Centre d'étude de l'énergie Nucléaire
Boeretang 200
BE-2400 Mol
Belgium

Phone +32 14 33 21 11
Fax +32 14 31 50 21

http://www.sckcen.be

Contact:
Knowledge Centre
library@sckcen.be

## Preface

In 1958 I got as research topic the study of radiation damage by magnetic susceptibility measurements. An apparatus for measuring the magnetic susceptibility of small solid samples by the Faraday method has been constructed.

The essence of most subjects studied have been reported in literature. The separated publication is not well suited for showing the underlying connection. The present paper concerns the connection, the interaction between electric currents which is the basis of magnetism. The basic ideas needed to understand susceptibilities are written in a simple story. The restrained number of subjects treated allows a clear overview. The paper reveals how science is built up. Hopefully it demonstrates and propagates my enthusiasm for scientific research.

The story is consistently written in the rationalized SI system. “Magnetic Susceptibilities” in the title points to the exact scientific aspect of the present paper. However, even in the exact science there is room for interpretation. The story is told as the susceptibilities appear to me. The existence of magnetic monopoles not being observed experimentally, we discus the physics of magnetism in a simple and straightforward Amperian way. “An Amperian approach” refers, for the current-current interaction, to the soundness of the mathematical generalization of the results of Ampere’s work.

The physics behind each mathematical equation is stressed. The number of equations is reduced but even then, for those who are somewhat reluctant to digest mathematical equations, they can skip them without losing the general trend of the story.

I thank my wife, Betty, who showed a continuous interest in this work. She always urged me to try to express my ideas in a way somewhat comprehensible for anybody. I also am thankful that she took more than a proportional part of the domestic duties so that I got the time for this work.

Turnhout, 2008

**Contents**

# The leading thread running through my perception of quasi static magnetic susceptibilities

## 1 Introduction

The study of radiation induced effects in solid materials by magnetic susceptibility measurements was the mission I received at the solid state physics department of the Belgian nuclear research institute at mid 1958. At that time my knowledge on susceptibilities was very limited. I realized that the magnetic susceptibility of a specimen was related to the force exerted by a magnet on the material of a sample. As a child I felt the attraction of a piece of iron toward a horse-shoe magnet. Other materials also undergo the influence of a magnet, even when they are less susceptible. In the latter case more sensitive force detection is needed. Using a balance as the quantitative force detector the principle of our set-up becomes such as indicated in Fig.1.1.

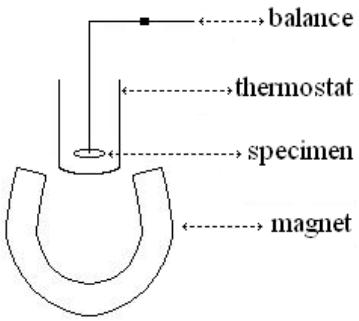


*Fig.1.1 shows an outline of an apparatus for measuring the magnetic susceptibility on small solid samples following the Faraday method.*

In nuclear reactors the neutron radiation that induces magnetic effects in solid materials, in certain cases, also induces radioactivity in the sample. The radiation level at the susceptibility measurement always was kept between acceptable limits by choosing a small mass for the sample of the material under study. Small samples need a sensitive force detector.

A sensitive vacuum microbalance has been built and used as the force meter in our apparatus. The concept of the balance is a compromise between sensitivity and precision [1].

As the Faraday method works with small samples, it seemed us the most promising for measuring susceptibilities on our specimen.

An electro-magnet exerts force on a sample. The electro-magnet has the practical advantage that it can be put on and off in a relatively simple way. The “off” “on” transition allows measuring the quasi static magnetic susceptibility of a sample. “Quasi” is the expression for indicating that a measuring period is not indefinitely long. “Static” means that we did not look for transient processes. The magnetic state of a sample was considered to be stable at the “on” period of the measurement.

The energized magnet exerts a force on the sample. The force, in the physics world of magnetism, relates to the interaction between electric currents.

For a first level in understanding magnetism it is not necessary to introduce elementary particles as charge carriers in the electric currents. The number of charged particles in the considered currents is very large, as water molecules in a river. Just as for water, we approached their behavior as a current of a continuous medium. It is neither necessary to know the theory of relativity for moving electric charges. Nevertheless, the effect of relativity, the force between two electric moving charges must be introduced in the expression for the force between electric currents.

At a susceptibility measurement no currents come in or out the sample. Electric currents flow inside the sample. We only consider the steady-state part of the susceptibility. The magnetic effect on a small sample therefore can be simulated by the effect of the magnet on a closed electric circuit, in free space, in which an electric steady-state current flows.

A flat circular electric circuit is the primitive unit we use in our models. It interacts magnetically with other units. It is simple, anisotropic and relatively symmetric. The property of anisotropy is necessary to understand directional dependences in magnetism. The circular symmetry facilitates calculations.

$$\mathbf{F}_2 = 10^{-7}\, I_1\, I_2 \oint_1 \oint_2 \frac{d\mathbf{l}_2 \times (d\mathbf{l}_1 \times \mathbf{r}_{12})}{r_{12}^3} \qquad (1.1)$$

Equation (1.1) is the mathematical expression formulating the force ($\mathbf{F}_2$) between two primitive current circuits. The current ($I_1$) in circuit 1 exerts, by magnetic interaction, a force on circuit 2 in which the electric current ($I_2$) flows.

The force is proportional to the product of the two current intensities, $I_1$ and $I_2$. The proportionality factor $10^{-7}$ takes care of the numerical equality on both sides of the equation, when the physical parameters are expressed in the SI units (mksA). The rest will be discussed later.

## 2 The coil-coil experiment

The primitive circuit is a powerful tool in explaining magnetic experiments by simulating models. Using such units, we carried out a simulation of a magnetic susceptibility measurement by measuring the force between two geometrically well defined current circuits. The aim of the experiment was to find out how far we understand the mathematical generalization of the results of Ampere's work. As the precision on the force, measuring the interaction between only two primitive units was to low, we simulated the susceptibility measurement using two stacks of primitive units. A coil in the experiment simulates one stack in the calculations. We measured the force between two coils in a simple geometrical situation [2a]. The set-up is shown in Fig.2.1.

The current in coil 2 simulates the current in the sample on the balance. The iron-less coil 1 is the primitive concept of an electro magnet.

The force, measured by the balance in a single series of experiments, agreed within three percent with the calculations. Taking in account that i) each complete turn of the wire, helically wound on the coil, is approximated by closed rings and ii) the relative position of

the coils was not very precisely known, we accepted that the equation used describes well the interaction between currents. We believe that we sufficiently understand the equation we got from text books. Therefore we did not spent more time on the improvement of the simulation experiment. Our mission was not of a metrological order.

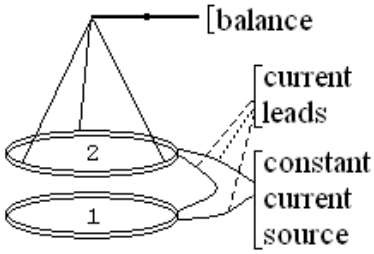


*Fig.2.1 shows the set up of a coil-coil interaction experiment*

The coil-coil experiment, as expected, reveals that, when the current in both coils flow in the same sense in the same direction, both coils attract each other. When the coil currents flow in opposite sense then the coils repulse each other. I memorise the former case remembering that a constant current in a helicoidally spring always contracts the spring. It does not matter what is the sense of the current in the spring.

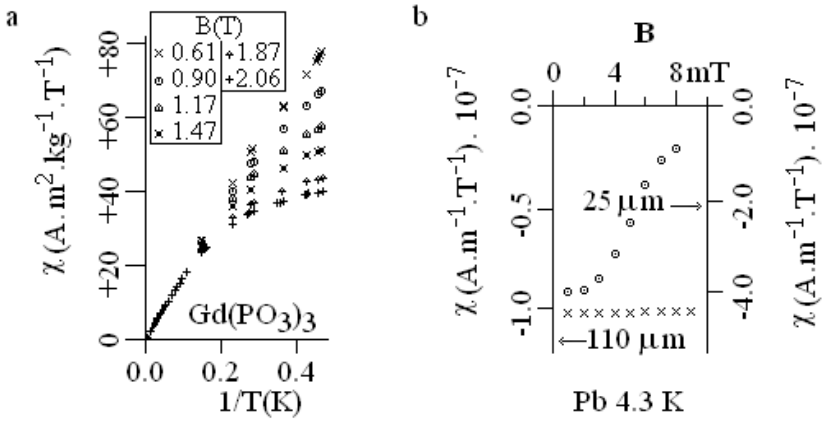


*Fig.2.2 shows the magnetic susceptibility as measured a) on a sample of gadolinium phosphate glass; b) on lead discs of different thickness [2b].*

In measuring susceptibilities also the sample is attracted to the magnet in one case, while it is repulsed in the other. In Fig.2.2 we

report on susceptibilities giving, by their sign, expression of this effect.

The gadolinium phosphate glass sample is attracted to the magnet. It's paramagnetic and its susceptibility is positive. The lead discs are repulsed from the magnet, they are diamagnetic and their susceptibility is negative.

In the above discussion is coil 2 the sample equivalent while coil 1 simulates the magnet. However, both coils are identical. The nomination only formally breaks the symmetry in the experiment in which both current circuits are equivalent. The situation resembles the situation on mooring a boat.

It does not matter whether the sailor, who pulls the rope, is ashore or on the boat. The rope tension pulls on boat and quay. Because the quay does not move the rope tension forces the boat to approach the quay.

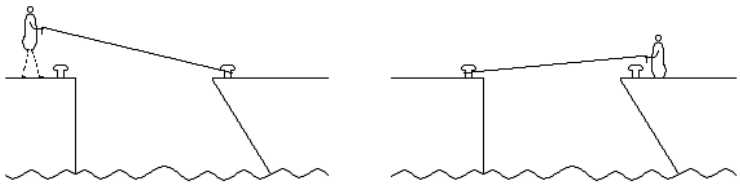

*Fig.2.3 indicates that to moor a boat it does not matter whether the sailor, who pulls the rope, is ashore or on the boat.*

In the coil-coil experiment, for the calculation of the force on the balance it does not matter which of both coils is called the magnet. However, the coil that hangs on the balance is clearly the coil that responds to the force (a boat resembling reaction). The magnet simulating coil 1 was fixed (a quay resembling situation).

At the magnetic susceptibility measurement the situation is similar. The magnetic interaction between currents results in a tension between sample and magnet. The magnet is strongly fixed in space. The sample lies on the pan of the balance that registers the effect of the tension. At the susceptibility experiment the magnetic effect can be as well pushing as pulling. Therefore, the comparison with the above boat situation bears not very far as it would be difficult to push the boat offshore with the rope.

The coil-coil experiment teach us further that the total effect of the spiral coil 1 on coil 2 is the sum of the effect of coil 1 on each of the turns of the spiral coil 2. The total effect is the sum of the partials.

What the experiment does not teach is how many turns are there in coil 2. Indeed, the force is related to the "ampere-turns" in the coil. The same force can be generated as well by few turns on which flow an intense current of many amperes as by many turns on which flow a low intensity current. The situation knows an equivalent in the magnetic susceptibility measurement. One force measurement does not indicate the current configuration in the sample but only indicates what is possible.

Many force measurements, taken at different situations, can help in interpreting the susceptibility data. Pattern recognition is a helpful technique to rely the data to a model that describes the physics.

Fig.2.2 shows that the susceptibility can depend on the magnetic induction field, **B**(T), on temperature, T(K), and on geometry. In part "a" in the figure the dimension of the susceptibility $\chi$, ($A.m^2.kg^{-1}.T^{-1}$) is different from that in part "b" ($A.m^{-1}.T^{-1}$). It indicates that the word "susceptibility" covers different meanings. One has to ask "what is susceptible to what for what?"

## 3 The current-current interaction

The agreement between the coil-coil experiment and its calculation shows that the summation holds also for parts of turns.

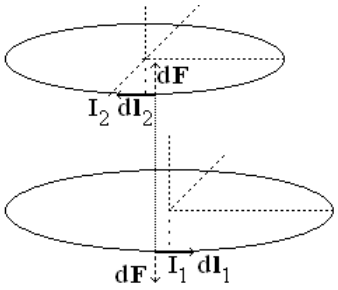


*Fig.3.1 shows the forces exerted by two current parts, $I_1 d\boldsymbol{l}_1$ and $I_2 d\boldsymbol{l}_2$, on each other. The parts are of two different circular circuits. The currents flow in the same direction but in opposite sense.*

In Fig.3.1 two parallel rings simulate what happens at a susceptibility measurement [3]. One of the rings simulates the sample while the other simulates the magnet.

Here also for two currents, flowing in the same direction but in opposite sense, the net effect is pushing both away from each other.

The current, I, flowing over a small part of a ring, a small piece of length d**l**, is considered as a current element, Id**l**. The interaction between current elements is the basis of the resulting force calculation.

At force calculations, the interaction between current elements fit's a two step picture. In the first step a current element in coil 1 generates, at the location of a current element in coil 2, an element of the magnetic induction field, d**B**. In the second step, the field element interacts with the local current element and results in the force element, d**F**. This vision is quantitatively sustained by the vector calculus. A bold letter indicates that the considered entity is a vector.

---

$$\mathbf{F}_2 = I_2 \oint_2 d\mathbf{l}_2 \times B_2 \qquad (3.1)$$

Equation (3.1) expresses the force in an other way but is equivalent to equation (1.1). Herein is $\mathbf{B}_2$ the magnetic induction field generated by the current of circuit 1 at the location of the considered current element in circuit 2.

---

Fig.3.2 outlines a simple case of two parallel current elements, both with the current directions perpendicular into the paper plane. The elementary magnetic induction field and the force element are in the plane of the paper.

The field direction at location 2 is perpendicular to the plane defined by the direction the current flows at location 1 and the line from the current 1 element to the current 2 element. The force direction at 2 is perpendicular to the plane defined by the current 2 direction and the field direction. Here, $d\mathbf{F}_2$ points towards location 1.

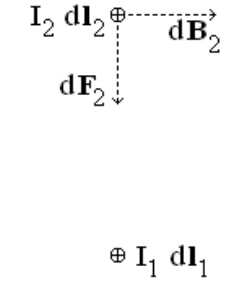


*Fig.3.2. A current element in ring 1, $I_1 d\boldsymbol{l}_1$, generates a magnetic induction field element, $d\boldsymbol{B}_2$ at the current element location in ring 2. The induction field element results in a force element, $d\boldsymbol{F}_2$.*

It must be mentioned that there is no "rope" at a magnetic interaction! In the case of the rope the force always pulls, not pushes, in the direction of the rope. The situation at the magnetic interaction is quite different, as shown in Fig.3.3.

Fig.3.3 shows that the force at current element 2 is not along its positional direction from the current element 1. $d\mathbf{F}_2$ is perpendicular to current 2 and to the field.

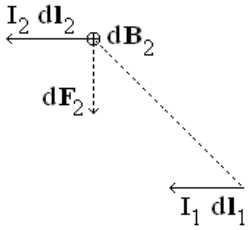


*Fig.3.3 shows that the force at current element 2 is not along its positional direction from the current element 1. $d\boldsymbol{F}_2$ is perpendicular to current 2 and to the field.*

Our cork-screw helps me to memorize the sense of the field at the current element 2 as generated by 1. On turning the screw the thread simulate the sense of the field when the screw is at the position of current element 1, lying in the direction and progressing (on turning) in the sense of the current element.

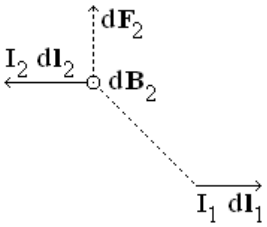


*Fig.3.4. An inversed sense of current element 1 results in an opposite sense of the field and the force.*

The right hand helps to memorize the sense of the force. When the fingers, in the direction of the field, point in the sense of the field and

the current element (here 2) points into the palm of the hand, then the thumb indicates the sense of the force.

We considered in the above paragraph the interaction between one current element in the sample and one current element in the magnet. However, the force felt by a current element in the sample simulating ring 2 is the sum of the contributions of all current elements in ring 1. The step for making the sum is treated in next paragraph.

## 4 The magnetic induction field's direction

The two steps in the force calculations between two current elements are independent. In the first step a current element 1 generates a magnetic induction field at the location of element 2. However, for the field generation it is irrelevant whether or not there is current at the location of element 2.

For the susceptibility measurements it means that, as long as the sample does not influence the currents in the magnet, one can discus the field of a magnet, without taking in account the presence of the sample.

We now focus on the field direction generated by the current ring 1 which again simulates the magnet.

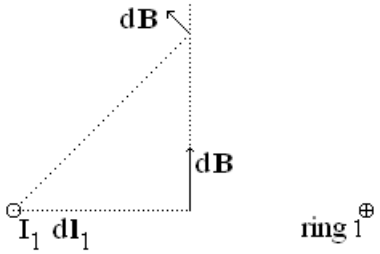


*Fig.4.1. A current element Id**l** generates a magnetic induction field at the target location. The direction of the field is perpendicular to the direction that joins the location with the current element.*

In agreement with a former statement, the current in the ring generates a field which, in a location in the plane of a ring always is perpendicular to the plane of that ring. This is not the case anymore for locations out of the plane of the ring.
The field contribution, due to the component of the current element, is perpendicular to the direction which joins the location with the current element. When the latter direction is out of the ring plane, the field direction is not anymore perpendicular to the ring plane.

For each location, the symmetry of the ring allows choosing a mid plane on which the location is situated. The mid plane is the median plane perpendicular to the ring plane, placed at a diagonal of the ring. Considering only the effect of one single current element, the symmetry of the ring allows choosing that element which situates at the mid plane, as all current elements are equivalent in the ring. In a ring a current element is perpendicular to the diagonal. The magnetic induction field direction lies in the mid plane. In Fig.4.1 the mid plane is in the drawing plane.

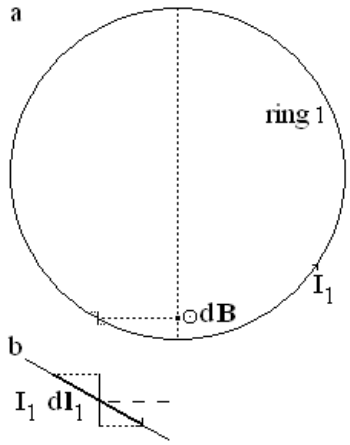


*Fig.4.2 indicates that in ring 1, the current element only contributes to the component of the magnetic induction field at the location by its component that is perpendicular to the direction which connects the element to that location. Part b) shows a detail of the general view, given in part a). The statement holds for each current element.*

Once the mid plane chosen, the other current elements are not anymore on the mid plane

The current flow in an element of a ring, in most cases, is not perpendicular to the direction that connects the element to the location. For each current element, the contribution to the field is due to the component of the element which is perpendicular to that direction. For one current element, the statement is visualized in Fig.4.2.

We now consider the result of the addition of two field components. Again we consider at first the special case in which both current elements and the location are on one mid plane. The cross section of the situation is pictured in Fig.4.3. The mid plane is in the plain of the drawing. The plane of the ring is perpendicular to that of the paper. At the right of Fig.4.3, the current flows into the paper plane. At the left, it is coming out.

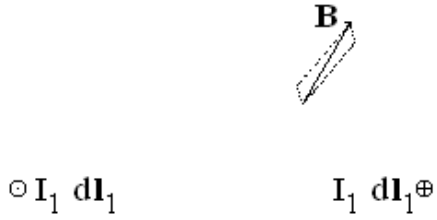


*Fig.4.3 shows, for the neighbourhood of ring 1, the direction of the magnetic induction field, as due to two current elements.*

At a certain location on the mid plane, the magnetic induction field is mainly due to the nearby current element. In the case we report in Fig.4.3, we consider only two current elements. The elements are diametrically opposed in the ring. The field is the resultant of two components. To an off centre location one element is closer than the other. The magnitude of the field component due to the nearby current element is larger than that due to the further off element. The magnitude of the field contribution decreases with the square of the distance between the current-element location and the field location. The field at the location is the combination of both field components; it is the vector sum of the components.

In the more general case in which two current elements are not situated at the chosen mid plane, the symmetry of the ring has the consequence that for each current element in the ring there exists one in a position symmetrical versus the mid plane. For each current element, the field vector can be decomposed in two components. The direction of one component lies in the mid plane while that of the other is perpendicular to that plane. The perpendicular components, due to the two current elements, cancel each other. The components in the mid plane add to each other.

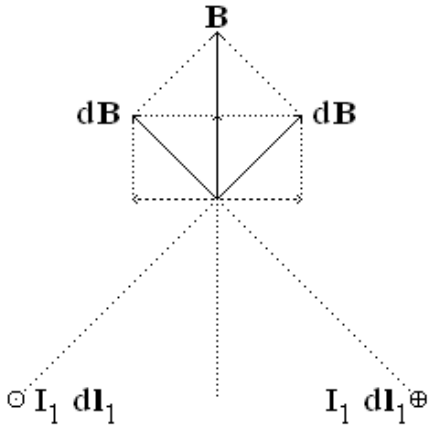


*Fig.4.4 reports on the magnetic induction field generated by two current elements which positions are symmetrical versus the mid plane. The field contributions of the two elements combine into one resultant.*

At the magnetic susceptibility measurements, the magnetic induction field at the sample place is the resultant of the contributions of all current elements in the magnet.

## 5 Magnetic lines of force

Due to a current ring, the direction of the magnetic induction field, at any location, always lies in a mid plane. For practical reasons, we only treat a fraction of the infinite number of possible locations. Fig.5.1 shows a typical result.

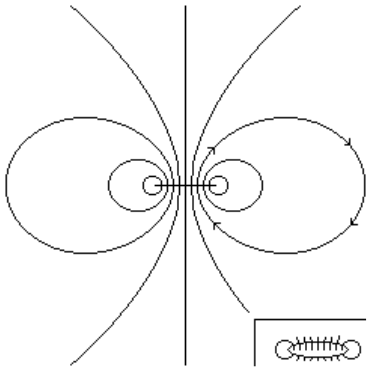

*Fig.5.1 shows a field line pattern in a mid plane of a ring. The mid plane lies in the drawing plane. In the lower right figure corner, a somewhat declined ring sketches the situation of the field lines at the diagonal.*

To get Fig.5.1, we started on five locations inside the ring on its radius. The starting points are 0.0, 0.2, 0.4, 0.6 and 0.8 times the radius. As stated before, in the plane of the ring all field directions are perpendicular to that plane.

Following the path indicated by the direction of the field, we designated a new location, positioned at a small distance from the starting point. We reconsider the field direction at the new location which lies out of the ring plane. Many times, for each of the newly obtained starting positions, we repeated the same process reconsidering the field direction after a small displacement.

For off axis locations the influence of the nearest current elements forces the field direction to deviate from a straight line. The calculation process results in closed lines, the so called magnetic lines of force. The ring current forces a freely moving needle of a compass to follow the local direction of the line. The south to north seeking pole-sense of the compass needle and the field-sense are the same. For

one of the lines, we indicated the sense of the field.

The magnetic induction field, due to a circular constant current circuit, lies, at any location, in a mid plane. The geometry of the ring results in a rotational symmetry about the axis of the ring and in a mirror-inversion symmetry about the ring plane. By mirror-inversion we mean that the geometry of the field direction at one side of the ring is the mirror image of the geometry of the field direction at the other side of the ring plane. The expression inversion indicates that at the mirroring the sense of the field inversed.

When the radius of the ring is taken as unity, then all field line patterns are the same for all rings.

What comes in the ring on one side gets out on the other side. What gets out the ring on one side returns back, by a closed loop outside the ring, to the other side. The field lines are closed and never cross each other. The field lines remind me the stream lines in a non turbulent liquid. It always fascinated me that an immaterial pure mental construction, invented by men for helping to calculate the force between electric currents, behave as the flow of a real material liquid.

A current carrying ring inside a sphere crudely simulates the world magnetic situation. The ring plane is the equatorial plane when the centre of the ring and of the sphere coincides. The poles occur at the surface of the sphere on the central axis of the ring. On the surface of the sphere the lines of force simulate the earth magnetic field lines. They come out one of the poles plunging in the other pole. The two poles are different.

A current carrying ring-ring interaction model simulates a magnetic susceptibility measurement. The current in one ring simulates the currents in a sample. The current in the magnet simulating ring generates the applied magnetic induction field at the location of the sample simulating ring. By symmetry, the current in the sample simulating ring generates also a magnetic induction field at the magnet. The symmetry, however, breaks up when the magnet does not respond to that field. In such case, the field generated by the magnet, called the applied magnetic induction field $\mathbf{B}_a$, is independent of the sample-susceptibility.

## 6 The force direction

The choice of the force detection system imposes the direction of the component of the magnetic force we can measure. As force detector, we decided in favour of a torsion balance. Our expectation for a good sensitivity/precision compromise, for measuring the magnetic susceptibility of small solid samples, pushed us to this choice. Fig.1.1 outlines the set up. The force sensitivity of our balance is in the direction gravity works. This direction also is advantages for constructions needed for low temperature measurements.
Once the set up chosen, the magnet configuration in the susceptibility experiment must be adapted.

In view of the adaptation, we discuss the force direction for simple ring-ring configurations. Herein again, simulates ring 1 the magnet and ring 2 the sample. The diameter of ring 1 is larger than that of ring 2. The currents in the rings are opposite in sense.

In a first configuration, both rings lie in the same plane. The direction of the magnetic induction field, generated by ring 1 at the current path in ring 2, is perpendicular to the ring plane. The force on each part of ring 2 is directed to the centre of ring 2 in the ring plane.

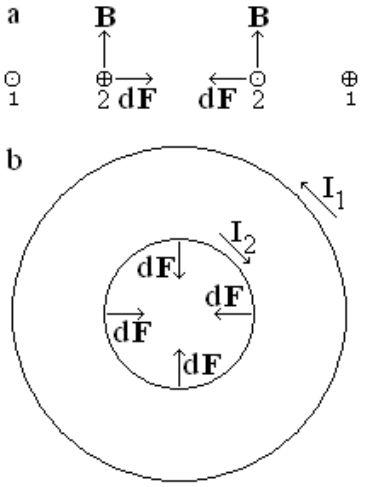


*Fig.6.1 shows ring 2 at the centre of ring 1, being in the same plane. a) Side view, all fields at the current elements in ring 2 are, by symmetry, equal in magnitude. b) Top view, the magnitude of all forces is equal. The magnitude of the forces is proportional to the magnitude of the local field.*

When the centre of ring 2 coincides with the centre of ring 1, (Fig.6.1) the magnetic induction field at each current element in ring 2 is the same. The geometrical situation of one of the ring 2 elements versus all the current elements of ring 1 is the same. Consequently, all

forces on ring 2 are equal in magnitude. There is no net force that tries to move the ring 2.

The forces tend to compress ring 2. In the case the currents in the rings would flow in the same sense, the forces would tend to expand the ring.

In our work, we never had to deal with changes in sample dimensions. We consequently neglect magnetostriction in our discussion.

A net force results when ring 2 lies off centre in ring 1. The geometrical situation of one of the current elements in ring 2 versus all the current elements of ring 1 is not the same for that of another ring 2 element (Fig.6.2). In ring 2 the magnetic induction field at one current element differs from the field at another one. The field is stronger in points closer to the current path of ring 1. The current intensity is the same everywhere in the ring. Consequently, the forces on the elements are proportional to the magnitude of the magnetic induction field. The net force on ring 2 is the resultant of all forces.

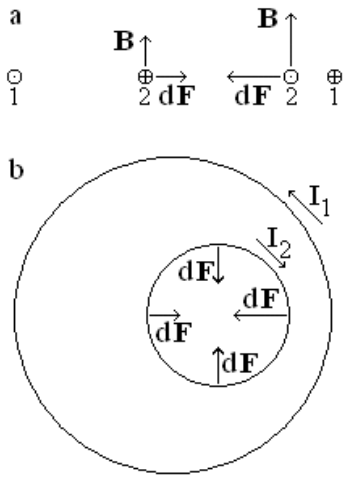


*Fig.6.2 shows ring 2 off centre in ring 1 but in the same plane. a) Side view at mid plane, the magnitudes of the fields at different current elements in ring 2 are different. The larger fields occur at locations that are closer to ring 1. b) Top view, the magnitude of the forces is different too.*

The net force tends to push ring 2 onto the centre of ring 1 when the current in ring 2 flows in an opposed sense the current in ring 1 flows. In the case the sense of the two flows is the same, the net force tends to push ring 2 still more out of centre.

In the configuration that both rings are in the same plane the net force is in that plane. To introduce the configuration into the

susceptibility experiment, the direction of the force should be the direction of the balance's sensitivity. The ring plane must be vertically positioned, the common mid plane diameter following the gravitational direction.

In the next configuration, both rings lie parallel but in different planes, their centres on the common axis perpendicular to the planes. By symmetry, no net resultant force remains in a direction in the planes. The resultant force acts along the axis. At each current element in the sample simulating ring 2 the radial component of the field, indicated in Fig.6.3 by Br, yields a force component. For horizontal rings, the force contributes to the resultant which is measurable by the balance.

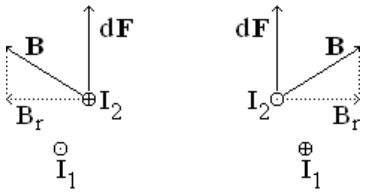


*Fig.6.3 shows the magnetic induction field component in the plane of ring 2 that generates a force in axial direction.*

## 7 The field direction at the sample

A sample can be magnetically anisotropic. In search for "how susceptible is that sample to a magnetic induction field?" one needs knowing the field direction at the sample's location.
In principle, we like to measure the magnetic susceptibility of a sample in all directions. However, there are some practical obstructions.

In exceptional cases we constructed on the balance pan a device allowing orienting the sample in different positions versus the applied magnetic induction field. Such a system was cumbersome, time consuming and certainly not practical at all.

In most cases a simple solution suffices, laying the sample on the bottom of the small squared balance tray. The balance tray hangs freely inside the tail of the cryostat that sets the temperature of the sample. The magnetic field at the sample is generated by the magnet outside the cryostat.

In our research we used two magnet configurations. We outline here their principle.

In the simplest sample/magnet configuration the direction of the field to which the sample is subjected for the susceptibility measurement is vertical. The configuration allows the magnet generating coil to be fixed over the tail of the cryostat that sets the sample temperature.

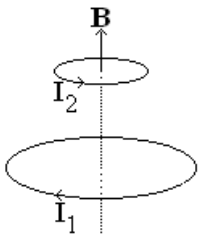


*Fig.7.1 shows the simplest geometrical sample magnet configuration. The sample is at the central axis of the magnet simulating ring.*

Fig.7.1 shows the simulation of the simplest configuration. The vertical central axis of the horizontally mounted magnet simulating ring is the geometrical place of the sample position.
The set up does not allow changing the direction of the field. However, the sense of the field is easily reversible by switching the current sense in the magnet ring.

In the simplest configuration, as stated in Fig.6.3, only the radial component of the field generates the force in the direction the balance is sensitive. In order to get a force signal, the field must diverge at the sample. The susceptibility measurements need a well defined magnetic induction field, known all over the sample. A conflicting situation arises when, on the one hand, we tend to get a homogeneous field which constancy is simplest to treat, while, on the other hand, we need a non homogeneous field to get signal.

Before getting into the compromise, we introduce a second basic magnet configuration.

In a somewhat more complicated configuration the field direction is horizontal. The construction allows relatively easily setting the magnet in whatever angle in a horizontal plane about the sample in the tail of the cryostat.

In the present simulation also is the axis of the magnet ring horizontal. The sample can not be in the plane of the ring, keeping the magnet outside the cryostat. We therefore simulate the magnet by a pair of identical current rings, located on a common axis, as outlined in Fig.7.2.

In the plane halfway the two rings the direction of the magnetic induction field has no radial component. The field, by symmetry, is purely horizontal and consequently does not result in a horizontal force component.

Out of axis, the field decrease results in a force, in the vertical direction, that can be measured by the balance.

Also in the present configuration the conflicting situation persists. The contradiction remains in a quest for a homogeneous field, allowing simple data treatments, and the need for non homogeneity to get the force, the latter being essential for the susceptibility measurement following the Faraday method.

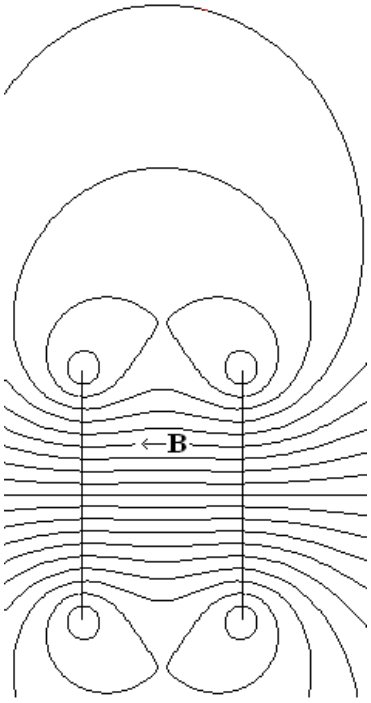


*Fig.7.2 outlines the field situation at mid plane of a "Helmholtz" pair of current rings. The planes of the rings are vertical. The two rings are perpendicular to the paper plane, simulating their vertical mounting. At locations halfway the two rings the direction of the field is horizontal, by symmetry. Out of axis, the field gradient yields a resulting force in the vertical direction, the sensitivity direction of the balance.*

## 8 A homogeneous field

In search for an honourable compromise between homogeneity and non homogeneity, we start discussing the way to generate a homogeneous magnetic induction field.

Fig.5.1 indicates that for locations, in the neighbourhood but out of the plane of a single circular current circuit, the magnetic induction field diverges. The field is not homogeneous. More primitive circuits together can yield better homogenous fields. In fact we yet introduced the technique in the Fig.7.2 configuration. A second identical primitive ring, positioned on the same axis as the first one, influenced the path of the magnetic lines of force, also called the field lines.

The influence of the second ring on the field line path depends on the distance between the two rings. When the distance is much larger than the radius of curvature of the field line at the first ring, the influence of the second ring is negligible. The closed field line embraces only one ring.

By symmetry, it is equivalent to call the left or the right ring in Fig.7.2 the second one.

When the radius of curvature of the field line at the first ring is much larger than the distance between the rings, the field lines enclose both rings.

An off centre field line leaving the first ring drifts away from the axis. Up to half the distance between the two rings, the first ring dominates the evolution of the field line. Beyond half way, the influence of the second ring takes over. By symmetry, the second ring leads the field line path into the plane of the second ring at an equivalent location it left the first ring.

Generalizing the observation, parallel identical current rings on one single central axis keep the field lines together. The effect spectacularly comes to expression in the simulation of a very long solenoid, as indicated in Fig.8.1.

For generating a homogeneous magnetic induction field we consider, as magnet coil, an extremely long straight solenoid. The coil-length is orders in magnitude larger than the coil diameter. The wire-diameter is much smaller than the coil-diameter. The wires are

closely and homogeneously wound on a mono layer. In the coil flows a constant current. There are no other currents influencing the field.

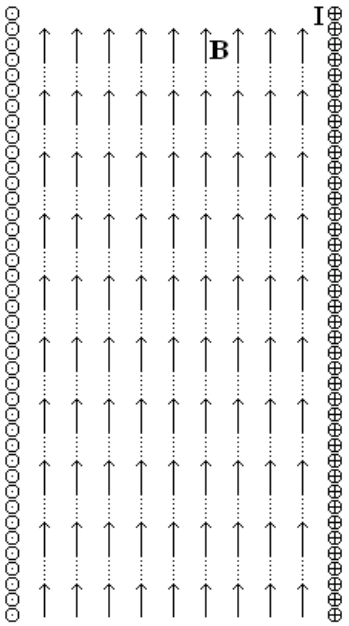


*Fig.8.1 represents a section of the simulation of a very long straight solenoid. The field lines are parallel. The direction and the sense of the magnetic induction field is the same over the total solenoid volume. The magnitude of the magnetic induction field is the same at all places. From the latter only a fraction is indicated. In short, the magnetic induction field is homogeneous.*

At the field calculation, the solenoid is simulated by a stack of identical rings. All centres of the current carrying parallel rings are on a straight lined single axis. The rings are closely packed. We neglect here the pitch of the solenoid as the wire diameter is much smaller than the coil diameter. In Fig.8.1 the diameter of the wire is exaggeratedly represented, allowing indicating the current sense. The intensity, the direction and sense of the current is the same in all rings. The calculation shows that the closely packed rings do not give much space to the field lines to escape from the stack.

In conclusion, the magnetic induction field, inside the coil far from the coil ends, is practically i) parallel to the coil axis, ii) independent of the radius of the coil, iii) independent of the place inside the coil, and iv) proportional to the intensity of the current flowing in the coil times the number of wire turns per unit length. The sign of the field is related to the sense of the current in the coil.

The field is strongly related with the technical specification of the solenoid, the “ampere turns per meter”. In the latter expression, ampere means the intensity of the current flowing in the solenoid. The

expression does not specify whether there is a high current intensity and a low number of turns or a low current intensity and a high number of turns. The expression in fact means "(ampere per turn) times the number of turns per meter". Herein is "(ampere per turn) times the number of turns" nothing else than the total intensity of the current that flows per meter. The latter current intensity leads to the "ampere per meter", the current density unit ($A.m^{-1}$) often used in magnetism.

## 9 A diverging field

In the above discussions we approach the magnetic induction field in a solenoid by calculating the effect of a stack of current carrying circles. In a further step of abstraction in the simulation, we represent the solenoid by a cylinder on which curved surface flows an infinitely thin current layer. The current flows in a plane perpendicular to the cylinder axis. The surface current density is homogeneous; it is the same over the total length of the cylinder. The abstraction of the wire dimension allows to get rid of the field effects in the current leads. The latter effects are for the moment of no importance to get the picture of the basic ideas.

Fig.9.1 shows some magnetic lines of force at the mid plane of a current carrying cylinder. The calculation of the five lines started at -40 times the radius length, i.e. at about the middle of the cylinder. The radial coordinates of the starting points are 0.1, 0.3, 0.5, 0.7, and 0.9 times the cylinder-radius distant from the central axis.

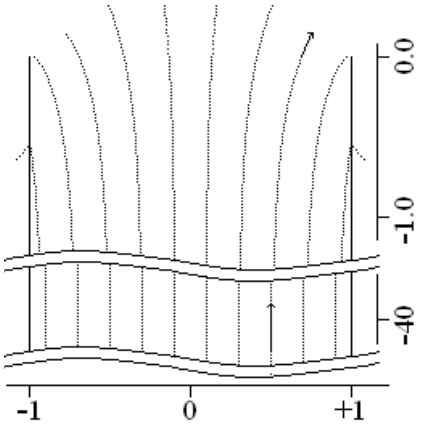


*Fig.9.1 shows some magnetic induction field lines for two parts of a cylinder which length is hundred times its radius. The upper part represents the field pattern at an end of the cylinder; the lower part at about the middle, 40 times the radius length from the end.*

At the end of the cylinder the lines diverge fan-wise. In the region of divergence, the magnetic induction field has a radial component. This component generates, in a simple geometrical sample magnet configuration (Fig.7.1), a force in the axial direction simulating a magnetic susceptibility experiment following the Faraday method. In the latter, the balance measures the axial force in a vertically positioned magnetic coil. An honourable compromise between homogeneity and non homogeneity of the magnetic induction field at the sample location situates at the end of the coil.

The above discussion yields enough information for starting qualitative susceptibility experiments. However, before doing so we look somewhat closer to the field pattern.

We start considering the theoretical model, an infinitely long cylinder with an infinitely thin homogeneous current layer on its curved surface. The current flows in a plane perpendicular to the cylinder axis. In this theoretical configuration is the magnetic induction field the same, everywhere in the cylinder. The field vector is parallel to the cylinder axis. The magnitude of the field is proportional to the surface current density. In many papers the letter **J** ($A.m^{-1}$) refers to that density.

In a cylinder with finite length, the field inside the cylinder is less than that in an infinite long one with the same surface current density. The cylinder parts omitted beyond the ends do not contribute anymore to the field. Nevertheless, in the middle of the cylinder with a length versus radius ratio hundred, as discussed in Fig.9.1, the field component in the axial direction is only 0.2 pro mille less than that of the theoretical infinite case. At the coordinate -40 (indicated at the right in Fig.9.1) the extra decrease of the axial field component is $3x10^{-5}$. At the same location for all positions between 0.0 and 0.9 times the radius, the radial field component is negligible; its magnitude is less than ten parts per million of the axial component value.

At an open end of a one half infinitely long cylinder, the axial component of the magnetic induction field is one half of that in the middle of the whole infinitely long one. It is logic, as only half of the current contribute to the field. The 50 percent reduction practically occurs also at the 0.0 coordinate (indicated at the right) in the Fig.9.1.

However, this is not the whole story. At the end of the cylinder radial components of the field find expression. Indeed, the radial components at the end of one half-long cylinder are not annihilated by the contribution of the currents on the missing half. The mirror-inversion symmetry makes such annihilation to happen at the middle of the cylinder.

## 10 The magnetic flux

To get feeling for the magnetic induction field pattern inside the cylinder, we discus some similarities it shows with the flow field, represented by streamlines, of an incompressible frictionless fluid in a diverging pipe. For a laminar flow in a steady state, the conservation of mass results in: “what is coming in the pipe is coming out”. The rate of mass flow is constant over the pipe.

Switching to magnetism, in the middle of a very long cylinder we state that, similarly to the flow rate in fluid dynamics, the product of the magnetic induction field times the area of the cross-section of the cylinder is the normal local magnetic flux. Normal indicates that we relate to the field component perpendicular to the considered area. The area is part of a flat plane. The specification “normal” is often omitted nevertheless supposed in literature. The flux, referred to by the symbol $\Phi$, is expressed in weber (Wb).

At the middle of the cylinder our statement holds. On the one hand, the area is the flat section of the cylinder, taken perpendicular to the cylinder axis. On the other hand, the magnetic induction field is constant all over the section of the cylinder. The field is perpendicular to the area.

In our solenoid simulating cylinder, one off axis field line together with the rotating symmetry, about the cylinder axis, result in an immaterial diverging tube. The tube and the cylinder are coaxial. To keep it simple, we consider only the tubes whose field lines leave the cylinder by the open end.

For fixing the idea we take, in Fig.9.1, in the middle of the cylinder the radius of the tube half the cylinder radius. The local flux is the local field times the cross-section of the imaginary tube. At the end of the cylinder, the axial field component is half that in the middle of the

cylinder. Calculations show that at the end of the cylinder the local cross-section of the tube is twice that in the middle of the cylinder. So, the flux through the “flux-pipe” is constant.

The middle and the real end of a cylinder are special in the way that the axial field component is constant all over the area of the cross section. However, for other sections in the cylinder the field component is not constant.

Fig.10.1 shows the axial field component, calculated along two lines of force which started at -40 times the radius length, i.e. at about the middle of the cylinder. The field component is expressed as the fraction of the magnetic induction field that exists inside an infinitely long cylinder carrying the same surface current density. The radial coordinates of the starting points of the field lines are 0.1 and 0.7 times the cylinder-radius distant from the central axis.

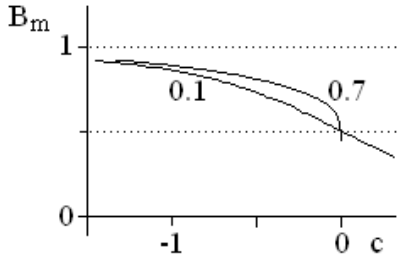


*Fig.10.1 reports on the axial field component fraction at different depths in the cylinder. The depth c is expressed in radii.*

At coordinates between the middle and the real end of the cylinder, the total flux over an area is build up by flux elements in the area. A flux element is the product of the local magnetic induction field times an infinitesimal small part of the area. With local we mean that the magnetic induction field can be considered as constant over the small area. The magnetic induction field therefore can be seen as the flux density. One can generalise the flux through an area as the sum of all infinitesimal flux elements in the area.

Similarly to the mass conservation in the fluid dynamics, in a flux tube holds: what is coming in is coming out.
The flux conservation does not hold anymore when the field lines of the diverging tube cross the current layer on the cylinder. The latter situation is not relevant for the susceptibility measurements, because we chose the sample dimensions small enough to avoid this inconvenience.

## 11 The gradient

The magnetic field lines pattern shows some similarities with the stream lines pattern of a laminar flowing incompressible frictionless fluid in a diverging pipe. The similarity helps us visualizing the occurrence of the radial field component on a sample simulating ring.

We need a radial field for generating the force in a set up we used for measuring magnetic susceptibilities. The set up in mind relates to the simple basic configuration that is outlined in Fig.7.1. In the present simulation is the magnet ring replaced by the half infinitely long cylinder. Fig.11.1 outlines the simulated sample/magnet configuration under attention.

The sample simulating ring here is the curved surface of an ultra short cylinder, i.e. the curved surface of a thin disc. The thickness or height of the disc is smaller than its diameter. The ring figures coaxially at the end of the magnet simulating cylinder.

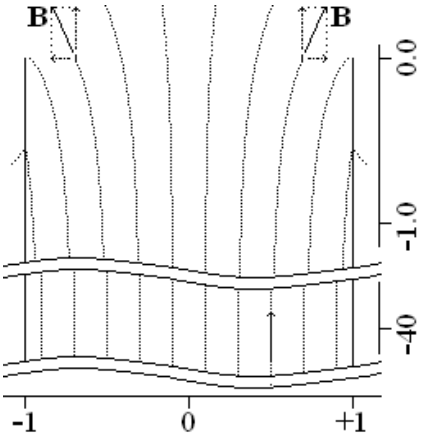


*Fig.11.1 indicates the magnetic induction field decomposition into an axial and a radial component. It concerns the field at a sample simulating ring at the end of the magnet simulating cylinder in a simple configuration.*

In our perception, the ring situates on an immaterial diverging flux-tube. In such a flux-tube is the flux constant. In the ring is the diameter constant. Therefore it is obvious that the diverging flux in the ring is not constant. Only part of the flux that is coming in on one flat open end of the ring comes out on its other flat open end.

Keeping in mind the similarly to the mass conservation in the fluid dynamics, the flux that is coming in on one flat open end of the ring comes out the ring. However, not all is coming out via the open end of the ring. Part is coming out via the curved “wall” of the ring. This part

is the difference between the fluxes that comes in and out via the open ends of the ring.

The local flux density at the side face of the ring is the radial magnetic induction field component we are in search for.
The rotational symmetry of our configuration keeps the picture simple. We reduce the problem even more by taking the height of the ring small. We take it so small that the flux density, at the ring's surface, practically is constant all over the height. Consequently, the density of the flux that leaves the ring via the curved surface is everywhere practically the same.

The configuration allows calculating the radial flux density simply as the quotient of the open end flux difference divided by the total curved surface area of the ring. The ring surface being the product of the circumference with the height, we can rearrange the formulation of the flux density. We introduce here the flux gradient as the quotient of the open ring ends flux difference divided by the height of the ring. The introduction results in the following formulation.

The radial magnetic induction field component at the ring is the quotient of the flux gradient divided by the circumference of the ring.

The same flux gradient, but divided by the area of the cross section of the ring, yields an average value for the axial component of the magnetic induction field-gradient. The latter component, consequently, is related to the radial magnetic induction field component at the ring.

The axial component of the magnetic induction field-gradient depends on its location in the ring. The relative deviations become less when the radius of the ring is smaller than the radius of the magnet simulating cylinder. In practise the value of the field-gradient, at the cylinder axis, is used as an approximation for the average gradient.

## 12 The magnetic moment

Above, we outlined the train of thought that led us to the element of the magnetic induction field that is needed for calculating the force on a sample. To know the field is the first step in the calculation of the interaction between the current in a magnet coil and the current in a

sample. To let the field interact with the current in the sample is the second.

We discuss the second step on a sample simulating ring in the sample/magnet configuration as outlined in Fig.11.1. The half infinitely long cylinder simulates the magnet that creates the field and gradient at the sample. At the ring, the radial magnetic induction field component is everywhere the same. It is the quotient of the flux gradient divided by the circumference of the ring. In our "gedanken experiment" we consider a constant current flowing in the ring. We choose a current intensity.

The force on the ring is that current intensity times the circumference of the ring times the radial magnetic induction field. The radial magnetic induction field component at the ring is the quotient of the flux gradient divided by the circumference of the ring. Consequently, the force on the sample ring is the current intensity times the flux gradient. The flux gradient is the area of the cross section of the ring times the average value of the axial component of the magnetic induction field-gradient. The force therefore is the current intensity times the cross section of the ring times the average value of the axial component of the magnetic induction field-gradient. The intensity of the current on the ring times the cross section of the ring is the magnetic moment of the ring.

Finally, the force on the ring is the product of the magnetic moment of the ring times the average value of the axial component of the magnetic induction field-gradient.

---

$$F_s = \mu_s.G \qquad (12.1)$$

Equation (12.1) expresses the force on the ring in the model, simulating the force on the sample at the susceptibility measurement. Consequently, the force on the sample is the product of the sample moment $\mu_s$ times G, the average value of the axial component of the applied magnetic induction field-gradient.

---

In search for a simple analysis of measuring data we try to uncouple, as far as we can, the parameters related to the apparatus from those related to the sample. Practically, we only succeed in the

way we can keep the magnetic induction field-gradient constant over a sample. In such a case is the magnetic moment practically only related to the sample. The measured force divided by the applied field-gradient, by construction, relates only to the apparatus.

The magnetic moment as induced in a sample by a magnetic induction field is the basic ingredient of our susceptibility studies. The magnetic field influences the sample, inducing a magnetic moment in it. The sample is susceptible to the magnetic field for creating a magnetic moment. The easiness of influencing is the topic of our research. We measured the susceptibility for different kind of samples. We try to model the data. A model is fruitful when not only it explains the physics beyond the observations but also predicts new observations.

## 13 A sample/coil configuration

After discussing theoretical models, we converge now to the discussion of one of our set-ups for measuring the magnetic susceptibility of a sample. Fig.13.1 outlines the subject of our attention. The magnet/sample configuration relates to the basic situation outlined in Fig11.1.

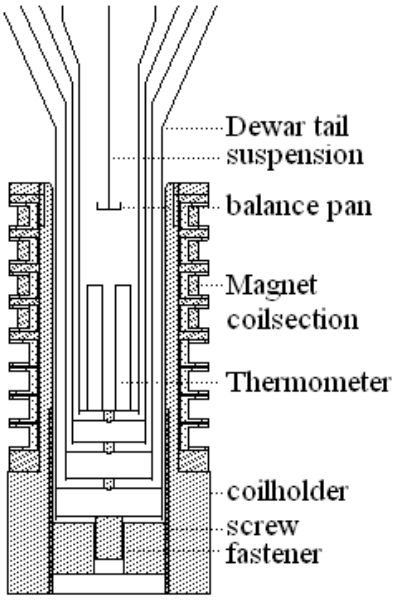


*Fig.13.1 shows the sample-magnet configuration. The sample lies on the balance pan. The sample is inside a cryostat which takes care of the sample temperature. Thermometers measure the temperature. Outside the Dewar generates a magnet coil the induction field and gradient. The position of the sample in the field of the coil is adjusted, along the coil axis, by a crew.*

Because we need only the divergent magnetic induction field pattern at the end of the cylinder, a short coil suffices in practice for generating the radial field component.

The day we built the coil our theoretical knowledge of the field was less developed. We were experimenting with four coil sections, 125 turns of copper wire each. The sections were connected in series, in a circuit powered by a constant current device. Therefore the current in the magnetic field generating coil was independent from the magnetic moment in the sample.

The sample in the pan hangs down, from the balance, in the Dewar tail at the axis of the coil [13].

The coil, on its holder, fitted the Dewar tail on the outside. By screwing up or down the holder, the coil position can be changed versus the position of the sample.

The sample dimensions are much smaller than the diameter of the coil. A relatively larger coil diameter results in a relatively smaller deviation of the value of a local field-gradient in the sample from the averaged value. The calculated value of the field-gradient at the cylinder axis is used as an approximation for the averaged value of the gradient.

The coil current generates heat due to Ohm's resistance of the wires. The heat increased the temperature of the coil. Copper spacers between the sections reduced the effect. Nevertheless, we limited the current to one ampere at the susceptibility measurements. For measuring samples showing large susceptibilities the set up was convenient. We did not felt the need to change the configuration.

For every location in the sample, the applied magnetic induction field-gradient is proportional to the current intensity in the coil. The statement also holds for the applied field. Due to the current limitation in the coil, the maximum magnetic induction field-gradient used on our sample was about 0.5 $Tm^{-1}$ (tesla per meter). The maximum magnetic induction field was 10 mT (milli tesla).

The limitation of the coil current, together with the small magnetic susceptibility of the balance pan, kept the force on the empty sample holder beyond the sensitivity of the balance. Measured in this set-up, the force on a sample does not need a correction for the empty sample holder.

The cooling of the cryostat results in the shrinking of its inner part, as shown by the X-ray picture given in Fig.13.2. It shows a doubly exposed film. At the first exposure all was at room temperature, at the second the inner part of the cryostat was cooled, the room temperature Dewar tail holding the film.

F*ig.13.2 is an X-ray picture of the balance pan. The picture is a double exposure, one of the tray at room temperature and one at liquid nitrogen. The film, on the outside of the Dewar tail, remained at room temperature. Cooling causes the shrinking of the copper wires that suspend the sample holder, lifting the latter.*

The double picture of the balance tray is the result from the shrinking of its suspension wires. The position of the sample in the Dewar depended on the cooling of the cryostat. The protocol for cooling allowed relating the sample position to the sample temperature.

Heat shields in the cryostat help homogenizing the temperature for the sample-thermometers configuration. A certain protocol for cooling the cryostat allowed relating the sample temperature to the thermometer reading to better than 1 % over the temperature region from room temperature down to 2 K.

## 14 The volume susceptibility

The current-current interaction is the basic idea behind the physics of magnetism. We deduced a sample/magnetic coil configuration which practically allows measuring the magnetic moment of a sample. A field-gradient that is constant all over the sample results in the

uncoupling of the magnetic moment from the parameters of the apparatus. The smaller the sample the closer the local field-gradient approaches everywhere in the sample its average value. The dimensional reduction of the sample however is limited by the limited sensitivity of the force detection.

In the next step of our discussion, we relate the magnetic sample moment to the magnetic sample susceptibility. For fixing the ideas, we discuss the simple case of a pure vanadium disc, in the balance pan, at low temperature. At 3.2 K, the vanadium is superconducting [14].

Putting the current in the coil "on" induces a magnetic moment in the sample. The magnetic induction field at the sample represents the in-between for the interaction with the coil current. Our question therefore becomes: what is susceptible to the applied magnetic induction field for creating magnetic moment? Knowing that the superconducting electrons can flow over the whole volume of the sample and that the kind of material that is superconducting may be of less importance, we consider the volume of the sample as representative for the sample. In our question becomes the sample volume the "what" that is susceptible to the field. In conclusion, we put the product of the sample volume times the volume susceptibility times the field equal to the magnetic moment of the sample.

---

$$\mu_s = v\, \chi_v\, B \qquad (14.1)$$

Equation (14.1) expresses the magnetic moment of the sample as the product of the sample volume v times the volume susceptibility $\chi_v$ times the field on the sample B.

---

For coil currents produced by the constant current device, we got force signals in the region wherein the balance functioned well measuring on a disc for which the dimensional compromise was 0.2 mm thick and 3.0 mm diameter.

Susceptibility measurements on a field-less cooled vanadium disc taught us that the sample is diamagnetic. The sample is pushed away by the coil current.

We understand the experimental fact as a consequence of Lenz's law. In a conductor, a changing external field creates current loops opposing the changed field. In a superconductor the current loops persist when, during the measuring period, the field remains constant. For temperatures for which vanadium is not superconducting, the currents die out, i.e. do not persist.

In the case the applied magnetic induction field is "off" when we cool the vanadium, the sample is a field-less cooled disc. At the cooling, the material changes from the normal conducting- to the superconducting state. In the field-less cooled sample we expect no persistent currents flowing in the disc at the onset of a susceptibility measurement. The force exerted on the disc at the measurement then only is due to the persistent currents induced at the field change. The force is independent of the flow sense of the current in the coil. At a fixed sample versus coil position is the force proportional to the square of the coil current intensity.

More quantitatively, at a given sample position we measured forces up to $3x10^{-5}$ N. The uncertainty on the proportionality constant relates to the variation coefficient 0.035% or the force detection-limit $1x10^{-9}$ N (newton), whichever is the larger.

We explain the experimental fact assuming that, at the temperature- and field-region we worked, the susceptibility of the vanadium disc is constant, independent of the applied field. The susceptibility times the sample volume also is constant. The force consequently is proportional to the field times the field-gradient.

In the sample coil configuration considered, in which no external currents occur, the applied field as well as the applied field-gradient is proportional to the intensity of the coil current. The agreement between model and experiment supports our explanation.

The experiment not only taught us that, at the given conditions, the volume susceptibility of the superconducting vanadium disc is diamagnetic and constant versus the applied field. It also tells us something on the apparatus. The variation coefficient is an indication for the overall precision. It concerns as well the balance as the constant current device and the geometrical stability.

## 15 On the applied field and gradient

The susceptibility of the superconducting vanadium disc was constant. The statement followed from measurements carried out for different coil current intensities but at a fixed sample location.

The constancy allowed us to check the axial field and gradient pattern, measuring for different locations but at a constant coil current intensity. For a given current intensity, the field and its gradient depends on the geometry of the sample coil configuration.

Fig.15.1 shows the normalized function we calculated with the before mentioned approximations for the applied field (**B**), the applied gradient (**G**) and the product of both. The normalization means that we converted the maxima to 1, i.e. 100% (scale on the left). The sample location, always on the coil axis, is given by the bottom scale. Zero is at the end of the coil. Minus means a location inside the coil while plus means outside.

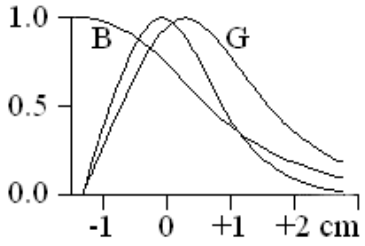


*Fig.15.1 shows the calculated normalized field (**B**), gradient (**G**) and the product of field and gradient.*

On the superconducting vanadium disc at 3.2 K, we carried out, in a single day experiment, force measurements at different coil versus sample locations. The given coil current intensity was 0.3 A. We analyzed the force data minimizing the relative deviations accepting that the susceptibility here also was constant. The experimental force versus coil position curve matched the calculated field times gradient curve versus sample position [14].

Systematic errors were less than 0.5%. In the quantitative analysis we took in account only forces larger than one third of the maximum force.

When we take the calculated field and gradient as the applied ones, the average experimental susceptibility values agreed within 0.44% with the one resulting from the measurements at fixed location.

The overall precision on the measurements, carried out on the superconducting vanadium disc at 3.2 K, gives faith to our knowledge of the experiments. It concerns as well the balance, the constant current device, the geometrical configuration as the calculated fields and gradients. The care we took in constructing the Dewar tail with low susceptibility materials was fruitful. Internal consistency indicates that the sample, at the inside of the Dewar, practically felt the field and gradient generated by the coil at the outside.

## 16 On the susceptibility of superconducting discs

The comparison of the magnetic susceptibility of lead with that of vanadium in the superconductive state bears out the assumption that, at low field and temperature, the kind of constituting material of the sample is of less importance.
We compared the susceptibility of discs that have the same diameter but are of different thickness.

The magnetic susceptibility of the 0.11 mm thick lead disc at 4.3 K (Fig.2.2) is in such a way similar to the vanadium one that its susceptibility practically is constant, independent on the field. The statement holds in the temperature and field region considered. Numerically however, the susceptibility of the thinner lead disc is much larger than that of an about twice times thicker vanadium one.

The experiment shows that the product of the sample thickness times its susceptibility for both samples is about the same.

The magnetic moment induced in the disc is about proportional to the flux passing the disc. We remind: the moment is the product of the sample volume times the susceptibility times the field. In other words: the moment is the product of the sample thickness times the susceptibility times the sample surface times the field. The sample surface times the field is the flux through the disc.

The experiment suggests that the flux is the driving entity for inducing the magnetic moment, the persistent currents in the sample.

For thinner discs, however, the dependence on the field of the susceptibility becomes different. In the 0.025 mm thick lead disc (Fig.2.2) the magnetic moment responds to the magnetic flux with the

same proportionality factor only at low fields. In the thinner discs the diamagnetic susceptibility for an increasing field switches over, at a certain value, from the constant- into a decreasing-regime.

We interpret the experimental fact accepting that in the thin discs there are not enough superconducting electrons sustaining all induced currents to persist. Some currents die out, like eddy currents do in a normally conducting metal.

## 17 Persistent moments

In the former part of our discussion on superconducting discs, we treated the proportionality of the induced magnetic sample moment to the applied field flux. The proportionality is only constant when the disc of a certain thickness is measured in low magnetic fields at low temperatures. In the following we consider cases for which the field or temperature is not low enough. The proportionality is not constant anymore but depends on the field and temperature. The persistent magnetic moment that we can induce in the superconducting disc is limited.

We carried out single susceptibility measurements with a too large field in a zero-field-cooling experiment. The susceptibility is lower than expected for a non limiting case. After such a single measurement the disc traps flux while it did not before the measurement.

We perceive the limitation as caused by lack of superconducting electrons available for sustaining the expected moment. When, at the application of the field, all superconductive electrons are consumed by the reachable moment, the overflow on induced currents dies out. Bringing the applied field to zero at the end of the susceptibility measurement, the field decrease generates sample-moment which sense is opposite to that of the moment generated at the field increase.

The field decrease, at first, compensates the moment that was induced by the field increase. Then, it generates a resulting persistent sample-moment, being in case limited too.

The experiment generated in the disc a magnetic moment that persists at zero-field. The moment is of the same kind as that

generated during the susceptibility measurements.

What happens at the susceptibility measurement of such a sample? Putting the coil current "on" for a low applied field, the total sample moment is increased or decreased depending on the sense of the current in the coil. Changing the coil current from "off" to "on" also changes the field-gradient from zero to a certain value. The difference in gradient results in the difference in force on the balance. The latter force difference relates to the total sample moment at the measurement. The total moment is the algebraic sum of the moment induced by putting "on" the applied field at the susceptibility measurement and the moment that existed before.

Measuring the magnetic susceptibility following the Faraday technique, one has to take care of a possibly trapped persistent moment at the interpretation of the measured force.

---

$$\mu_s = v\,\chi_v\,B + \mu_p \qquad (17.1)$$

The introduction of the persistent moment $\mu_p$ in equation (14.1) yields constant sample susceptibility.

---

One can separate the two moment components carrying out two consecutive measurements but with different coil current sense. Changing the sense of the coil current changes the sense of the force that is due to the persistent moment. However, it does not change the sense of the force due to the freshly induced moment. Half the algebraic sum of the forces red at the two measurements is the force component related to the induced moment. Half the difference of the two forces is related to the moment that existed before the measurements.

The experiment indicates that the persistent moment, when unperturbed, is stable in orientation. Indeed, changing the coil current sense changes the gradient sense and changes the force sense. It means that the persistent moment reacts paramagnetic or diamagnetic depending on the sense of the field-gradient.

Concluding, we define here the volume-susceptibility as the sample-moment-density-per-tesla factor that relates the proportionality of the sample moment to an applied field-change. Such definition allows stating that: the magnetic susceptibility of a superconducting disc at low temperature and low magnetic field is diamagnetic and still can be considered as a sample constant.

## 18 Dimensional equations

The dimensional equations allow following qualitatively the logic of the physics at the path of an exposure.

The dimensional representation of the current intensity is capital I. The representation of a length is l. I/l express the dimensionality of a magnetic induction field. Indeed, the vector calculation of the field incorporates the current intensity of the field source. Also involved in the calculation is surfaces divided by volumes. A surface is a two dimensional entity, here represented by l times l or l square ($l^2$). The volume is a three dimensional entity represented by l cube ($l^3$). Just like in normal algebra, the division of l square by l cube is reciprocal l (1/l). When we combine the current-intensity with geometrical aspects it results in the dimensionality I/l for the magnetic induction field **B**.

A similar reasoning yields for the dimensionality of **G**, the gradient of the field, $I/l^2$.

The same reasoning holds for the magnetic moment. There is the current in the sample that results in the dimensionality I. The surface of the current loop yields $l^2$. The dimensionality of the moment is the product of both, I times $l^2$.

The dimensionality of the exerted force F is I $l^2$ $I/l^2$. The algebraic result of $l^2/l^2$ is unity. As we do not consider numeric values in the dimensional equations we state that $l^2/l^2$ is dimensionless and we omit it in the equations.

Consequently, the dimensionality of the force here is $I^2$. This expression is nothing else than the original acceptance the magnetic force is due to a current-current interaction.

The dimensionality analysis may be handy for not losing the track of the logic of physics while arguing some experimental facts; it does not indicate the technical implications your reasoning may have. Example, you need quite a different apparatus for weighing the mass equivalent of one thousand kilogram than one thousands of a kilogram.

## 19 Units

Quantitative analysis asks for numerical equations. In analyzing your experimental data you handle a number of units of a certain entity.

The newton is the force unit in the international system SI. The basic units in the SI system are the meter (m), kilogram (kg), second (s), ampere (A) etc. The newton is often expressed in the basic units: length, time and mass. In mechanics is the newton one kilogram meter per square second, $kg.m/s^2$. It relates to Newton's law: force equals mass (kg) times acceleration ($m/s^2$). The balance, calibrated in newton, is our instrument to measure the force at the susceptibility measurements.

The relation of the force with the magnetic interaction asks for quantitatively formulating our former dimensional expression: the force is proportional to the square of the current intensity.

In our susceptibility studies, we were able to keep the quantitative formulation rather simple: the force, expressed in newton, is the product of the magnetic sample moment times the gradient of the magnetic induction field ($F_s = \mu_s.G$), as formulated in equation (12.1). The coherent formulation is very handsome for the experimentalist. There is no proportionality factor different from 1 involved. The apparatus and the sample related entities are rather well uncoupled. The force as well as the gradient practically is only related with the apparatus. The moment concerns only the sample.

For the magnetic moment there exists a unit that carries a name, the Bohr magneton. It is used in the quantum theoretical approach of magnetism. However, in our context, the Bohr magneton is too small to be handsome. Equation (12.1) would need the huge extra proportionality factor of $1x10^{23}$.

We showed that the moment $\mu_s$ is related to the product: a current intensity times a surface. It is not illogical to fall back on the SI basic units and use “ampere square meter”, $A.m^2$, as the, for the moment nameless, practical unit for the magnetic sample moment.

As far as I know, there is no magnetic induction gradient unit that carries a name. G relates also to current intensities. However, when we would introduce the ampere, the SI basic unit for the current intensity, the unwished proportionality factor should be unavoidable. We are fairly content using for the gradient the tesla per meter ($T.m^{-1}$). The tesla is the name of a unit for the magnetic induction field. Using the tesla keeps the extra proportionality factor out of the force equation (12.1). Of course as we will discuss later, we can not avoid the extra proportionality factor. It will show up when we relate the tesla to the ampere.

## 20 The field-intensity

The magnetic induction field is the driving entity that generates magnetic moment in the sample material. In a technical context, a certain field relates to the generating currents in a solenoid by a value expressed in ampere-turns/meter. In a more abstract formulation, we relate the field **B** in a cylinder to the surface current density **J** ($A.m^{-1}$) expressed in ampere/meter. In the density formulation relates the word “ampere” to the total current intensity over one meter of length in the axial direction.

In paragraph 8, we saw that for a straight infinitely-long homogeneously wound solenoid the inside field relates univalent with the ampere-turns/meter value. The field inside the solenoid is everywhere the same and the current density along the solenoid is constant too.

In paragraph 9, we saw, for a solenoid simulating cylinder of limited length, that the relation **B** to **J** is not univalent. Indeed, the relation magnetic induction field versus surface current density depends on the geometry of the situation. In a rather long cylinder of finite length the axial field at the middle is about that calculated for the infinitely long case. At the end of the cylinder it is only half that.

In off axis locations at the end of the cylinder off axial field components show up. Although the surface current density is the same over the total length of the cylinder the magnetic induction field depends on the geometrical situation of the location that we have in mind.

For complex cases it is common use to introduce, for the location under attention, an “effective surface current density”, a kind of weighed average value.

In paragraph 2, the coil-coil experiment showed that the mathematical generalization of the results of Ampere’s work reproduce well the experimental force. The generalization takes care of the geometry of the situation. For a certain location in the cylinder, the calculation yields field and gradient values which accurately lead to the force. To calculate, we split up the surface current on the cylinder into small parts, the current elements. Each element contributes to the field. The local field is the sum of all contributions. The contributions are weighed. Example given, current elements that are farther off the considered location contribute less to the resultant field. A constant factor appears in the calculation. The calculation yields an accurate value for the magnetic induction field **B**(T) expressed in tesla.

To relate the field **B** in a unique way to an “effective surface current density” we return to the infinitely long cylinder. Indeed, when the field expression in tesla is proportional to the field-intensity expression in ampere per meter, then it also holds in the case that the field/surface-current-density relation is univalent. It holds for an infinitely long cylinder with its axis parallel to the direction of the field vector and the current sense adapted to the field sense.

---

$$\mathbf{B} = \mu_o \mathbf{H} \qquad (20.1)$$

Equation (20.1) expresses the magnetic induction field **B** as equal to the product of the proportionality factor $\mu_o$ times the field-intensity **H** the latter also being called the field-strength.

---

In the rationalized SI system is the numerical value of the field-intensity **H** the numerical value of the weighed average surface-current-density i.e. the numerical value of the surface current density that, for an infinitely long cylinder, results in the magnetic induction field. It consequently is expressed in $Am^{-1}$. As far as I know, there is no particular name for this field-intensity unit in the rationalized SI system.

---

$$\mathbf{H}_{12} = I_1 \frac{1}{4\pi} \oint_1 \frac{d\mathbf{l}_1 \times \mathbf{r}_{12}}{r_{12}^3} \qquad (20.2)$$

Equation (20.2) formulates the field-intensity in the rationalized SI system. The proportionality factor $(4\pi)^{-1}$ in the formulation equalizes the field-intensity value $\mathbf{H}_{12}$ with the effective surface current density. The effective surface current density (expressed in ampere per meter) is the surface current density **J** on an infinitely long cylinder carrying a homogeneous current layer on its curved surface which yields an identical $\mathbf{H}_{12}$. Consequently, the factor $\mu_o$ in equation (20.1) is $4\pi$ times the proportionality factor in equation (1.1).

The geometrical factor $\mathbf{r}_{12}/(r_{12})^3$ results, for an identical relative orientation of the field location versus the current element I**dl**, in a field decrease which is proportional to the square of the distance $r_{12}$.

---

The factor $\mu_o$ in (20.1) is the free space permeability. The term free space emphasizes that no other currents are involved in the problem than those we are considering here. The value of the proportionality factor is $\mu_o = 4\pi \times 10^{-7}$. It converts the field-intensity value into the magnetic induction field value. An effective current density 1 $A.m^{-1}$ relates to a magnetic induction field $4\pi \times 10^{-7}$ tesla. The practical unit tesla relates to a much larger field than the SI based unit $A.m^{-1}$. You need less tesla than ampere per meter to get the same effect.

I did no historical research on the origin of the factor but its numerical value suggests that it comes from the conversion from the earlier Gauss system into the rationalized SI system. As finishing touch, the definition of the ampere is chosen to confirm the value of $\mu_o$.

The calculation of **H** is identical to that of **B** exempt for a constant factor. One makes the same effort to calculate an accurate value for the "effective surface current density" than for calculating the magnetic induction field itself. In most cases personally I felt it as a slight detour, when you calculate at first **H** for arriving at **B**. However, at the discussion of current densities the use of **H** can be practical. In such cases the proportionality factor is not needed.

## 21 The mass susceptibility

We introduce the "mass susceptibility" because we present here some work we performed on a piece of Gadolinium Meta-phosphate glass [21].

Again we start looking for an answer to the question: what is susceptible to the applied magnetic induction field for creating a macroscopic sample moment? Knowing that each Gadolinium ion is paramagnetic, that the expected moment is proportional to the number of magnetically active ions and that the number of ions in the sample is proportional to the mass, we consider the mass of the sample as representative for the sample.

In our question becomes the sample mass the "what" that is susceptible to the field. In conclusion, we put the product of the sample mass times the susceptibility times the field equal to the magnetic moment of the sample. The susceptibility here is expressed as the moment per kilogram per tesla.

---

$$\mu_s = m_s \chi_m B \qquad (21.1)$$

Equation (21.1) expresses the magnetic moment of the sample $\mu_s$ as the product of the sample mass $m_s$ times the mass susceptibility $\chi_m$ times the field in the sample B.

---

Fig.21.1 reports on results of susceptibilities that all have been measured at the magnetic induction field 9.05 mT. The susceptibility is paramagnetic, about proportional to one over the temperature. It approximately follows Curie law.

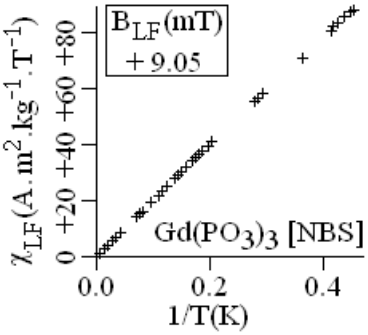


*Fig.21.1 shows the mass susceptibility of a Gadolinium Meta-phosphate glass sample versus reciprocal temperature as measured at the magnetic induction field 9.05 mT.*

The Curie law states that the susceptibility equals a "Curie-constant" divided by the temperature. The constant relates and to the number of paramagnetic centres in the sample and to the magnetic moment of each centre. In the sample, the paramagnetism is overwhelming. All other contributions to the moment are negligible.

---

$$\chi_m = C / T \qquad (21.2)$$

Equation (21.2) is the Curie law.
C is the Curie constant.
T the temperature.

---

The negligibility allows keeping the analysis simple. We accept that no magnetic impurities contaminate the glass. The final result indicates that the sample we measured was magnetically pure. We assume: i) that only Gd is magnetically active; ii) that all Gadolinium atoms are in the $Gd^{+3}$ state and iii) that each of them carries the same kind of paramagnetic centre. Quantum mechanics attributes to $Gd^{+3}$ an intrinsic magnetic moment that is the same for all $Gd^{+3}$ ions. The maximum component of the moment along a magnetic field is the product of the Lande factor times the total angular momentum factor times the Bohr magneton. We consider here the Bohr magneton as a basic unit for expressing the magnetic moment of a paramagnetic centre.

Only one Gadolinium atom occurs in each chemical $Gd(PO_3)_3$ group. The molecular weight of such group, one mol, contains Avogadro's number molecules. The number of molecules in a sample

is a fraction of Avogadro's number. The fraction is the sample mass divided by the molecular weight. The number of $Gd^{+3}$–ions in the sample is that mole fraction of Avogadro's number.

The number of Gd atoms in the glass sample we consider here is constant. It does not depend on the measurement. The quantum theory says that the intrinsic moment per Gd is constant too. One concludes that the average contribution, to the sample magnetic moment, depends on temperature.

## 22 The sample temperature

The susceptibility of our Gadolinium Meta-phosphate glass sample, shown in Fig.21.1, clearly is temperature dependent. A metallic helium cryostat, reported in Fig.22.1, allowed reaching temperatures between 2 and 300 K.

This paragraph contains data taken from my paper in Progress in Vacuum Microbalance Techniques, 2, 147 (1973) Publ. Heyden & Son [22].

The cryostat is fixed on the balance house in a way that the balance pan hangs freely in its tail.

For temperatures below 60 K we filled the upper refrigerant vessel with liquid nitrogen and the lower vessel with liquid helium. For temperatures higher than the boiling point of liquid helium at a normal atmospheric pressure (about 4.2 K) the boiled off gas flow over the sample room determinates the sample temperature.

In this situation is the cryostat not really a thermostat in which the temperature is kept precisely constant. However, the thermal evolution at the measurement is kept so slow that, in the case of pure lead, the superconductive transition at 7.193 K was detected with a precision of 0.01 K. Measurements carried out in a period of 15 years, yielded, within this precision, the same value.

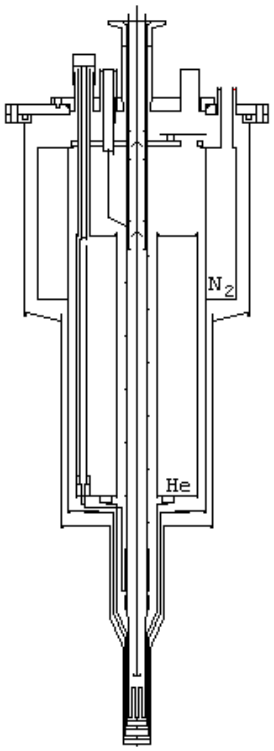


*Fig.22.1 shows an overview of our helium cryostat which allowed susceptibility measurements for temperatures between 2 and 300 K. For temperatures below 60 K the upper refrigerant vessel is filled with liquid nitrogen and the lower one with liquid helium. The boil off helium gas flow over the sample room determines the sample temperature. Pumping off He yielded temperatures below 4.2 K.*

For lower temperatures the helium was pumped off but still the gas flow over the sample room sets the temperature.

For temperatures higher than 60 K the lower refrigerant vessel is filled with liquid nitrogen. The controlled gas flow sets the temperature. In the region just below room temperature, the temperature of the vessel and sample room, after having been cooled by gas, evolves slowly enough for the measurements.

The sample-room temperature was measured with calibrated resistances, platinum for above and germanium for below 57 K. The reading of the thermometer depends on the magnetic induction field. In the set-up, the thermometer value used at the susceptibility measurements is the interpolation between the value red before the magnetic field has been turned on and that red after the magnetic field has been turned off.

In the temperature region below 5 K the sample temperature deviated from the thermometer readings. The deviation is due to the

limited thermal contact between sample and thermometer. Fig.13.2 shows the balance pan versus thermometer houses configuration.

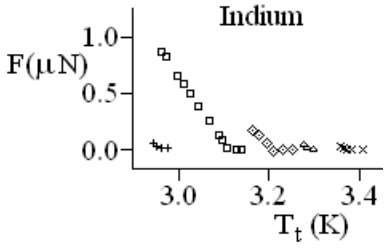


*Fig.22.2 shows the forces measured on an Indium disk at different thermometer temperatures and different coil currents.*

The measurement of known critical temperatures of low temperature superconductors, as reported in Fig.22.2, yielded corrections for better relating sample temperatures to the thermometer readings. We treat the Indium case as an example.

As it is much easier to adjust the coil current than the temperature, we measured the sample while its temperature rose slowly.

The thermometer reading of the transition temperature between the superconducting and the normal metal state is by 0.074 K higher than measured in good thermal contact. The sample is colder than the thermometer reading. We carried out similar experiments on other superconductors.

The introduction in the calculation program of a correction term for the temperature and a protocol for cooling the cryostat resulted in an error on the sample temperature less than 1%.

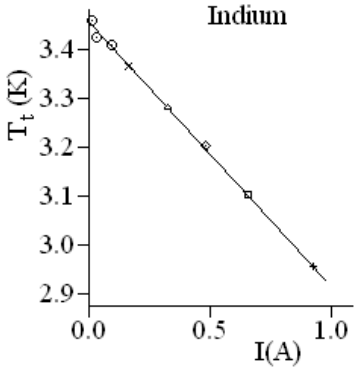


*Fig.22.3 reports on the thermometer readings, as obtained from Fig.22.2, the crossing of the slopes with the zero force line, versus the coil-current. The extrapolation to zero coil-current is the transition temperature of Indium.*

## 23 The sample location

The applied field and its gradient are independent on the magnetic moment of the sample. The applied field and gradient are calculated for locations in the neighbourhood of a solenoid. However, to know the precise field and gradient at the sample place, one has to know the precise sample/coil geometry.

In the case of the superconducting disc, we pointed out the sample location by matching the experimental force versus coil position curve to the calculated-field-times-gradient curve versus sample-position. Fig.15.1 shows the calculated curve. A precise matching was possible because the measurements were carried out at constant temperature.

We measured the susceptibility of the Gadolinium Meta-phosphate at different temperatures. Fig.21.1 shows that the mass susceptibility depends on temperature. The sample position in the cryostat depends also on temperature (Fig.13.2). The shrinking of the suspension wires of the balance pan, on cooling, displaced the sample at low temperatures from the room temperature position.

With the aid of a small ferromagnetic sample, we located the sample versus coil position at different temperatures [13]. The localization study allowed us to set up a protocol for cooling the cryostat in such a way that we were able to reproduce the sample position. The location related corrections for the field factors are incorporated in the computer programs.

## 24 The Brillouin centre

Fig.21.1 reports on the mass susceptibility of a Gadolinium Meta-phosphate glass sample versus reciprocal temperature. The paramagnetic susceptibility is about proportional to the inverse of the temperature. The proportionality is rigid in the Curie law. Looking closer, the susceptibility deviates from the Curie law. At low temperatures, the susceptibility is somewhat low compared to the rigid proportionality theory.

We explain the deviation in terms of the quantum theory of paramagnetism. A paramagnetic centre contains an intrinsic magnetic moment. In a magnetic induction field, the possible moment

components parallel to the field are quantized. The state wherein the moment is attracted by the magnet is energetically the more favourable. Less favourable are the states wherein the moment is pushed away from the magnet. The centres tend to become in the more energetically favourable state. However, the thermal "agitation" opposes to such tendency. Thermal agitation switches centres from one componential state into another state. The Brillouin function expresses for macroscopic systems the fraction of the theoretical intrinsic moment each centre has as a weighed average. The value of the Brillouin function [24] can be seen as an expression for the degree of polarization of the centres.

For high temperatures and low fields the thermal agitation wins over the ordering and the resulting macroscopic sample moment is low. In the "high-temperature/low-field" domain the Curie law holds. In the low-temperature/high-field domain the ordering wins and the sample moment is large. In an extreme case, all centres are in the lowest energetic state. The magnetic moment is saturated. It does not help anymore to lower the temperature or to increase the field for increasing the sample moment.

---

$$\mu_{ps} = N_G \, \mu_G \, \Psi (z)_G \qquad (24.1)$$

Equation (24.1) is the mathematical expression of the paramagnetic component to the sample moment $\mu_{ps}$ following the Brillouin theory for one kind of paramagnetic centre (here the $Gd^{3+}$ ion). The subscript G indicates that only $Gd^{3+}$ ions are considered.

$N_G$ is the total number of "Brillouin centres" in the sample.
$\mu_G$ is the maximum component along the magnetic induction field of the intrinsic moment of one single centre.
$\Psi (z)_G$ is the Brillouin function with z as the argument.

$$z = (\mu_G \, B)/(k \, T) \qquad (24.2)$$

k is the Boltzmann constant.
T is the sample temperature.

---

The Brillouin function describes quantitatively the order disorder competition result. The Greek letter $\Psi(z)$ refers to the function. Its argument z is a dimensionless fraction, the ratio of two energies. It is the quotient of the energy related to the centre-moment in the field divided by the energy related to the temperature. The numerator in the fraction z relates to the energy that the intrinsic centre-moment would release when, in maximum attracting position, it would be brought from a zero field into the final one. In the denominator figures the product of the Boltzmann constant k times the temperature.

The Brillouin function approaches unity for large z values. Unity expresses maximum polarization of the centres. One then says that the sample is magnetically saturated.

In the Gadolinium Meta-phosphate glass, considered in Fig.21.1, the susceptibilities at low temperatures deviate from the Curie law. We interpret the deviation as the expression of the onset of saturation. We attribute the temperature dependency mainly to the presence of "Brillouin" centres. We define a Brillouin centre as an ensemble of isolated paramagnetic states the effect of which results in an average paramagnetic moment per centre that is given by the product of its intrinsic related moment times the Brillouin function.

The Gadolinium Meta-phosphate glass is a thankful subject. On the one hand, the concentration on paramagnetic $Gd^{3+}$-ions is rather small indicating that interactions between paramagnetic centres will be small. On the other hand, the concentration is large enough so that the paramagnetic contribution prevails.

We can neglect the atomic diamagnetism. The glass we got from Mangum NBS (USA) was magnetically pure. We have not to take magnetic contaminations in account.

The favourable situation allows a rather precise analysis of the paramagnetism.
From the point of view of the Brillouin theory is the sample moment the product of the number of Brillouin centres in the sample times the intrinsic moment of the centre times the Brillouin polarization degree.
From the point of view of the magnetic susceptibility is the sample moment the product of the sample mass times the mass susceptibility times the magnetic induction field.

Combining both points of view relates the susceptibility to the Brillouin function. The latter function is dependent on the ratio, obtained by dividing the magnetic induction field by the temperature. Consequently, the susceptibility depends on both, the magnetic induction field and the temperature.

We calculated back the experimentally observed magnetic sample moments from the reported susceptibilities, using sample-mass, applied field and temperature. The experimental magnetic moment does not depend on an interpretation of the sample magnetism. It is the result off a measurement that is carried out with a sample independent apparatus.

When the sample moment could be attributed to Brillouin centres, then the quotient, the moment divided by the Brillouin function value, would be a constant, related with the number of centres.

The applied magnetic induction field, used as the driving entity in the argument of the Brillouin function for the Gadolinium Meta-Phosphate glass sample, results in a concentration on Gd ions that slightly depends on the sample temperature.

As the number of Gd atoms does not change with temperature, the temperature dependency indicates that the present interpreting model is not complete.

## 25 The Weiss field

The differences in the calculated Gd ion concentration indicate that we miss a parameter in the understanding of the physical basis of the magnetic susceptibility. The use of the applied magnetic induction field as the driving entity in the Brillouin function results in a slight difference between experiment and theory. We consider here a correction to the applied field. The correction is attributed to the degree of saturation of the sample moment.

Weiss introduced the idea of an intern magnetic field which is proportional to the magnetization of the sample. In other words, the magnetic induction field that governs the sample is the sum field, the sum of the applied field together with an intern generated extra field that is attributed to the presence of the magnetic centres. We therefore

put the Weiss magnetic induction field equal to a proportionality constant times the Brillouin function.

We used the total magnetic induction field, the sum field, as the driving entity in the argument of the Brillouin function. We analysed the Gadolinium Meta-Phosphate glass sample results, reported in Fig.21.1, in that way. We observed that a constant fitted Bo value results in a constant calculated concentration of Gd ions. The introduction of the Weiss field allowed to obtain an intern consistent model.

---

$$\mathbf{B}s = \mathbf{B}a + \mathbf{B}_W \qquad (25.1)$$

Equation (25.1) expresses a magnetic induction field **B**s that governs the sample as the sum of an applied and a Weiss field.
**B**a is the applied magnetic induction field.
$\mathbf{B}_w$ is the Weiss field and we approximates it by:

$$\mathbf{B}_W = Bo\ \Psi\ (z) \qquad (25.2)$$

---

The Gd concentration, as derived from the fitting, differs by a few percent from the value indicated by the chemical formula unit. We therefore introduce in our analysis $Gd_x(PO_3)_3$ as the chemical constitution of our glass sample.

In our Weiss field approach we separate the field and temperature independent terms from the degree of polarization. Bo is the field generated by full saturated magnetization of the sample. For analytical convenience we split it up in two terms, x the relative Gadolinium concentration and Bf. The Bo value is the product of x times Bf.

For the Gadolinium Meta-Phosphate glass sample the best fit for Bf has a negative value. Bf incorporates a sample geometry-related factor. The minus sign indicates that the Weiss field, in the example, reduces the applied field.

The situation about the magnetic moment is clear. The experimental value for the moment depends only on the “well known” apparatus. The situation about the susceptibility can be considered as

less clear. To which of the two fields, the applied field or the sum field, is the sample susceptible?

For Brillouin centres in a high temperature region, the Curie-Weiss law approximates well the temperature dependency of the applied field related susceptibility, here referred to by the apparent susceptibility. The Curie-Weiss law is an adaptation of the Curie law in which latter the effect of the Weiss field is expressed as a temperature component. The law states that the susceptibility equals a "Curie-constant" divided by the temperature minus the Weiss constant.

---

$$\chi = C/(T - \theta) \qquad (25.3)$$

Equation (25.3) formulates the Curie-Weiss law expressing the paramagnetic susceptibility.
C is the Curie constant.
T is the temperature.
The parameter $\theta$ , the Weiss constant, practically is constant in the temperature region wherein the Weiss field is and a small fraction of the applied field and inversely proportional to the temperature.

---

The susceptibility which is related with the sum-field Brillouin function in our case indicates the magnetization of the $Gd^{+3}$ ions follows precisely the Brillouin theory.

As the magnetic moment is beyond question the two susceptibilities are related to each other. For both, the product of the susceptibility times the related field is the same.

## 26 The magic angle

We discuss here the physics behind the Weiss field as the effect of a long range magnetic dipole interaction between Brillouin centres.

The model starts with our basic primitive unit, the circular closed electric circuit in free space. In the circuit flows an electric steady-state current. The unit simulates the Brillouin-centre as field

generator. We refer to the field by a magnetic lines of force pattern. Fig.26.1 shows a field line pattern in the mid plane of the unit ring.

The Brillouin centre feels a rather homogeneous applied field. The field tends polarizing each Brillouin-centre. In a magnetically fully polarized sample, all Brillouin-centres orient the direction and sense of their own field, at their magnetic symmetry axis, in the direction and sense of the applied field.

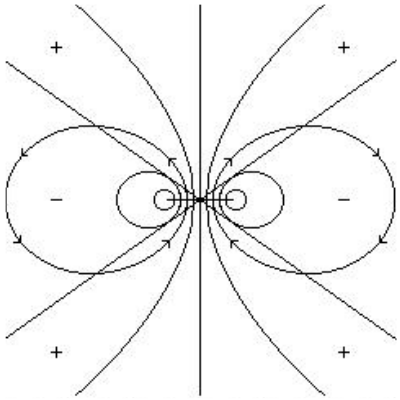


*Fig.26.1 shows field lines of a Brillouin-centre. At magnetic saturation is the direction and sense of the centre's own field at its symmetry axis the same as those of the applied field.*

The oriented Brillouin-centre generates its own magnetic induction field. We now follow the path of a field line. To fix the idea we consider, in Fig.26.1, the closed loop marked with arrow points which indicate the field sense. We follow the journey starting inside the ring in the plane of the current ring. In the plane of the ring is the centre's own field parallel with the applied field. The sum of the fields is larger than each part. Leaving the ring plane, the own field is not anymore parallel to the applied field, but still has a parallel component. Following the path of the field line we observe a turning point. Here the centre's own field starts contributing to the applied field with an anti-parallel component. The component has the same direction as the applied field but has an opposite sense. In other words, in part of the loop the centre field increases the applied field, while in the other part it decreases the applied field.

How one Brillouin-centre's field influences the field felt by another one? In other words, what is the field contribution of one Brillouin-centre, called the source, at the location of the other centre, called the target. The contribution depends on the source target location geometry. It depends on the angle between the applied field direction and the direction of the target location. In the case the radius of the

centre can be considered negligible; the field pattern around the source is a dipole one.

The Regions around the source wherein the applied field increases are referred to by a plus sign, indicating addition. The region around the source wherein the applied field decreases is marked by a minus sign, indicating subtraction.

We focus on a field line loop of the source centre. For all loops, starting inside the centre, its contribution to the applied field switches from “increasing” to “decreasing”. The switch locates at the extremes, of the loop, in the applied field direction. For larger distances, all turning points lie on a straight line. The line passes the middle of the source.

For fixing the idea, we consider the right upper quadrant of Fig.26.1. It shows that for a target distance about five times the unit radius, the statement practically holds. However, when the target Brillouin-centre is closer to the source, the statement does not hold anymore. The smallest loop drawn in Fig.26.1 even does not touch the line. However, the straight line is a rather good border line between the plus and minus regions in the case of a dilute Brillouin-centre system. Dilute means here that the centres are not very close to each other.

Spinning the sample about the angle the borderline makes with the applied field improves in some cases the resolution in magnetic resonance spectroscopy. May be, wondering the improvement is at the origin of the adjective “magic”. Time averaging of the plus with the minus effect results in the resolution improvement.

## 27 The spheroid

The Weiss field model takes in account the joint influence of all other Brillouin centres in the sample on each of them separately.

The basic step is the interaction between two centres. The symmetry of the Brillouin-centre’s field pattern involves that, for a distant pair of fully polarized centres, the influence of each of them on the other is the same. We take one centre as the target and all the others as sources.

We have to integrate the effect off all source centres in the sample on one target centre. We have to do it for every place in the sample. To keep the calculations relatively simple, we consider simple sample geometries, spheroids. The spheroid is derived from a sphere by a uniaxial compression or elongation.

The spheroid allows different shapes, from the longer slender prolate one, over the bulbous sphere to the short stout oblate spheroid. Different spheroids allow simulating different sample shapes.

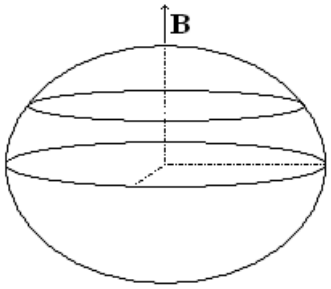


*Fig.27.1 outlines an oblate spheroid with its rotational symmetry semi-axis along the applied magnetic induction field.*

The spheroid has rotational symmetry. The rotational symmetry semi-axis lies along the applied magnetic induction field. At the calculation of the Weiss contribution to the applied field we avoid the impossible task of taking the Brillouin centres one by one. We group them in small volume elements. The magnetic moment of such a group is the local magnetization times the elementary volume, dv. Because we here add the effect of volumes, we use as definition of magnetization the magnetic moment per unit volume. The magnetization here is the number density, the number of $Gd^{3+}$ ions per unit volume, times the Brillouin average magnetic moment per Gd ion. In our calculations we assume that the Brillouin-centre distribution is homogeneous.

The field on our target by distant Brillouin centres is the difference of the effect of centres, located in one region, and those, located in the other region. The difference is function of the shape of the spheroid. It depends on the ratio of the rotational-symmetry semi-axis of the spheroid versus the radius. The radius is that of the equatorial circle in the plane perpendicular to the applied field vector. The function value is larger, more positive, for the prolate spheroid than for the sphere. It is less for the oblate spheroid. The thinner the spheroid the smaller the function value is.

On its turn the number density introduces a difficulty in calculating the Weiss field at the location of our target Brillouin centre. At which distance from the target have we to stop the continuously smeared out influence of distant Brillouin centres? Close to the target the dipole approximation does not hold anymore. We correct for the non dipole character introducing in the model a small magnetically inert region about the target centre.

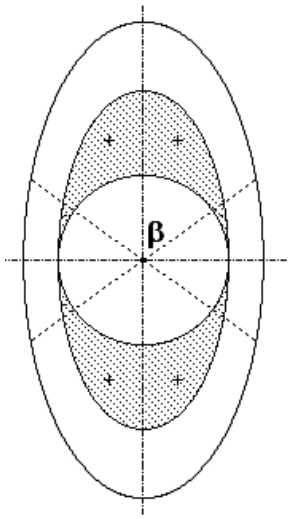


*Fig.27.2 shows a prolate spheroid shaped sample. A spherical magnetic inert inner region encloses the target centre which situates at the middle of the spheroid. Only the dotted regions contribute effectively to the Weiss field. The magic angle separates the plus and minus regions.*

Once again, for keeping the calculations simple, we consider the inner inert region having a spheroid shape. The introduction of the inert region results in a Weiss field that depends on the difference in shape of the sample and that of the inner region.

As an example we consider a prolate spheroid shaped sample, referred to in Fig.27.2. The long semi-axis is in the direction of the applied field. The target Brillouin centre is at the middle of the spheroid surrounded by a spherical inert region. For the analysis, we consider two internal regions. The first one, a circle represents the small spherical magnetically inert inner region. As there are no Brillouin centres in this region, it does not contribute to the Weiss field. The second internal region we consider has the same shape as the sample. Although it is smaller it has the same ratio semi-axis versus radius as the sample spheroid. Its radius is the same as the radius of the inert inner sphere. As the shape of the prolate inner region is the same as the shape of the sample simulating region, the plus and minus contribution cancel each other. From the region

between the two prolate spheroids there is no net contribution to the Weiss field.

When Brillouin centres are homogeneously distributed in a spheroid, only a small fraction of the source centres is magnetically active in generating an intern Weiss field. For the prolate spheroid, as indicated in Fig.27.2, the plus region is more important. The Weiss field in the prolate spheroid adds to the applied field. By the same reasoning, for an oblate spheroid the minus region is the more important and the Weiss field reduces the applied field.

When the Brillouin centres are homogeneously distributed in the sample, the spheroid is a special case in the sense that, once its shape and orientation specified, the Weiss field is the same all over the volume of the sample. The Weiss field is homogeneous in the sample. It makes the calculations simpler as all centres feel the same magnetic induction field. The argument in the Brillouin function is the same for all centres. Consequently, the magnetization is homogeneous in the sample.

The calculations allow stating that when the longest semi-axis is along the applied field direction the magnetic induction field at the target is larger than the applied one. When the longest semi-axis is perpendicular to the applied field direction the magnetic induction field at the target is lower than the applied one.

The Weiss field is proportional to the magnetization but the proportionality constant can be positive or negative.

## 28 The Gadolinium experiment facing the Weiss model

The Weiss model, as exposed above, is relatively simple. The applied field was homogeneous. The paramagnetic centre distribution in the sample is homogeneous. The sample has a spheroid shape, resulting in a homogeneous Weiss field and consequently in a homogeneous magnetization.

The homogeneity has as a consequence that for each case the entities field and magnetization are univalent. They have the same value all over the sample volume. The question rises: how good fit our real sample in this idealized model?

At the time we measured the $Gd(PO_3)_3$ glass sample we were not aware of the possible impact of the Weiss field. The laboratory notes do not mention the geometry of the sample. Neither is the sample orientation indicated. Nevertheless we submitted the susceptibility data to the Weiss analysis for constant fitting parameter x and Bf.

For the Gadolinium Meta-Phosphate glass sample the best fit resulted in a relative Gd concentration x equal to 1.0395 and Bf equal to -0.066. The precision on the measurements find its expression in the standard relative deviation, 0.66 %. From the point of view of the statistical analysis, we estimate the uncertainty on the relative Gd concentration x on +/- 0.15%, which is about the standard error of the mean.

The fitting result concerns all measurements carried out at temperatures below 25 K. The upper limit is somewhat arbitrarily but it answers the purpose to select the more precise data related to the larger paramagnetic susceptibilities.

The precision of the analysis indicates that it is meaningful to use average values for sample field and magnetization. We therefore accept that the analysis respects the general trend.

The fitting parameter $Bf < 0$ indicates that the longest sample dimension was perpendicular to the applied field direction. This is plausible as the sample laid down on the bottom of the balance pan and the field direction stands perpendicular to the bottom plane of the pan. On the assumption that the sample was platelet like, an oblate spheroid approximates best the geometry and is numerically acceptable. It indicates that, at the lowest measuring temperature, the magnetization reduces relatively the applied magnetic induction field by 6 per cent.

The result of the analysis asks for reproducing the $Gd(PO_3)_3$ glass study in a proper way. The sample should have a spheroid shape. It should be measured for different orientations in the applied magnetic induction field. Such spheroid sample can be considered as a one single geometrically well known homogeneous cluster. Cluster is an expression used in the terminology of the magic angle spinning high resolution nuclear magnetic resonance analysis. An orientation dependent susceptibility study may yield information about the best approach to the shape of the inner inert field region. We chose for a

sphere on the meagre argument that vitreous material can be considered as isotropic. Whatever the shape, it should at least allow for a plus as well as for a minus sign for the magnetic dipole interaction effect. How well the final version of the shape will allow fitting the data, it still remains an approximate simulation of the real magnetic ion distribution about the targets.

Cautious as we are, we always keep in mind that, even for well fitted data, the result of a susceptibility study only indicates what physically is allowed. It is prudent to be aware that other possibilities may exist.

## 29 The relative susceptibility

The introduction of the Weiss field created a drastically changed situation. For the sample magnetization generating field, we switched over from a sample independent applied magnetic induction field to the magnetization dependent "sample field". Nevertheless, the basic principle, the current-current interaction, remains the same. The magnet, by the applied field, generates net currents in the sample by orienting moments of the paramagnetic centres. These net currents on their turn, by the Weiss field, also generate net currents in the sample.

---

$$\mathbf{B}s = \mathbf{B}a + \mathbf{B}_W = \mu_o\,(\mathbf{H}a + \mathbf{H}_w) \qquad (29.1)$$

Equation (29.1) expresses equation (25.1) in another way. The magnetic induction field that governs the magnetization of the sample is the sum of the applied- and the Weiss-field.

Weiss introduced the field-intensity $\mathbf{H}_w$ as proportional to the magnetization **M**. It allows expressing the sample magnetic induction field by:

$$\mathbf{B}s = \mu_o\,(\mathbf{H}a \pm \alpha\mathbf{M}) = \mu_o\,\mathbf{H}a\,(1 + \chi_r) \qquad (29.2)$$

Herein is $\chi_r$ the relative magnetic susceptibility.

$$\chi_r = \alpha\,\mathbf{M} / \mathbf{H}a \qquad (29.3)$$

---

The Weiss field-intensity, as the applied field-intensity, is for any location in the sample the expression of an “effective surface current density”. The field is proportional to the magnetization. The proportionality factor $\alpha$ in equation (29.2) is often omitted in literature. Although the omitting in certain cases is defensible in general it is not.

The relative susceptibility $\chi_r$, the Weiss field divided by the applied field, expresses the current-current interaction is susceptible to the applied field-intensity for generating a difference in field-intensity due to the sample magnetization.

Here again the word susceptibility is used. The word “susceptibility” behaves somewhat like the word “beauty”. The meaning is different when different situations are considered. The meaning of the word “beauty” depends on the object to which it is related, as architecture, or flowers, or even mathematical equations. So the meaning of the word susceptibility is different when used in different contexts. A difference between the notion of “susceptibility” and “beauty” is that in the susceptibility case, once the situation is defined then the effect can be treated quantitatively, while, as I feel about, this is not the case when “beauty” is considered.

The relative susceptibility as defined here differs from the mass susceptibility treated in Fig.21.1. In our $Gd(PO_3)_3$ glass case is the former negative while the latter is quite strongly positive. A strong magnetization can, in certain cases, reduces the effect of the applied magnetic induction field. The reduction depends on the sample/field geometry.

## 30 The Curie temperature

A quality of a good physical model is that it not only gives an interpretation to your data but also suggests new experiments.

The Weiss model interprets the fine tuning of the sample magnetization as observed in our susceptibility data as a pure long-range magnetic dipole-dipole interaction effect. In the model the sample magnetization increases or reduces the effect of the applied magnetic induction field.

What happens when there is no applied field? No applied field means no imposed direction. In the case our model nevertheless would hold in such drastically changed situation, a Weiss field should be the only contribution to the total sample magnetic induction field.

What foresees the Brillouin model? Using only the Weiss field in the argument of the function, putting the applied field value zero, allows solutions below a critical temperature.
The pure magnetic dipole interaction model suggests the appearance of spontaneous magnetization below the critical temperature. That critical temperature, the Curie temperature is the highest transition temperature separating the high temperature region in which the sample is paramagnetic from the low temperature region in which the sample is ferromagnetic.

The temperature of the onset of ferromagnetism can easily be derived for small values of the argument of the Brillouin function. For small values of $z = \mu_G \mathbf{B}_W/kT$ one can eliminate the Weiss field out of the $\mathbf{B}_W = Bo\ \Psi(z)$ equation that determines the Weiss field. It results in a Curie temperature being proportional to the product of the sample material saturation magnetization times the maximum moment component of the Brillouin centre times the sample form factor. We consider a sample magnetization along the longest dimension of a prolate spheroid as this spheroid has a positive form factor.

Fig.30.1 reports on calculated relative magnetization data for a $Gd(PO_3)_3$ glass prolate spheroid that is two times longer than large. In the case the inert inner region is spherical; the Curie temperature is 0.13 K.

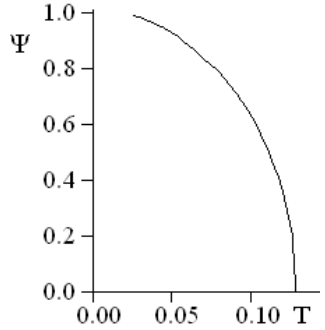


*Fig.30.1 shows the relative magnetization that, without applied field following a Weiss model, can appear in a prolate spheroid sample of $Gd(PO_3)_3$ glass. The data results from a calculation for a prolate spheroid that is two times longer than large.*

Following the theory, the Curie temperature should depend on the geometry of the sample. However, the theory relates to a homogenous magnetization of the sample. In practice fluctuations may occur resulting from non-homogeneities in the Gadolinium distribution. The sample then may be considered as build up of many sub-clusters of different shape. It consequently is not excluded that magnetization relates to ferromagnetic domains. Whatever, we expect indications for the occurrence of ferromagnetism. The upper limit for dipole-dipole interaction ferromagnetism in Gadolinium Meta-phosphate, 0.8 K, is a temperature beyond the reach of our apparatus.

Our calculation result, ferromagnetism as the consequence of a pure magnetic dipole interaction model, surprised me. Indeed, textbooks I was aware of describe the correct nature of the ferromagnetic coupling as the exchange coupling. However, the pure magnetic dipole interaction model can afford a Curie temperature above room temperature. In the dipole-dipole model, the main contribution must come from a very large maximum moment component per Brillouin centre. The exchange coupling comes here into play for building up very large moments by the much smaller atomic once.

## 31 Exchange coupling

The Weiss field model is a long range model. The dipole-dipole interaction is felt all over the sample. The exchange coupling, at variance, can be considered basically as a short range interaction. It is a quantum mechanical expression of the interaction between the spins of neighbouring electrons**.**

A lucky effect of the exchange interaction is Hund's rule. It states that electrons in the incomplete f-shell of the gadolinium atom combine to yield the large permanent magnetic moment for the ion. The half filled shell contains seven electrons whose spins all combine ferromagnetically.

The Gadolinium Meta-phosphate glass is special. On the one hand it is a relatively dilute system. There is on the average only one Gd of the thirteen atoms that constitute the chemical formula unit. On the other hand, Gd has a relative large magnetic moment. The total angular momentum is seven times larger than that of one unpaired

electron. The large moment allowed us to detect dipole-dipole interaction in the relatively dilute system.

The exchange interaction between electrons of different atoms leans on the overlap of their wave functions. The overlap falls off very rapidly with distance. That is why we refer to the exchange interaction as basically a short range interaction.
In $Gd(PO_3)_3$ the Gd ions are quite a distance apart. However, the f-electrons of a Gd ion can couple by exchange with electrons, of intermediate non-magnetic ions, which then couple with the f-electrons of a second Gd ion. The mechanism is known as super-exchange. In what follows we analyse our susceptibility data, as referred to in Fig.21.1, without taking in account the long range dipole-dipole interaction. At low temperatures the susceptibilities are low compared to the (Weiss-field-less) Brillouin expectation value. We therefore consider the exchange coupling to be antiferromagnetic. To fit our data closely the antiferromagnetic interaction must be temperature dependent. To keep the analysis simple, we accept that each Gd ion is or isolated or belongs to a pair. In a pair the magnetic moments are fully compensated by each other. The isolated Gd ions behave as expected by the Brillouin law. The concentration on isolated Gd ions depends on temperature. At low temperatures the non magnetic pairs are energetically favoured. We attributed to the pairs an effective antiferromagnetic coupling energy. The energy is, by the Boltzmann constant, related to a reference temperature, here expressed by Ta. The coupling energy competes with the thermal agitation.

For high temperatures the thermal agitation wins over the pairing, resulting in a macroscopic sample moment related to the active Brillouin centres. Lowering the temperature decreases exponentially the remaining concentration on magnetically active Brillouin centres.

For the Gadolinium Meta-phosphate glass sample the best fit on this pair forming model resulted in 1.03918 for the Gd concentration and 0.1338 K for the reference temperature, the expression of the coupling energy. The standard relative deviation of 0.67 % indicates the precision on the measurements carried out at temperatures below 25 K. At the lowest measuring temperature, following the pair model, about 6 % of the Gd ions should occur in pairs.

The Gd concentrations resulting from the Weiss- and the pair-model analysis are, to a high precision, the same. Also the standard relative deviations are the same. Our apparatus is not precise enough

to differentiate, for the susceptibility data used, between the Weiss- and the pair-model.

Measuring the susceptibility of a prolate spheroid $Gd(PO_3)_3$ glass sample, the magic angle along the applied field direction, can, in principle, indicate whether or not short range antiferromagnetic coupling does occur. Susceptibility measurements at temperatures below the region spanned by our apparatus can indicate whether the sample becomes ferromagnetic or looses drastically its magnetic moment.

I like to comment here on the need of exchange coupling to explain, from the viewpoint of the Weiss field model, the Curie point of ferromagnetic materials. In the Weiss dipole-dipole interacting model is the Curie point proportional to the magnetization at saturation times the maximum component of the intrinsic moment of the Brillouin centre times a form-factor. For the latter factor, we consider that of a prolate spheroid sample two times longer than large. We calculate the magnetization at saturation of iron in our example case.

The Curie point of pure iron, following the literature, is 1043 K. For fixing the idea we consider the hypothetical case all atoms have five uncompensated ferromagnetically coupled electrons. Taking in account the mass density, the molecular weight, the number of Avogadro, the maximum moment component per atom, we obtain for the magnetization at saturation a value that is eleven times larger than that for the Gadolinium Meta-phosphate. The high saturation magnetization clearly does not suffice for reaching the experimental Curie point. The mayor contribution increasing the point then has to come from the intrinsic moment of the Brillouin centre. Here the exchange coupling comes into play. The magnetic moment of neighbouring iron atoms are ferromagnetically coupled by exchange interaction. The interaction energy has to be high, to resist the high temperatures. When we consider a group of a certain number of iron atoms as one single Brillouin centre, how many iron atoms on the average need such group for explaining the Curie point? The number of iron atoms per group, calculated from the Curie point of iron for the prolate spheroid considered, is 842. Such a number of iron atoms take the volume $(2.1\ nm)^3$. Is the high Curie temperature a nanometre size effect?

Grouping the iron atoms does not change the saturation magnetization. Indeed, the moment per centre is larger but the number of Brillouin centres is lower.

The Weiss dipole-dipole interacting model is certainly not the whole story. The model yields a homogeneous magnetization for a homogeneous Brillouin centre distribution in the sample. A piece of pure iron at room temperature not exposed to an applied field does not show the effect of the homogeneous magnetization. The magnetic dipole-dipole interaction model considers only shapes but not dimensions. In a sample that is not subjected to an applied field, Weiss assumed that magnetized domains may reorient themselves in the field of neighbouring domains, reducing strongly the long range dipole effect.

The dipole-dipole model is in severing crunch when we consider the magnetically inert inner region about one Brillouin centre. In the Gadolinium Meta-phosphate case the distance between two centres can be considered as large compared to the own centre dimension. This is certainly not the case in the iron related story. Moreover, for fitting the Brillouin theory we need the moment of about thousand atoms to be ferromagnetically exchange coupled. Why should it stop at thousand? The three dimensional chained mail coupling can extend over a domain that contains hundred times more iron atoms.

I only crudely discussed the exchange interaction. The work I did in the field of short distance interaction is limited. However, we need the basics on ferromagnetism for explaining the magnetic field dependency of the energizing current in an electro-magnet. We now discuss the electromagnet in our set-up for measuring magnetic susceptibilities.

## 32 The electromagnet

In paragraph 7 we discussed two basic configurations for simulating sample/field situations. The first of the two concerned a sample/coil configuration that we considered in paragraph 13. We now pass on to the second basic configuration. Herein is the magnetic induction field direction at the sample horizontal. The electromagnet generates such field. Fig.32.1 outlines the magnet. The use of the electro-magnet gave some advantages over that of the coil.

Thanks to the presence of iron, the electromagnet allowed susceptibility measurements at much higher induction fields. The mounting on a turntable, allowed setting the magnetic induction field direction at different angles in a horizontal plane about the sample in the tail of the cryostat.

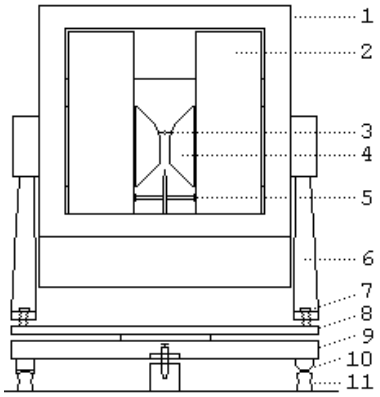


*Fig.32.1 outlines the front view of the magnet. The main items are: 1)the yoke, 2) the coils, 3) a viewer, 4) the pole shoes, 5)a centre rod, 6) the support, 7) the screws, 8) the turntable, 9) the carriage, 10) the wheels and 11) the rails.*

The better possibilities at measuring susceptibilities with the aid of the electro-magnet ask their price. The manipulations became much more complex. I'll save you the cumbersome evolution in time.

At variance with the coil, the magnet was too heavy to be fixed on the cryostat. It was loaded on a carriage. We rolled it back on rails for changing the sample. Crowns on the wheels, on one side, provide lateral guidance. The replacing of the magnet was reproducible to a fraction of a millimetre. After the sample was put on the balance pan, the magnet was rolled in place on a fixed position, locked by a pin. We then positioned the balance house, the free hanging pan above the centre rod. The centre rod, fixed between the pair of coils, indicates the central axis about which the magnet turns. The height of the magnet was adjusted using the screws on the supports. The vertical positioning of the magnet brought the pan in the target area of the viewer. Again, the position was adjusted to a fraction of a millimetre. For mounting the cryostat, the magnet was driven back. The cryostat in place, the magnet is rolled forward again. The tail of the cryostat was centred between the pole shoes, once more to a fraction of a millimetre. The turntable allowed the magnet to turn about the tail of the cryostat. Hampered by the leads the angle was limited to about 180 degrees. The yoke kept the stray field to an acceptable level.

The pole shoes of the magnet also underwent evolution. At the beginning, the gap between the shoes was 1.5 inch. In the final version, when the skill of making cryostats had been improved, the gap between them was reduced to 1 inch. The tapered pole-pieces started being cones with a round base. After milling, their shape resulted in a gap that slightly widens under a constant angle in the neighbourhood of the sample. We believe that the latter shape increased somewhat the reproducibility of the susceptibility measurements for certain magnetic induction fields.

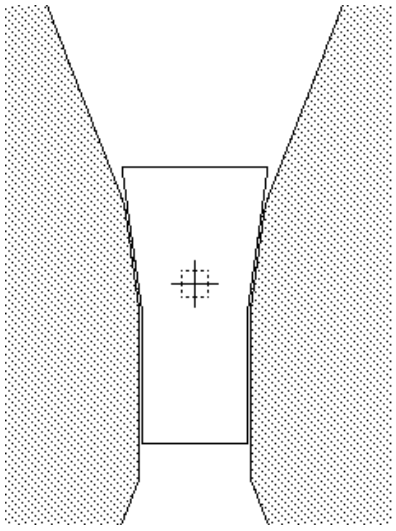

*Fig.32.2 shows the outline of the mid-plane section of the pole shoes. The gap slightly widens with height in the neighbourhood of the sample. A Plexiglas piece, shaped to fit closely the pole shoes' gap, allows positioning the viewer. On its turn, the viewer allows vertical positioning of the magnet to a fraction of a milli-metre.*

A piece of Plexiglas has been shaped to fit closely the pole shoes' gap. We used it for positioning the viewer. We placed the Plexiglas piece between the pole shoes of the magnet in backward position. The reference cross drawn on the Plexiglas piece was highly reproducibly located in the gap. The picture of the cross was focussed on the ground glass of the viewer. The sharpness of the picture indicated the sample/viewer distance. The viewer was clamped horizontally between the coils of the magnet at the height of the sample pan. The viewer position aimed at was realized when the picture of the cross on the Plexiglas co-insides with the cross etched on the ground glass.

The Plexiglas removed and the magnet replaced, we adjusted the height of the magnet by bringing the picture of the pan at the cross of the viewer's ground glass.

## 33 The force/moment relation at the electromagnet

The electro magnet generated at the sample location a magnetic induction field which direction is perpendicular to the sensibility direction of the balance. The situation relates to the second basic magnet configuration, discussed in paragraph 7. The electromagnet configuration is different from the iron-less coil one. The latter one, the first basic magnet configuration, we used for measuring the superconducting lead.
At variance with the situation in the first configuration, in the second one the force on a current ring is not due to the smaller radial component of the magnetic induction field. In our case of the electro magnet the major component of the field causes the force. However, here also a homogeneous field do not exerts force on the ring. For a force signal, we need a gradient. We discuss the situation on Fig.33.1.

The horizontal magnetic induction field **B** works on a vertically positioned flat circular electric current circuit, our primitive unit in our model. Only the horizontal components of the currents in the ring feel a force in the vertical direction, the sensitivity direction of the balance. When the field at the top location of the ring is smaller than at the bottom, the force at the top will be less than at the bottom. When the gradient of the field can be considered as constant over the ring, then the force on the balance can be calculated to be equal to the current intensity times the surface of the ring times the gradient of the field. This formulation, related to the field at the electromagnet, is exactly the same as that stated for the iron-less coil configuration. For the electromagnet we also are in search for an honourable compromise between homogeneity and non homogeneity.

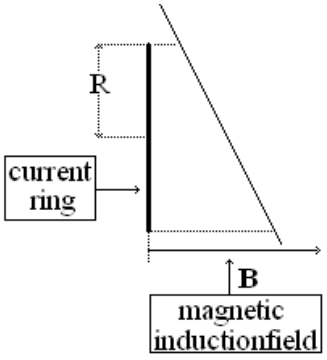


*Fig.33.1 outlines the magnetic induction field-gradient at a ring current. In the figure is the ring perpendicular to the drawing plane. The larger induction field at the lower part of the ring generates the higher force.*

## 34 Field measuring

In search for an honourable compromise between homogeneity and non homogeneity, we start discussing the way to know the magnetic induction field. The huge amount of ferromagnetic material in the electromagnet makes the field calculation too complex to be practical. The precision of the calculating result was nothing to be desired. So we measured the field in relation to the coil-current.

At variance with the simple situation reported in paragraph 13, the value of the electromagnet's induction field at the sample location was not univalent related to the coil current. The advantage offered by the electromagnet (to allow higher fields) has a certain drawback. The field depends on the history of the magnetization. We studied the field/coil-current relation. It allowed us to optimize the reproducibility of the field setting by energizing and de-energizing the electromagnet at a controlled coil-current intensity ramp velocity.

The coil-current/field study was rather time-consuming. To keep the time spent on the precision analysis within reasonable bounds, we restricted the study to six coil current intensities, 1.8, 1.4, 1.0, 0.8, 0.6 and 0.4 ampere. The precision on the current intensities was to about 0.02 per cent.

The field measurements evolved during the period we measured susceptibilities. We started with a small flip-coil, red out by a galvanometer. Our more precise measurements resulted from a calibrated rotating coil magneto-meter. We evaluated the precision at 3 mT. We took the centre of the 3 mm diameter probe as the measuring location.

We located the probe of the magnetometer between the pole shoes of the magnet in a highly reproducible way. In the pole shoes' gap fits closely a shaped piece of Plexiglas with holes. The magnetometer's probe fits precisely in the holes. One of the holes is at the reference location. We measured the field, the magnet in backward position.

The holes have been drilled all along the central line in the middle between the pole shoes. Our limitation to the centre line is based on the assumption that, by symmetry, the field vector is horizontal and that, for all parts of a small sample, close to that line, the vertical component of the field is negligible.

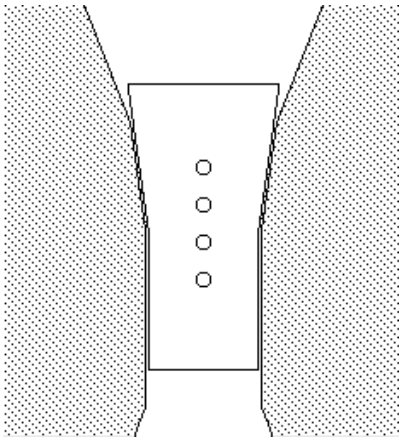

*Fig.34.1 shows the outline of the mid-plane section of the pole shoes. A shaped Plexiglas piece with holes fits closely the pole shoe's gap. The holes allowed to precisely and reproducibly setting the field-measuring probe.*

To obtain an acceptable approach to a univalent field/coil-current relation, we measured susceptibilities in series, following a constant pattern. At first we carried out some measurements for the highest coil current. So we cycled the ferromagnetic material of the electromagnet a few times up and down the highest magnetization. Then, the so called proper measurements took place by pairs for each of the six current intensities. The measurements started with the highest current intensity then lowering the intensity and finally ending the series at the lowest current intensity.

In our later papers, the six magnetic field values measured at the reference location for the six current intensities appear as nominal values.

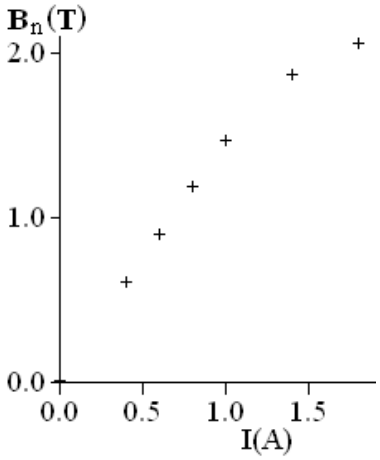


*Fig.34.2 reports on the six nominal values 2.06, 1.87, 1.47, 1.17, 0.90 and 0.61. The values of the magnetic fields are expressed in the unit tesla. The fields were measured at the reference location for the six current intensities.*

The rather precise field measurements allowed observing deviations in time. Compared to summer time, in autumn the field

increased by about 0.1 to 0.2%. The smaller value relates to the higher fields. We think that the temperature of the magnet has some influence. The temperature of the cooling water for the electromagnet was not stabilized. As it was on the limit of our reproducibility we did not studied the effect any further.

At the susceptibility calculation we took care of the change in the sample's position depending on the sample's temperature. Magnetic fields, measured at different locations, were the basic data for a location dependent field equation. Taking in account the sample's location-temperature relation, the field-location equation allowed introducing in the computer program a temperature dependent field-value adapting term.

## 35 The relative permeability

The current in the coils of the electromagnet only slightly contributed to the field at the sample location. At that place, the magnetization of the ferromagnetic material generated the main contribution to the field.

For the electromagnet, the calculation of the magnetic induction field at the sample location proceeds, in principle, in the same way as for the sum-field in the Gadolinium Meta-phosphate case. However, while in the Gadolinium case discussed in paragraph 28 the considered location lies inside the magnetized medium, in the electromagnet case it is outside. The applied field for the sample in between the pole-shoes of the electromagnet is the sum of the field component due to the coil current and the field component due to the magnetization.

When we talk about an "applied field" we mean a field that intentionally is generated at a considered location. In our susceptibility measurements it is the field that we put on the sample in order to study the sample's reaction. Precise susceptibility measurements ask for precisely known applied fields. At susceptibility measurements carried out with an iron-less coil as in the Fig.13.1 configuration, the applied field component at the sample location is only due to the coil current. At the susceptibility measurements carried out with the electro-magnet, the applied magnetic induction field felt by the sample is the

sum of the applied field felt by the electromagnet plus the field due to the magnetization of the pole shoes.

---

$$\mathbf{B}s = \mu_o (\mathbf{H}a + \alpha\mathbf{M}) = \mu_o \mathbf{H}a (1 + \chi_r) = \mu_o \mu_r \mathbf{H}a \qquad (35.1)$$

Equation (35.1) expresses equation (25.1) once more in another way.
$\mu_r = (1 + \chi_r)$ is the relative permeability.

---

The relative permeability expresses how many times the magnetic induction field felt by the sample is larger than that generated by the coil-current alone. You can interpret the amplification factor as the result of the ferromagnetic material being permeable to the field lines. The interpretation leans on the field line path in parallel current rings as discussed in Fig.7.2. Generalizing the picture, the parallel magnetic moments in the magnetized material guide field lines in the material.

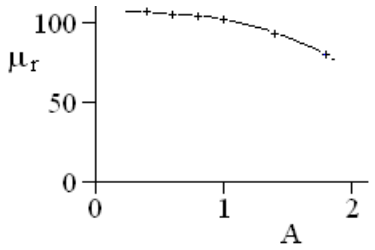


*Fig.35.1 reports on the relative permeability, for six different coil current intensities, calculated for the sample location.*

Due to the ferromagnetic medium, the amplification factor for the magnetic induction field in our electromagnet is about two orders in magnitude. The relative susceptibility $\chi_r$ is positive and much larger than unity.

It appears to me that the fact, that the magnetic induction field felt by the sample can be orders in magnitude larger than that generated by the coil-current alone, may have led to the terminology “magnetic induction field”. The use of the adjective “induction” raises a sense of injustice to me. Agreed, in the electromagnet the magnetization of the ferromagnetic material is the major contribution to the field at the sample. However, it is not the only contribution. I did no historical research for supporting my impression. Nevertheless, I give you another argument. The definition of the field-intensity in an earlier

system, the Gauss system, is different from that presently used in the rationalized SI system. For an iron-less coil in the Gauss system, the values of the magnetic induction field and the field-intensity are the same. It is quite normal then to differentiate between the fields by an adjective. Consequently, they got a different name.

In the rationalized SI system we do not need the adjective "induction". The magnetic field, **B** expressed in the unit tesla, is the one needed for calculating the Lorentz force. The omission of the adjective will not lead to confusion with "field-intensity" when we strike the latter expression out of our terminology. We find here the term "field" misleading. In fact, **H** expresses a weighed average surface-current density. So you should not call it "field" anymore. You should give it another name, preferably a short and easier one.

Adjectives nevertheless remain practical for specifying which field or part of fields we consider. E.g. in the Gd case is the "sum" field the sum of the "applied" field and "Weiss" field.

## 36 Remanence

The electromagnet generates the field applied to the sample with a good degree of reproducibility.

The field/coil-current relation is different from what the pure magnetic dipole interaction model suggests. The dipole model allows a spontaneous magnetization. Taking in account the high Curie temperature for iron, the ferro-magnetic material of the pole pieces can, at room temperature, magnetize up to 97% of saturation.

The effect of such a spontaneous magnetization does not show up at the sample's place. Weiss explained the observation introducing the concept of domains, each magnetized practically to saturation. The magnetization vectors of these domains are oriented in such a way that the resultant magnetic moment is strongly reduced. The bulk magnetization occurs when some of these vectors are caused to align themselves more or less parallel to the field generated by the coil-current. In our set-up, the bulk magnetization of the pole shoes is about proportional to the coil-current in the lower current intensity region. For higher current intensities an onset of saturation appears.

After removal of the current through the coils of our Varian-Ass-V-4012A electromagnet, the magnetic field at the sample location did

not returned exactly to zero. The material of the electromagnet showed remanence. The remanence depended on the speed the coil-current was shut down. The controlled de-energizing resulted in a remanence of about 10 mT.

The remanence fit the picture we have on magnetism. The remanence is a magnetization that remains after the applied field is removed. In a certain way it reminds the persistent moment in the superconducting disc we discussed in paragraph 17. In both cases the magnetization remains stable in orientation.

We did not observe such stability in the Gadolinium case. We interpret the difference in stability in the difference in the easiness of reorientation of spin versus orbital systems. The magnetism of the Gadolinium 3+ ion is a special case. It practically is due only to the spin of its seven 4f-electrons. The ion, in the ground state, has no orbital magnetic moment. The f-electrons have practically no interaction with the valence electrons. The spins reorient relatively easily. At variance with 4f-electrons in the rare earths, the d-electrons in the iron group are less well shielded from interaction with the valence electrons. The valence electrons are on the basis of the chemical bounds, which on their turn result in crystal fields. The ground state of the iron 2+ ion has a relatively large orbital moment that, to certain extend, is pinned by the crystal field. It depends on the symmetry of the surrounding whether the orbital will be relatively easily reoriented. Néel explained certain remanence on the presence of elongated single domain particles. As the ground state of the iron 3+ ion has no orbital moment we expect the spin to reorient rather easily. The ferromagnetic material of our electromagnet was rather soft. Soft means that the effect at the sample location of the larger part of the magnetization was reduced by intern reorientation.

The power supply of the electromagnet generated a direct current of a constant sense. In the higher current intensity region, the voltage on the magnet was rather high. We had no idea of the electric insulation of the current leads in the magnet. Consequently, we did not switch the current sense to reduce the remanence by a coercive field. As my mission was not the study of the susceptibility apparatus itself, we lived with the relatively small remanence. The soft ferromagnetic material of the electromagnet allowed a rather wide window in the value region of fields. Nevertheless, for reason of precision, we measured susceptibilities only at the higher fields.

## 37 The force on the empty pan

The advantage of the electromagnet, allowing measuring at relative high fields and gradients, results in an effect we had not to bother about in the formerly discussed field/coil configuration. The energized electromagnet exerted on the empty balance pan a measurable force which can not be neglected anymore [37].

We tried a copper nickel alloy of feeble susceptibility for the balance pan, to reduce the zero force. However, the susceptibility could be considered as feeble only in a limited temperature region. Moreover, its susceptibility changed with time. So, we switched over to a gold-copper alloy, a material stable in time. It was diamagnetic over the total temperature range reached by our apparatus. Of course the alloy resulted in a force we had to correct for. As the force was reproducible the correction was no major problem. Fig.37.1 reports on the force data.

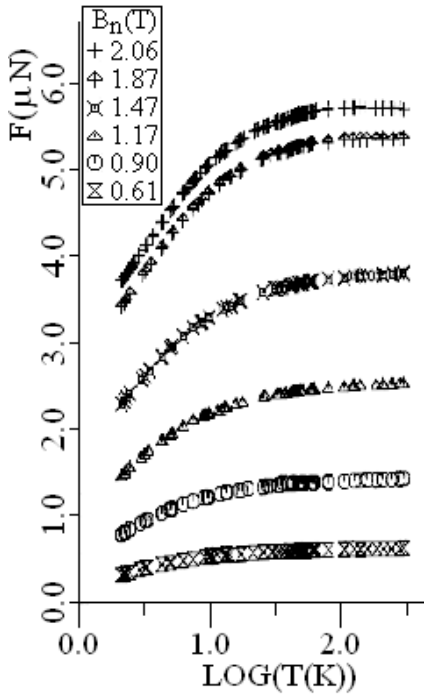


*Fig.37.1 reports on the force on the bare balance pan, with cover, made of a gold-copper alloy. The data were taken at six different nominal magnetic fields. The plot, force versus the logarithm of temperature, allows a rather well resolved view of all measurements, as well in the higher as in the lower temperature region.*

For making the pan and cover, we fold a glossy alloy sheet. The glossy surface reduced the sticking factor for oxygen. The oxygen, as a trace in the heat exchange Helium gas tends to adsorb on rougher

surfaces at low temperatures. Oxygen, when adsorbed on the pan, introduces parasitic effects as it is paramagnetic.

Treating the Helium and a protocol of sample cooling, for sticking the oxygen at the surface of the inner wall of the cryostat at a location above the balance pan, increased the reproducibility of the zero force measurement.

The diamagnetism of the balance pan and cover had also a positive effect; it tens to drive the pan to the same place between the pole shoes, increasing the reproducibility.

The force on the sample holder, in fact, depends on two parameters. It depends and on temperature and on field. However, the field can be reset within a minute to a preset value by energizing the magnet. For simplification, only fixed values of the field setting are used. Then, for each of these values, the force can be considered to depend only on one single variable, the temperature.

The limited number of applied field value settings results in a spatial separation of the measuring point marks in the drawing, Fig.37.1. The systematic allows pattern recognition as a helpful technique for detecting erroneous data. The mark of a bad measurement situates, in most cases, somewhere isolated in the drawing. Even an inexperienced investigator immediately recognizes the measurement affected by an accident. The method saved considerably time as it becomes superfluous to check every data of the measurements.

For each nominal field we considered four fitting regions of temperature. The limitation is a compromise between desired precision and the time to spend on the fitting.

We fitted the forces on the empty sample holder to simple smooth equations, expressing the superposition of a constant diamagnetic–like and a Curie-Weiss-like behaviour. The equations allow correcting for the force on the balance pan with cover. The equations are introduced in the susceptibility calculating computer program. The difference between the measured force on the pan and cover and the computer approximation is plotted in Fig.37.2.

Fig.37.2 reveals that, at the susceptibility calculations, we have to deal with an uncertainty on the force on the bare sample. It is due to

the uncertainty on the compensation for the force on the sample holder. The pattern in Fig.37.2 is quite different from that in Fig.37.1. The force data taken on the empty sample holder for the six different nominal magnetic induction fields are well separated from each other in the drawing. For all of the six, the forces evolve in a gentle way with temperature. At variance, the distribution of the force error marks mixes up for the six fields. The distribution resembles that for accidental errors about the mean. It would be very time consuming for further reducing systematic errors.

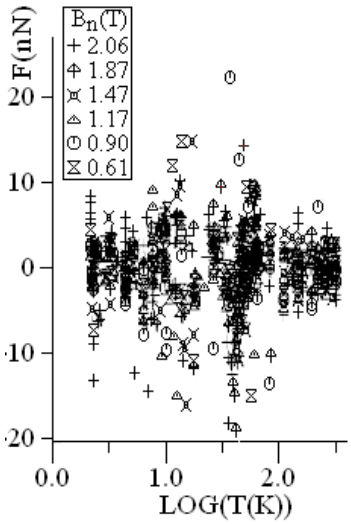


*Fig.37.2 reports on the force error on the sample, i.e. the force on the bare balance pan, with cover, minus the approximation of this force by the computer program, plot versus the logarithm of the sample temperature for different applied magnetic induction fields.*

We did not study the law of distribution. As the effect of the systematic errors is of the order of the spread of the data we accept, for the discussion, that, in a crude way, the Gaussian law of errors applies. We estimate the standard deviation to be about 10 nN (nano-newton). The uncertainty is one order in magnitude larger than that due to the force detection limit of the balance, as discussed in paragraph 14. We tend to believe that the larger uncertainty is due to the limited reproducibility in the field/current relation of the electromagnet.

The force measurements on the empty sample holder indicate that the reproducibility is about 0.18% for the highest field and 1.7% for the lowest field. From the point of view of the electromagnet, the reproducibility not only relates to the magnetic induction field applied to the sample location but also to the field-gradient at that place. In the next paragraph we will discuss the measurement of the field-gradient.

## 38 Field-gradients

In the early days while setting up the susceptibility apparatus we used the Maxwell equation for getting an impression of the field-gradient. The equation in mind states that the change in time of the magnetic flux in a coil induces in that coil an electric tension.

We pulled up a small coil, in the middle between the pole shoes, in a vertical sense. We recorded the resulting tension. Fig.38.1 shows a record that was taken at maximum electro-magnet current.

The pattern gives good impression of the position-gradient relation. However, we could hardly consider it as a precise measurement. The coil, although small, was larger than our samples. The moving of the coil and of the recorder pen was motor driven. The speed remained not precisely constant during the measurement. The relative uncertainties became even larger at the lower intensities of the magnet energizing current for which the signal was smaller. The precision on the gradient was not very good in those days. However, it was good enough allowing studying radiation damage in single crystals of lithium fluoride. The effect of radiation was much larger than that you could question on the basis of the uncertainty of the gradient.

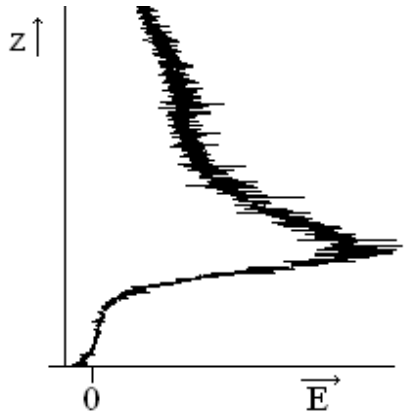


*Fig.38.1 shows a record of the electric tension E generated by a small coil moving in a vertical sense between the pole shoes. The average tension and the gradient are proportional to each other.*

The introduction of the rotating coil magneto-meter and an easier access to computer facilities allowed another approach for estimating the field-gradient. The technique consisted in fitting the field/place data to an equation and then differentiating the equation. Our statement “estimation” expresses that the procedure leans on the assumption that the magnetic induction field varies smoothly with

location. We have no elements that make us doubt on the assumption. Fig.38.2, as an example, reports on data measured with 1.8 A, the maximum current intensity we used for energizing the electromagnet.

The fields were precise to a fraction of a percent. The calculations can be carried out with great precision.

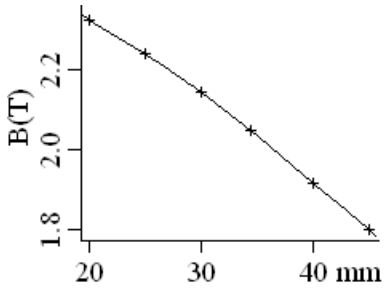


*Fig.38.2 reports on magnetic induction field data for different places in the middle of the mid-plane between the pole shoes in a vertical sense, for the highest current.*

The precise result however depends strongly on small changes in the data. We assumed the measuring location at the centre of the 3 mm diameter probe. An uncertainty of 0.1 mm on the field location difference in the neighbourhood of the sample results in a relative gradient uncertainty of the order of a percent. An uncertainty of 0.1% in the magnitude of a magnetic induction field results also in a relative gradient uncertainty of the order of a percent. The result is quite logic when we realize that the gradient relates to a small difference of two large values.

## 39 The gradient/field ratio

For the iron-less coil it is possible, for the sample location, to deduce the field-gradient from the magnetic induction field. In a constant coil/sample configuration is, for whatever location, the ratio, the value of the gradient divided by the field value, independent of the coil-current.

For the electromagnet this rule does not quit hold. The ratio depends on the magnetic saturation of the ferromagnetic material of the yoke and the pole shoes. The constant protocol for energizing and de-energizing the magnet results in a rather reproducible ratio. We report on ratios in Fig.39.1. The signs mark ratios we obtained with the fitting technique, discussed in paragraph 37. The + signs relate to

ratios calculated from averages of measured gradient and field values for an energized electromagnet.

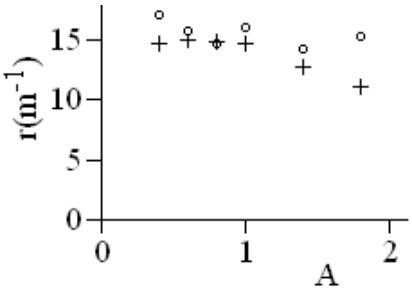


*Fig.39.1 reports on the ratio, the gradient divided by the field value, by the + sign for an energized magnet and by the o sign for the remanence.*

The magnet energizing current intensity is expressed in ampere (A). I interpret the pattern as consisting of two parts. In the region one ampere and below the signs does not indicate magnetic saturation of the ferromagnetic material in the electromagnet. The value of the ratio, the gradient divided by the field, is practically independent of the coil-current. The uncertainty on the ratio is attributed to the uncertainty on the gradient value. The uncertainty is of the order of one percent. In the region above one ampere where the onset of saturation is observed the ratio values are lower. The fitting technique was the same as that used for the low coil-current region. So we expect that the precision on the ratio values also is of the order of one percent. So the lower values of the ratio indicate the presence of a real effect which we attribute the onset of saturation.

The o signs in Fig.39.1 relate to ratios calculated from averages of gradient and field values measured after the magnet has been de-energized. No magnet energizing current means that the ratios concern the gradient and field due to the remanence. The uncertainties on the small field and gradient values make the uncertainty on their ratio larger. I felt somewhat surprised that the ratios are about the same as those obtained for the energized magnet.

## 40 The product of field and gradient

Our experience with susceptibility measurements introduced to us another method to evaluate the value of field-gradients. The force on a sample is the product of the sample's magnetic moment times the magnetic induction field's gradient. Samples with known magnetic moment will lead us to the field-gradient. The reproducibility on the

force we measured on a pure single crystal platelet of LiF, was about 0.3% for each of the nominal fields. Conclusion, the reproducibility of the gradient must be of the same order.

The reproducibility makes sense trying to put a value on the gradient. We shifted the uncertainty problem to the knowledge of the magnetic moment. Pure LiF is a diamagnetic material which, to the best of our knowledge, practically has a field independent susceptibility. For a material with constant susceptibility, the magnetic sample moment is proportional to the applied magnetic induction field. The situation allowed us to separate the apparatus related items from the sample related ones. On one side we have the force divided by the product of the field times the gradient. On the other side we have the sample mass times the mass susceptibility. Both sides are equal to each other.

On the assumption the magnetic susceptibility of LiF is field independent, the apparatus/sample separation allowed us to adjust the nominal field factor, magnetic induction field times its gradient at room temperature, to yield the same susceptibility values for all nominal fields.

The adjustment only is precise to 0.3%, the reproducibility of the measurements. A theory on relative small errors of observation states that the fractional error of a quotient is the sum of the fractional errors of all its components. The fractional error, the relative uncertainty on the measurement is 0.3%. The probability is large that the fractional errors of observation of and the field and the gradient are smaller than 0.3%. Also the error of observation for the susceptibility is probably about 0.3%.

The deviations larger than 0.3%, between susceptibilities measured at different nominal fields, should not be attributed to an observational error at the measurement of a sample with field independent susceptibility. The origin for the difference should be sought elsewhere.

At first, we look closer to the force. In fact, we measure the force difference, the difference between the force before and after energizing the electro magnet. Due to the remanence, the force is not zero at zero magnets current. However, the product, the field times its gradient, related to remanence is less than 0.05% of the product related to all nominal measuring fields. The effect is negligible.

Next, we consider the field. The field is known to a fraction of a percent. However, we measured the magnetic induction field outside the cryostat. In paragraph 15 we stated that the sample inside the Dewar practically feels the field and gradient as generated by the coil outside. The statement holds for the low field experiments. We now assume that the statement can be extrapolated to the higher magnet fields we consider in the present discussion.

Magnetic susceptibilities of non ferromagnetic materials were the main subject of our research. The product of field times its gradient was of direct concern. We took LiF as our reference material. Ferromagnetic contamination was a problem. We interpreted the most diamagnetic sample as the least contaminated. As we had no precise value for the susceptibility of LiF, we took the value obtained at the highest field factor as the more probable. To yield the same susceptibility value for all measuring nominal fields we adjusted their field factors, the product of the field times its gradient. Of course, the susceptibility value then still is subjected to the uncertainty on the gradient related to the highest field used.

For taking in account the sample displacement, caused by the shrinking of the suspension wires at lowering the temperature, we measured the field factors for three locations. We did it for each of the six nominal fields used. A smooth curve fitted through the three values versus location coordinate allowed adapting the product to the sample position.

For all six nominal fields the field factor is constant within 1%. The field factor depends only slightly on the location coordinate. The restricted measuring range extended only 1.6 mm upwards starting from the room temperature reference location near the maximum of the absolute value of the field factor. The field-gradients, the quotients of the field factors divided by the field values, therefore were precise up to 1%.

The values of the field factors were obtained from force measurements. The values of the magnetic induction field were measured with a rotating coil magnetometer. Does both data fit each other? We looked to the intern consistence by comparing the “experimental” field factor with the “calculated” one using the magnetic induction field. In the working region the relative deviations,

from internal consistence, range from +9% to -5%. The relative deviations are large in comparison with the reproducibility.

We realized the gradient is the difference of two relative large values. Small changes in field values restore the internal consistency. A magnetic induction field adaptation reduces the absolute values of the deviations from consistency to below 0.2% over the total measuring location range for all six nominal fields. In all cases, the consistency asked for a magnetic induction field adaptation less than 0.1%. In other words, our fields and field factors were adequate for calculating the magnetic susceptibilities from the measured force data. And so were the field-gradients, the quotients of the field factors divided by the field values.

The internal consistency also holds for slightly different field factors resulting from a slightly different choice of the reference susceptibility. The analysis does not remove the uncertainty on the susceptibility of our reference material.

## 41 Stainless steel 304

Stainless steel has some useful properties for constructing cryostats. In a cryostat the cold inner part has to be thermally isolated from room temperature. Stainless steel is available in thin walled vacuum tight tubes. The tubes allow suspending low temperature vessels in vacuum. High vacuum is a good thermal insulator. A thin wall keeps the cross section of the suspension material low. A small cross section on its turn limits the thermal flow. The thermal flow is even more reduced by the choice of stainless steel, as its material is bad thermal conductor.

The constitution of stainless steel is the main drawback for constructing a cryostat to be used in a magnetic susceptibility apparatus. As it mainly consists of iron, and we know that iron is ferromagnetic, it influences the magnetic induction field. When we know the susceptibility we can estimate a save distance the material should keep away from the measuring room. Fig.41.1 reports on the low temperature mass susceptibility of stainless steel 304.

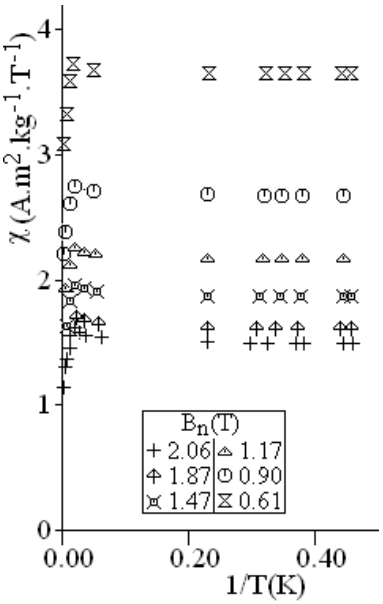


*Fig.41.1 reports on the magnetic susceptibility of stainless steel 304 at low temperatures.*

At low temperatures the susceptibility is practically independent on temperature but strongly dependent on the applied magnetic induction field. The dependency is typical for magnetic saturation of paramagnetic centres. The behaviour indicates the presence of ferromagnetism. Fig.41.2 shows susceptibilities, taken at 4.3 K, plotted versus reciprocal applied magnetic induction field.

We used the method of Honda and Owen for calculating the ferromagnetic contribution to the magnetic susceptibility, $\chi_f$. The analysis asks for ferromagnetic materials below the Curie point at high field showing magnetic saturation. It implies the magnetic moment per unit of mass $M = \chi_f B$ being constant. When all conditions are fulfilled, the susceptibility $\chi_f = M/B$ depends linearly on the reciprocal of the applied magnetic induction field B.

---

$$\chi_{si} = \chi_o + \chi_{fi} = \chi_o + M(1/B_i) \qquad (41.1)$$

Equation (41.1) expresses the sample susceptibility $\chi_{si}$ to be the sum of a field independent susceptibility component $\chi_o$ and a field dependent susceptibility. In the latter is the magnetic moment M of the ferromagnetic contribution field independent.

---

The fitted straight line does not include the origin of the set of axes, indicating the presence of a second susceptibility component.

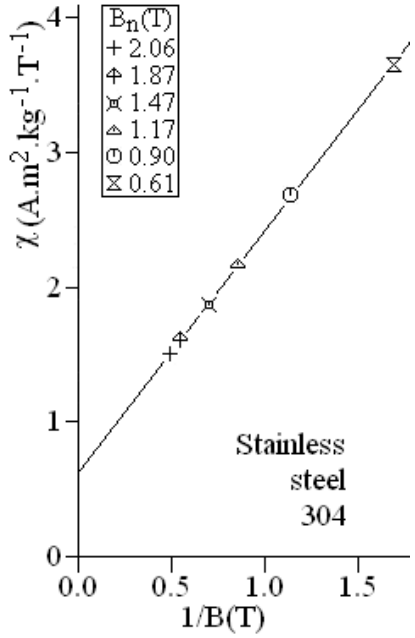


*Fig.41.2 shows the magnetic susceptibility at 4.3 K, of a sample of stainless steel 304, versus reciprocal applied magnetic induction field.*

The analysis of the measured data results in a magnetic moment M 1.79 $A.m^2.kg^{-1}$ and $\chi_o$ 0.62 $A.m^2.kg^{-1}.T^{-1}$. The analysis yields for the relative standard deviation on $\chi_{si}$ a value somewhat less than 0.6%. The precision mainly regards the gradient of the applied magnetic induction field. Indeed, the ferromagnetic contribution to the susceptibility is the largest for all measurements and the related magnetic moment is field independent. The force measured on a constant magnetic moment is proportional to the gradient of the applied magnetic induction field.

From the point of view of the construction of a cryostat, the susceptibility could have been worse. Stainless steel 304 contains about 18 percent chromium and about 8 % nickel. Except for small concentrations on other additives, the main remainder is iron. In spite of the large concentration on iron, the magnetic susceptibility result is much less than a hypothetical “bad case”. We explain. We approximate the constitution of the steel by the chemical formulation $Fe_{18}Cr_5Ni_2$ and its molecular weight 1.38 kg. For simplicity reason we consider only the spins of the unpaired electrons in the d-shell in the ground state of the atoms. The total number of electrons in one chemical formula unit then is 101. At magnetic saturation such a

number would yield a magnetic moment of 408 ($A.m^2.kg^{-1}$). The "hypothetical bad case" is 228 times more magnetic than the experimentally observed ferromagnetic component in the real steel. Less than 0.5% of the spins occur in a ferromagnetic state.

Most of the electrons couple antiferromagnetically with another one. A further indication for the antiferromagnetic coupling is the slightly protruding susceptibility values at the left in Fig.41.1. Non interacting magnetic centres evolve smoothly towards saturation on lowering the temperature as shown in Fig.2.2a. Antiferromagnetically coupled paramagnetic centres may evolve trough a maximum susceptibility on lowering the temperature.

## 42 The contribution of a NBS reference material

We tried to improve our experimental precision, measuring the magnetic susceptibility of an aluminium standard reference material [42]. We bought the material from the USA National Bureau of Standards. The material is paramagnetic. The difference in measuring technique, however, left room for interpretation. The NBS certified figure was measured following the Gouy method. The maximum field used at the NBS was 0.75 T, slightly higher than our lower field value. Ferromagnetic contamination was the problem.

We measured two samples. Fig.42.1 reports on the normalized ratios of their susceptibilities. Some values are different by more than the error of observation.

Each mark in the figure refers to its normalized ratio. The ratio is the quotient of the magnetic susceptibility measured at one of the six nominal fields divided by the susceptibility taken at the highest measuring field. As the susceptibilities are normalized to that taken at the highest measuring field, all ratios for the nominal field 2.06 T are 1. For clarity, these marks are omitted. As susceptibility values we used an average taken on more than 20 susceptibilities measured at temperatures in the neighbourhood of room temperature.

Also for clarity reason, Fig.42.1 reports only on the errors of observation on sample 2. The errors relate to the standard deviation on the susceptibility measurements. The standard deviations are about the same for the other samples.

The agreement between the ratios for sample 1a and 1b indicates the measurements are reproducible within 0.2%.

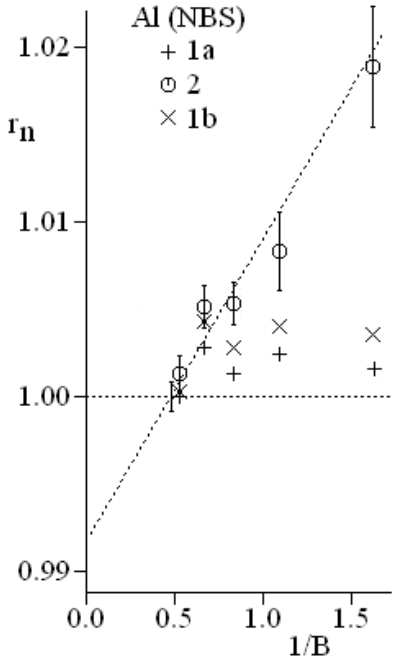


*Fig.42.1 reports on the normalized ratios of the magnetic susceptibilities versus one over the magnetic induction field. Sample 1 was measured before (1a) and after (1b) sample 2. Before being put on the balance pan each sample has been etched conform to the NBS handling instructions. Sample 1 has been treated a second time after measuring sample 2 and lost 7% of its mass during this operation.*

The differences from unity, the ratios show, indicate our uncertainty on the value of the product, field times its gradient. Indeed, we used the product that we adjusted to yield unity for all ratios of "our" reference, a LiF crystal.

We interpret the pattern of the ratios of sample 2 as an expression for the presence of a magnetic nearly saturated ferromagnetic contamination. The effect is equivalent with that of an iron mass fraction versus aluminium of a quarter of a million.

If we would tend to attribute, for sample 1, the deviation from unity also to a ferro magnetic contamination it would be impossible to conclude which sample is contaminated, the reference Al or the LiF. We assumed that our reference LiF was not contaminated. However, if the LiF were contaminated, the product, field times its gradient, would have been adjusted to a too low value. Then the ratios of sample 1 would have been closer to unity. The deviation from unity indicates an uncertainty which cause is not resolved.

In conclusion, the NBS aluminium standard reference material contributed to the knowledge of our susceptibilities, by the results on sample 1, indicating that our measurements are precise to within a fraction of a percent.

However, the accuracy remained uncertain. We have no answer to the question which of the two Al samples is the more representative for the certified reference figure? In our perception, the relative inaccuracy on our gradient may be about two percent.

The uncertainty on the susceptibility relates to the product, field times gradient. As we believe that the values of the applied magnetic induction field are less uncertain, we attribute the major part of the relative uncertainty to the field-gradient.

We also carried out the whole procedure of comparing the susceptibility of the NBS (USA) reference material to ours, at the temperature of liquid nitrogen. Except that the uncertainty at 77.7 K was slightly higher than at room temperature, the general conclusion remained the same.

## 43 On susceptibilities of $La_{1-x}Gd_x(PO_3)_3$ glass

Our discussion revealed that, except for a proportionality constant about unity, we know the values for the product of field and gradient for room and liquid nitrogen temperatures. We now consider experiments indicating that the product values still hold at the liquid helium temperatures.

The susceptibility measurements on superconducting discs indicated that the sample at the inside of the Dewar practically felt the field and gradient generated outside (paragraph 15). The statement is the conclusion resulting from experiments at low fields. Analyses on susceptibilities taken on $La_{1-x}Gd_x(PO_3)_3$ glass samples indicate that the statement also holds for higher fields as generated by the electromagnet.

For identifying our samples we allocated them a number. The number 710 refers to the $710^{th}$ sample we measured. The numbering is not restricted to the Gd containing samples. The analysis of low field data taken on number 710, a Gadolinium Meta-phosphate glass

sample, teaches us that the field and temperature dependence of the magnetic susceptibility of the Gadolinium ions relates tightly to the Brillouin function (paragraph 20 – 27).

The analysis, of data taken on the $Gd_x(PO_3)_3$ sample 711 (Fig.2.2a) at the higher fields generated by the electromagnet, yields the same conclusion.

The concentration on Gd ions in $Gd_x(PO_3)_3$, x about 1, allowed mutual interaction between paramagnetic centres. We assumed the interaction to be concentration dependent. For reducing the interaction we turned to a magnetically dilute system, $La_{1-x}Gd_x(PO_3)_3$. At first, we made in our institute a glass with a Gd concentration x about 0.2%. The basic materials, we used for the preparation, were the purest we disposed of. Nevertheless, more than one third of the magnetic moment of sample number 717 was due to impurities.

Wenzel and Blackburn NBS (USA) knew how to make iron free samples. We were happy to get two glass pieces, respectively with the Gd concentrations x about 1% and 0.1%. We could not find any indication for magnetic contamination on samples taken out of the materials. The magnetic susceptibility versus reciprocal temperature patterns are very similar to that shown in Fig.2.2a.

The magnetic susceptibility of number 754, a $La_{1-x}Gd_x(PO_3)_3$ glass sample with x about 0.001, is diamagnetic at room temperature, as reported by negative susceptibilities at the left side of Fig.43.1. In the very dilute Gd system at the higher measuring temperatures the paramagnetism of the Gd does not compensate the underlying diamagnetism.

At the lowest temperature the difference in magnetic saturation, as in Fig.2.2a, shows up by the spread of the susceptibilities for all the Lanthanum Gadolinium Meta-phosphate glass samples we measured. In the Brillouin context is the field/temperature ratio highest for the highest measuring field; the sample is nearly completely saturated. At the lower field only the numerical analysis reveals the onset of saturation. On the pictures it would be difficult to see the differences.

The similarity of the patterns for the glass samples with different Gd concentrations indicates that the saturation effect mainly is independent on the Gd concentration. It mainly relates to the individual paramagnetic centres.

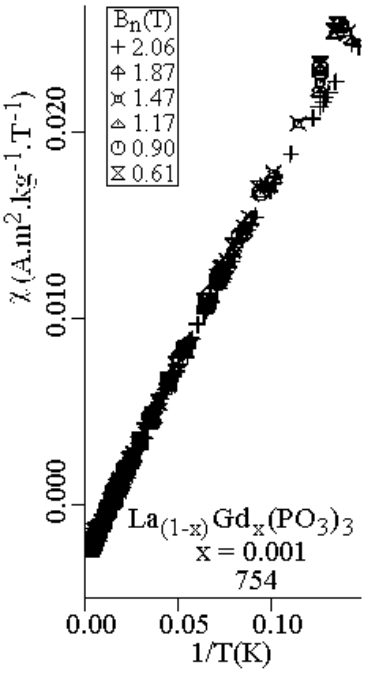


*Fig.43.1 shows the magnetic susceptibility of sample 754, a $La_{1-x}Gd_x(PO_3)_3$ glass sample with x about 0.001. At the higher temperatures the resultant paramagnetic effect of the limited number of paramagnetic centres becomes so small that the underlying diamagnetism prevails. The marks are one on top of another, indicating that the susceptibility is independent of the magnetic induction field.*

We checked the reproducibility of our measurements at low temperatures with the $La_{1-x}Gd_x(PO_3)_3$ sample 754. Our sample 754 weighed 5.91 mg. We measured twice the global susceptibility pattern. Fig.43.2 reveals that the result of both measuring series is practically the same.

Fig.43.2 reports on the differences the experimental values of the magnetic susceptibilities deviate, in percent, from theoretical ones.

The theoretical values are the ones calculated with one single Brillouin function for the analysis of the results of both series of measurements. No interaction between paramagnetic centres is taken in account. For the analysis of both series the concentration on Gd ions is taken the same as the studies concern the same sample. Also the underlying diamagnetism is kept equal for both studies. For all fields and all temperatures for both series of measurements, the calculations are carried out with one single set of two parameters, the concentration and the diamagnetism.

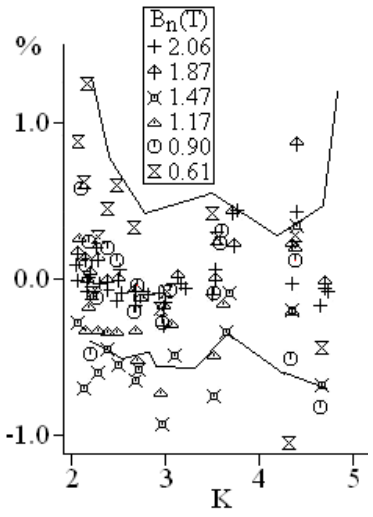


*Fig.43.2 reports on the percentage the experimental susceptibilities deviate from those expected on the theory of one Brillouin function for a $La_{1-x}Gd_x(PO_3)_3$ glass sample without mutual interactions. The marks relate to data taken in April 1982. The lines are contours for data measured in November 1980.*

In Fig.43.2 the marks reports on the data measured in April 1982. For clarity reason, no individual values are reported for data related to measurements taken in November 1980. The lines rely respectively the upper and lower extreme values. The series of measurements for the two patterns are practically independent from each other. Indeed, we cleaned the sample outside the Dewar before each series. The agreement between the results of both analyses is an indication for the long term reproducibility of our measurements.

At the first series of measurements, November 1980, an AuCu rather flat plate, number 647, covered the sample. In the second study, April 1982, number 776 covered also the sides of the sample. The idea beyond the cover change was to improve the prevention from oxygen sticking on the sample. The agreement between the results of both measuring series indicates that both covers were adequate.

From the batch for which the Gd concentration is about 1%, we measured the susceptibilities of different $La_{1-x}Gd_x(PO_3)_3$ glass samples. We used the samples for checking the homogeneity of the Gd concentration. Our analyses indicate that differences up to 1.6% occur in milligram samples.

Our analysis of the magnetic susceptibility data indicates that the $La_{1-x}Gd_x(PO_3)_3$ glass prepared by the NBS is magnetically pure. Over the whole temperature range covered by our apparatus, the magnetic susceptibilities relates tightly to the Brillouin theory. At the lower temperatures the susceptibilities changes drastically with the magnetic

induction field. Due to the difference in saturation, the susceptibility difference at 2 K is about a factor two. The material could function as a susceptibility reference material if the Gd concentration and it homogenisation could be certified. As the NBS material is not certified as reference, we feel that the uncertainty on the accuracy of our measurements remains unchanged.

## 44 On the sample magnet interaction

Measuring susceptibilities in a sample/iron-less-coil configuration (paragraph 13), the applied field and gradient were independent from the magnetic moment in the sample. Indeed, a constant current device kept the current in the coil constant. The constant current generates a constant field and gradient. The coil generated field therefore is independent from the currents in the sample.

The situation is different in an iron containing electro magnet. The magnetic polarisation of the pole shoes does not only depend on the current in the coils of the electromagnet, but also on the magnetization of magnetic materials in the neighbourhood.

We estimated the interaction between sample and pole shoes for our susceptibility measuring set up with the electro-magnet. Again, the model starts with our basic primitive unit, the closed circular circuit in free space, for simulating the sample. Fig.44.1 reports on the configuration.

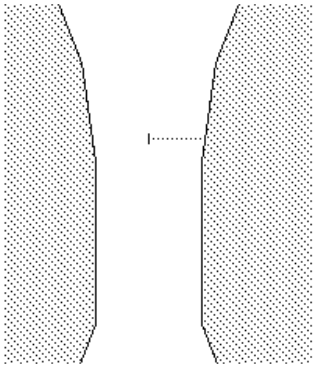

*Fig.44.1 outlines the sample position between the pole shoes. The magnetic moment of the sample is approximated by the moment of a closed current ring. The gap between the pole shoes is larger than the sample dimensions.*

As the sample dimensions are small compared to the distance from a pole shoe, the sample moment can be approximated by a magnetic dipole moment. The sample interacts on the magnet by the long range

effect of its magnetic dipole on the ferromagnetic material of the pole shoe. We interpret the interaction as due to the field generated by the sample moment on the ferromagnetic medium of the electromagnet. We consider the interaction at a location in the tip of a pole shoe close to the sample in its horizontal plane. The field at that location is proportional to the magnetic moment of the sample and inversely proportional to the cube of the distance. The distance is somewhat half the pole shoes gap. Taking in account the proportionality constants results in a field value, expressed in tesla, about one tenth of the moment value, expressed in ampere square meter.

For estimating the relative effect we compare, at the location considered, the field generated by the sample to the field generated by the coils of the electro magnet. For fixing the ideas, we concentrate on the lowest magnetic induction field used in our susceptibility study with the electromagnet, 0.61 T. Following paragraph 34 the relative permeability, at this nominal field, is about hundred. It means that, at the sample location, the field contribution due to the current in the coils of the electromagnet is one hundredth of the nominal measuring field. We take this figure, 6 mT, as estimation for the field at the considered location in the tip of a pole shoe. This field will be changed by the contribution due to the sample moment. We assume that the magnetization of the ferromagnetic medium of the electromagnet will follow the change about proportionally. When one accepts that a change by one percent of this magnetization would be hardly detectable, it means that the contribution to the fields, due to the sample, should be less than 60μT. In the given configuration, it is equivalent in saying that the effect will be negligible when the sample moment is lower than $6 \times 10^{-4}$ $Am^2$. The effect of a 3 mg piece of macroscopically fully saturated iron would be detectable. In our susceptibility research we never exceeded that moment limit. Indeed, we never had an indication for the presence of a sample magnet interaction.

## 45 The mole susceptibility

The mole susceptibility is the magnetic moment, per mole and per tesla, induced in a sample by the applied magnetic induction field. What is the reason for introducing one more expression for the magnetic susceptibility? To my feeling, it is the constant number of entities in one mole that makes the difference. When it is difficult to

study a physical property of one entity, it can be more practical to study the property of a larger number of them together. The large number considered here is Avogadro's number ($6.02x10^{23}$). Such number of $La(PO_3)_3$ entities weighs 0.375 kg. The molar weight of a material writes down in kg without the need for a large exponent.

A constant number allows relatively easy to compare, between different materials, the property under attention which mainly relates to the single entity. The interaction between the entities should be of minor importance. Example given, the volume of a stack of balls is the volume taken by one ball times the number of the balls. This is a good approximation as long as the balls are not strongly deformed e.g. by their own weight. Something similar happens with the diamagnetism of ions.

We applied the concept for explaining the diamagnetism which appeared at room temperature in our $La_{1-x}Gd_x(PO_3)_3$ glass sample. In the very dilute Gd system at the higher measuring temperatures the paramagnetism of the Gd does not compensate the underlying diamagnetism. In the present approach, we approximate the underlying diamagnetism by the sum of the components. The summing up is similar to that you do for calculating the molar weight. For the susceptibility of our glass sample, you sum up nine times the diamagnetism of the oxygen 2- ion, 3 times the value for the phosphorus 5+ ion and one times that for the Lanthanum 3+ ion. The underlying mole susceptibility for the Gadolinium 3+ ion is taken equal to the mole diamagnetism of the La 3+ ion.

For the mole susceptibilities we used the values based on a compilation by W. Klemm. These data are reported by P.W. Selwood, in his book "Magnetochemistry" [45]. After adaptation of the reported values to the presently used SI units, we obtained for our $La_{1-x}Gd_x(PO_3)_3$ glass sample a mole susceptibility $-13x10^{-4}$. Our experimental value, deduced from Fig.43.1 by extrapolating the reversal temperature to zero, is $-11x10^{-4}$. The absolute value of our result is only by 16% lower than the value estimated by the Klemm data.

The agreement suggests that it is meaningful to consider the experimental diamagnetism of our $La_{1-x}Gd_x(PO_3)_3$ glass sample as build up by the diamagnetism of the ions. However, the 16% deviation indicates that the model is somewhat oversimplified.

## 46 Diamagnetism of ions

We saw that, in a certain way, the ion can be treated, from the point of view of diamagnetism, as an entity on its own. We consider here ions which are no Brillouin centres and do not have a magnetic moment when they are out of magnetic induction field, but do have one when they are in a field. It means that out of the field there is no net current flowing over a closed circuit in the sample. However, putting on the field generates resulting currents. The interpretation leans on quantum mechanics which, for our purpose, I feel rather complicated. I will try to outline the basic effect as they appear to me.

Consider at first an ion out of field. The ion is build up by a positively charged nucleus surrounded by a number of negatively charged electrons. The dimension of the ion is much larger than each of the components. The internal kinetic energy opposes the attraction of charges of different signs, preventing the electrons to stick on the nucleus. The mass of the nucleus is heavy while the electrons are relatively lighter. The ions are buzzing with activity of the more mobile electrons. Although in the ion we can not follow the activity of each electron separately, the probability of finding an electron somewhere in the ion is structured. Probability relations, expressed as orbitals, yield an electron density distribution in the ion. From the more complex possibilities, we consider here the simple case of a spherical symmetrical one about the nucleus.

We now turn to the model we are familiar with. We consider a ring at the equatorial plane of the ion, the nucleus at the centre. When the ion is out of field, there is no net current flowing on the ring. However, reminding the buzzing activity in the ion, we can interpret the situation as the result of two currents, flowing in opposite direction, compensating the effect of each other.

We put on a magnetic induction field perpendicular to the plane of the ring. Fig.46.1 depicts the situation.

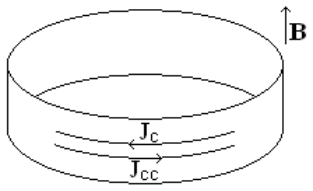


*Fig.46.1 outlines components of two closed electric circuits in which the currents are flowing in opposite directions in a magnetic induction field.*

Paragraph 6 treats the basic current field interaction. The current flowing in clockwise direction is subjected on its total circumference to a Lorentz force directing to the centre of the ring. The current circuit is under pressure. The circuit in which the current flows counter-clockwise the forces tend to expand the ring.

What is the reaction of the system on these forces? The reaction depends on the rigidity of the construction. This statement expresses one of the perceptions of the theorem of Miss van Leeuwen. The diamagnetism is the consequence of the ion reacting as a system on its own. Although we can not follow each electron in the ion, an orbital is attributed to each electron. The probability of finding an electron somewhere in the ion is structured. Certain energy is associated to each orbital. For elements early in the table of Mendeleev the energy of groups of orbitals are sufficiently different that the orbitals do not mix. The structure of the ion can be considered as rather rigid.

The rigidity of the ionic system can stand the pressure due to currents flowing in different senses. The force, due to the current in one sense is compensated by the force, due to the current flowing in the other sense. The ionic system does not react on the magnetic component of the Lorentz forces, the forces exerted by the applied magnetic induction field on the intern currents. However, the Lorentz force has not only a magnetic component but also an electric one. This electric component causes the induced magnetic moment [46]. We understand the induction as an effect of one of Maxwell laws.

Qualitatively, the Maxwell law in question states that a change in the applied magnetic induction field generates a curled electric field. The electric field acts on the electrons in the ion. We know that moving electrons are the basis of the electric currents. In the case outlined in Fig.46.1, the electric field acts on both current parts. However, for one of the current-flow senses, the electric field slows down the velocity of the electron. For the current part flowing in the opposite sense the same electric field fastens the velocity of the electron. The intensity of the current part flowing in one sense becomes less while that flowing in the other sense becomes larger. The addition of the effect of the electric component of the Lorentz force on both parts results in a net current flow.

In the perception the ionic system is rigid; the whole electron configuration rotates about an axis. The axis passes the nucleus and lies in the direction of the applied magnetic induction field. The

situation resembles somewhat that of a revolving door. You push it anywhere and it turns as a whole on its axis. Nevertheless, there is a large difference. When you stop pushing the door, friction puts the brake on the rotation. After a while the door stops turning. At variance, the electronic ion configuration keeps turning when you stop to change with time the applied magnetic induction field. In our perception of the magnetic susceptibility results, the situation resembles that of a superconductor in an applied magnetic field. Once the applied field is kept constant, the induced current flow persists. Even without driving force, the angular velocity of the ion construction remains constant.

We have experimental evidence for the persistence of the induced currents during several minutes. However, the long turn stability of our force detector, the balance, was not stable enough to prove the long turn persistence of the currents. Our apparatus allowed measuring precisely only the short term force change with the energizing current change of the electromagnet. At the setting up or cutting down of the energizing current of the electro-magnet the absolute value of the force change was the same but the sense of the force was opposite. What we were able to measure is in agreement with the current model of the diamagnetic susceptibility.

## 47 The fluor one minus ion

We now look more closely to one ion. We chose the $F^-$ ion as example because it responds rather well the model discussed in the former paragraph. As no material exists that is constituted of only F-ions, we were not able to measure the mole susceptibility of the fluor negative ion on its own. However, in the current perception the susceptibility of the fluor ion takes the major part of the susceptibility of LiF. We paid lots of attention to one single crystal of Lithium Fluoride, the crystal used as one of our reference materials.

The mole susceptibility we measured on the LiF single crystal was $1.08 \times 10^{-4}$ $Am^2mol^{-1}T^{-1}$. This experimental value is about 8% lower than the Klemm value, when the latter was adapted to the rationalized SI system. Chauvinism let me believe that our mole susceptibility value is somewhat more precise than the Klemm value. However, this feeling does not matter for discussing the susceptibility of the fluor ion. Following Klemm, the Lithium ion contributes only for five

percent to the susceptibility. Reducing our experimental LiF value by five percent, we obtain the value $1.03 \times 10^{-4}$ "ampere square meter per mole and per tesla" as the mole magnetic susceptibility of the fluor ion in the LiF crystal.

How compares the experiment with theory? As far as I know, the mole susceptibilities reported by Klemm are not yet replaced by more precise pure theoretical values. The "a priori" calculation of the magnetic susceptibility seems not yet advanced enough to do so. Calculating susceptibilities assume that we know all the orbitals, the wave functions with their eigenvalue. In practice, this is almost never the case. It seems that the repulsion between electrons is one of the causes that prevent the exact solution of the problem. Slater, estimating partial shielding of the electric charge of the nucleus by electrons in the neighbourhood of the nucleus, yielded a value for the mole susceptibility of the fluor ion which is about twenty percent lower than our deduced value.

The theory nevertheless expresses a perception of the physics governing the discussed diamagnetic susceptibility. In the present model, the mole susceptibility is the sum of the susceptibilities of all ions. All ions are equivalent. The susceptibility of one ion then is the mole susceptibility divided by Avogadro's number. In each ion the electric charge on each electron is the same. Also the mass of the electron is in all cases the same. The susceptibility contribution of each orbital contains a common factor, minus the square of the charge divided by six times the electron mass. This is the easy part of the calculation, as the common factor can be taken out the addition. The difficult part relates to the summing up of the distributions of the electrons in the ion.

Our approach will be rather simple. We turn back, for simulating the magnetic moment of the ion, to our primitive unit, the flat circular electric circuit. We consider all electrons of the F- ion to circle on an equatorial ring with radius r. We consider the F- ion containing ten electrons. The theory of the mole susceptibility of the ion then states that its value is Avogadro's number times the common factor times the number of electrons in the ion times the square of the radius.

For the mole magnetic susceptibility of the F- ion, the only value we deduced from experiment relates to only one unknown of the model, the radius. The model's resulting value for the radius is 0.0603 nm (nano-meter, $10^{-9}$m). We interpret the radius as a kind of location

average for the time averaged distance the electrons are away from the nucleus in the $F^-$ ion.

The susceptibility derived average radius of the $F^-$ ion is only about half the radii estimated from X-ray analysis. The X-ray data leans on the structure of LiF crystals. The nature of the structure is approximated by thinking of the ions as close-packed hard spheres. LiF has a face-centred cubic structure. In the hard sphere approximation, we can perceive a normal F- ion as an ion that takes place in a vacancy in the lattice. The experimentally observed diamagnetism indicates that, just as in theory, the model holds to a first approximation. In this approximation, the fluor ion can rotate freely in the available space, although the symmetry of the vacancy, hosting the F- ion in the crystal, is not spherical.

We have to weaken the hard sphere model. The outer part of the F- ion orbitals, the low electron density regions extend out of the vacancy. It interacts with the "crystal field" which is build up by the electron density orbitals of the neighbouring ions. The outer parts of the orbitals of neighbouring ions fill the vacancy with a low electron density. We also have to weaken our assumption on the rigidity of the ion configuration. I have great difficulty to grasp the duality, the limit between the "rigid versus non-rigid" complementarities.

The diamagnetism of ions nevertheless indicates that the overlap of orbitals does not prevent the major part of the ion to rotate freely. The relatively smallness of the average radius, as derived from the susceptibility considerations, indicates that the major electron density is close to the nucleus, away from the vacancy's walls.

## 48 The ionic moment

The magnetic moment of a single $F^-$ ion is the susceptibility of the single ion times the applied magnetic induction field. For fixing the idea, we consider the moment the fluor ion acquires in the field of 1 tesla. At such a field is the moment very small ($\mu_F = 1.71 \times 10^{-28}$ $Am^2$). It is only twenty parts per million that of the Bohr magneton.

In quantum mechanics the moment associated with a single electron expresses in Bohr-magneton. We did it for the unpaired electrons in the Gadolinium containing glass. It also holds for the

orbital momentum. However, in the fluor ion all electrons are paired, their spins being anti-parallel. Out of an applied field, the total angular moment is zero. The internal magnetic quantum effects compensate each other. The resulting magnetic moment is zero. In the model, the quantized fluor ion entity, put in an applied field, rotates as a whole and the resulting moment expresses in a non-quantized classical way.

We simulate the moment as generated by our primitive current ring. The magnetic moment of such a ring is the current intensity times the area embraced by the ring. With the ring-radius derived in the former paragraph the ring-area is known ($1.14 \times 10^{-20}$ $m^2$). Given the ring area we can calculate the current intensity (0.0150 μA).

We now express the current intensity in terms of moving electrons. The current intensity is the product of the linear number density of the electrons, times the electron's electric charge times the velocity. The current intensity at a certain point on the circumference of the circuit relates to the charge that passes per second that point. The charge is expressed in Coulomb. One Coulomb per second is the equivalent of one ampere. The linear number density is the number of electrons per unit length along the path in the circuit. In the simple model of the fluor ion, the ion carries ten electrons. Those electrons circulate on the circumference of the ring. The circumference ($2\pi r$) being very small, the linear number density is very large ($2.64 \times 10^{+10}$ electrons per meter). As each electron carries the same electric charge ($1.60 \times 10^{-19}$ Coulomb) we can calculate their velocity. The electrons circulate along the circumference of the circular current circuit at a drift velocity easily reached with a bike (12.7 kilometre per hour).

Knowing the velocity, we can calculate the number of electrons passing per second at one point on the circle. The number is high although the drift velocity is not spectacular. The height of the number (93 Giga electrons per second) results from the smallness of the radius. Giga in physics is the expression for billion in the sense of $1\ 000\ 000\ 000 = 1 \times 10^9$.

As on each revolution of the ion ten electrons are passing, we derive that the Fluor ion, in a magnetic induction field of one tesla, makes 9.3 Giga revolutions per second.

Yet in the early days of superconductivity London noticed the similarity between the superconductive and the molecular state.

We here go into the comparison between persistent currents as they appear in ions versus those occurring in low temperature superconductors. In both cases at low enough temperature and low enough applied magnetic induction field, a field change in time induces currents in the sample. In both cases, the reaction to the field setting is diamagnetic. In both cases, the induced currents persist when the field increase stops and the applied field is kept constant. In both cases there is no process that decreases the kinetic energy of the electrons. The difference between the two cases concerns the magnitude of the diamagnetic moment.

The Meissner-Ochsenfeld model [48], for certain cases, relates the induced magnetic moment of simple superconductive samples to the complete expulsion of the applied field from the interior of the superconductor. For geometrical simple sample models, the spheroids, one calculates that a constant surface current density can completely compensate a homogeneous applied magnetic induction field. It simulates the Meissner-Ochsenfeld state. A mathematical equation, which takes in account geometry and dimensions, expresses quantitatively the model. The equation for thin oblate spheroids approximates well the induced magnetic moment in a thin superconducting disc. The experimental moment value is derived from the data given in Fig.2.2.b. Even when one questions the physics behind the model, the equation yields the right moment. Assuming that the equation still holds for much smaller dimensions, we apply the equation to the F- ion. We still consider the F- ion to be spherical symmetric. The magnetic susceptibility (the magnetic moment divided by the applied magnetic induction field) of the ion is proportional to the volume of the superconducting sphere. The radius derived from the Meissner-Ochsenfeld model is 4.75 pm. One pico-meter (1 pm = $10^{-12}$ m) is one millionth of a millionth of a meter.

The calculated radius of the superconducting region in the ion is only 7.9% of the radius derived by the quantum mechanical model or 3.6% of the radius derived by the X-ray hard sphere model. In the superconductive model the fluor ion, put in an applied field, has not to rotate as a whole.

The superconducting model for explaining the diamagnetism of the ion asks for some comments. If the model holds, it would be an expression of superconductivity at room temperature and above. In the classical low temperature superconductors two electrons interact by phonons forming a Cooper pair. The question rises whether for the ion

the presence of one nucleus and the orbitals are sufficient for a similar interaction? Do we need another interaction process? The assumption that the radius of the superconducting region can be of the same order in magnitude as the Compton wavelength of the electron raises the question whether the quantum electro dynamics has to come into play?

The same kind of discussion holds for the Li+ ion. The magnetic moment of the Li+ ion, estimated from the Klemm data, is about five percent of the moment of the F- ion. The radius of the superconducting region in the Li+ ion then is the cube root of five percent of the radius in the F- ion. The radius of the superconducting region in the Li+ ion still is of the same order in magnitude as the Compton wavelength of the electron.

The superconductive model is a post-experimental theory. We can not state that the superconductive theory expresses the physics behind the experiment. One experimental magnetic susceptibility figure does not allow making a choice between theoretical models. Only a disagreement can state that a theory does not explain the experiment. Later on we develop arguments the Meissner-Ochsenfeld model does not apply here.

## 49 About unpaired electrons

The diamagnetism of pure single crystal platelets of LiF is practically temperature independent. In a show-case they were stable for years. However, energetic irradiation damages them. We experienced with thermal neutrons as well as with gamma rays. Fig.49.1 reports on the paramagnetic susceptibility of a thin sample irradiated with neutrons.

From the point of view of magnetic susceptibility is the field and temperature dependence of the neutron irradiated sample familiar to us. The susceptibility relates very well to the Brillouin function. However, compared to the Gadolinium Meta-phosphate (Fig.2.2a) the field dependence at low temperatures (right above in the figure) is much less in LiF. The reduced saturation effect expresses the reduced magnetic moment of the Brillouin centre in the LiF case. In the latter case, the pattern fits well with the theory of the moment of one single unpaired electron per Brillouin centre.

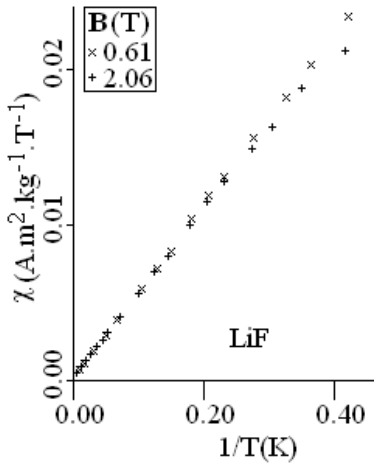


*Fig.49.1 reports on the paramagnetic susceptibility of a thin platelet of a LiF single crystal irradiated with $2x10^{19}$ neutrons per $m^2$. The magnetic susceptibility of the un-irradiated sample has been subtracted from the experimental value measured on the irradiated sample.*

The optical spectrum, taken on the crystal, indicates that more than one kind of colour centre occur in this alkali halide. The colour centres are attributed to F, M and R centres.

The Brillouin behaviour indicates all magnetically active centres carry only one unpaired electron and do not interact magnetically with other centres [49].

The "Brillouin" analysis of the susceptibility data yields an unpaired electron concentration. In the Fig.49.1 case, only 0.039% of the fluor ions are replaced by single electrons.

Fig.49.2 outlines one plane of the LiF crystal in a hard sphere approximation. Irradiation induces F centres. An F centre is the result of the escape of a fluor atom leaving one electron in the fluor ion vacancy. In the drawing, the square serves only to catch the eye. Two adjacent F centres result in an M centre. In the M centre the two electrons pair anti-parallel in a way no magnetic moment is left. An R centre is an F centre adjacent to an M centre. The R centre carries only one unpaired electron. From the point of view of magnetism, all magnetically active centres in our irradiated LiF crystal carry the moment of one unpaired electron. The M centre is magnetically not active.

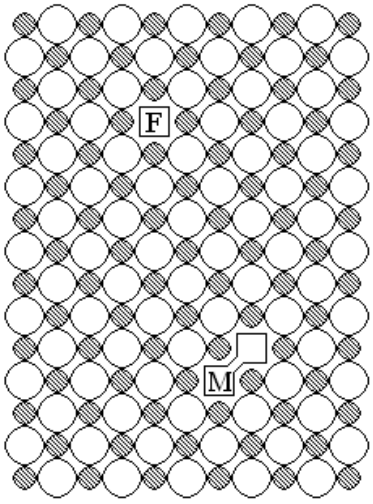


*Fig.49.2 outlines one plane of the LiF crystal in a hard sphere approximation. Irradiation induces F centres. The F centre is a fluor ion vacancy in which one electron is left. Two adjacent F centres result in an M centre. In the M centre the two electrons pair anti-parallel in a way no magnetic moment is left.*

The relative low concentration in a sample wherein different kinds of centres occur indicates an attractive interaction plays between the centres. The model implies an attraction range about 2 nano-meter. The susceptibility of the sample with different kinds of centres relates well to one single Brillouin function. Only the magnetic moments of single unpaired electrons were detected. It indicates, F centres are or isolated or aggregated. In the aggregations, the pairs are anti-parallel with the moments completely compensated.

At lower neutron doses, the optical spectra indicate the ratio of the F centres versus the M and R centres is larger. The F centres are the primarily formed defects at the irradiation. During irradiation newly formed primary F centres coagulate with existing aggregates.

The low concentration together with the relative small moment per Brillouin centre explains why the Weiss field can be neglected in the Brillouin analysis.

The following up of the evolution of the susceptibility of the LiF crystal with increasing irradiation dose was rather monotonous from the point of view of magnetism. In most cases, we reduced the boring effect by measuring only at three different temperatures. In the higher temperature region, not needing liquid helium, the Curie approximation was sufficient for our purpose. The susceptibility is practically field-independent. We needed two measuring points for defining the linear relation between susceptibility and reciprocal temperature, yielding an unpaired electron concentration. The third

measurement served for checking the linearity, i.e. the Curie law still holds in the particular situation.

In the LiF case, susceptibility measurements were only a utility tool for following the radiolysis of the crystal. However, we enthusiastically welcomed the appearance of the indication for the presence of the expected metallic lithium phase.

**50 The Pauli-paramagnetism** [50]

The model in which, during irradiation, newly formed primary F centres coagulate with existing aggregates not only holds for neutron irradiated samples but also for gamma irradiated crystals. The difference in the concentration density of the primary F centres at the irradiation only plays a minor role.

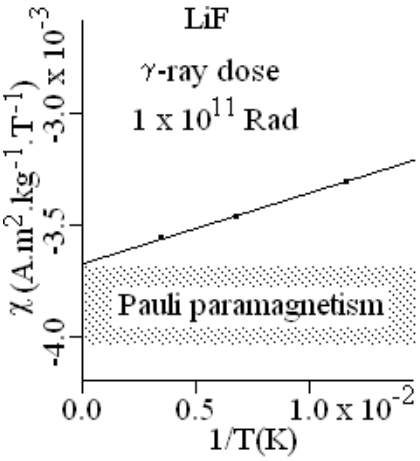


*Fig.50.1 reports on the diamagnetic susceptibility of a thin platelet of a γ-irradiated LiF single crystal. The dotted region indicates the presence of a temperature and field independent paramagnetic susceptibility, referred to as the Pauli paramagnetism.*

As we predicted, we observed also the indication for the radiolysis of LiF crystal by gamma radiation. Fig.50.1 reports on the essence of the statement. We analysed the marks in the figure, the experimental susceptibilities, as the superposition of two contributions, a temperature dependent part and a temperature independent part.

The temperature dependent contribution obeys the Curie law. The analysis of the data indicates that 0.021% of the originally present fluor ions are replaced by a magnetically isolated single electron.

The underlying temperature independent contribution is diamagnetic ($-3.65 \times 10^{-3}$ $A.m^2.kg^{-1}.T^{-1}$). Just as in the $La_{1-x}Gd_x(PO_3)_3$ glass sample with small x, at the higher temperatures the resultant

effect of the limited number of paramagnetic Brillouin centres becomes so small that the underlying diamagnetism prevails. However, the diamagnetism is not that of the un-irradiated LiF crystal. A practically temperature independent paramagnetism compensates partly the original diamagnetism. We interpret the compensation as due to the Pauli paramagnetism.

An F centre, with its single electron, always is adjacent to a Li+ ion. Such a configuration can be seen as a Lithium atom in a somewhat peculiar form. Larger aggregations of F centres therefore are nothing else than metallic Lithium. In the metal the inter-atomic distance is much smaller than the orbital a valence electron would occupy in a single Lithium atom in free space. In the metal the orbitals of the Li atoms mix in the whole neighbourhood. The electron does not stick to one single Li+ nucleus. The translational aspect becomes of greater importance. In the mathematical approach the Bloch function expresses the plane wave character of the state an electron occupies travelling through the lattice. No one electron has the same electronic state as another one. The Pauli Exclusion Principle holds. Each state is related to certain energy. The interplay between the wave character of the travelling electron and the periodicity of the lattice result in limitations of physically realisable states. The available energy levels situates in a band. In a metal all possible energy levels in the band are not occupied. The states with the lowest energy are preferentially filled. In the model at temperature zero all energy levels are filled up to the Fermi level. In this situation all electrons are paired as in the M centre. However, at variance with the situation in the M centre, in the metal at about room-temperatures the thermal agitation can excite electrons into more energetic states. One electron in an excited state is single and its magnetic moment is not compensated. The easiness of excitation depends on the energy level density near the Fermi level. At higher temperatures, the thermal agitation excites more electrons. However it also reduces the average moment of each electron. In a first approximation, the effect of a higher number of unpaired electrons is compensated by the reduction of the average moment per electron.

The magnetic susceptibilities of a LiF thin crystal platelet, irradiated to a high radiation dose, indicate that magnetically isolated Brillouin centres and metallic Lithium coexist. We did not observe any indication for something in between.

In the analysis of the data in Fig.50.1 we did not mentioned the diamagnetism introduced in the metal by a change of the magnetic induction field. Nevertheless the effect of the Maxwell law in question still exists. The currents induced are known as Eddy-currents (Foucault currents in the francophone regions). Differently with what happens in superconductors, in normal conductors the currents do not persist. Features as impurities, lattice misfits and distortions scatter electrons. The currents die out. The transient effect is not detected by our quasi static magnetic susceptibility measuring apparatus.

The magnetic susceptibility experimental data are interpreted in agreement with the models for the electronic conduction. However, the susceptibilities do not indicate why there is a difference in persistence between normal and superconducting currents.

## 51 Wiedemann's additivity law

The Wiedemann's additivity law states the magnetic mass-susceptibility of a mechanical mixture is the sum over all components of the product of the mass susceptibility times the weight fraction of each component [51]. Fig.51.1 reports on an experience we got with a mixture of copper aluminium powder.

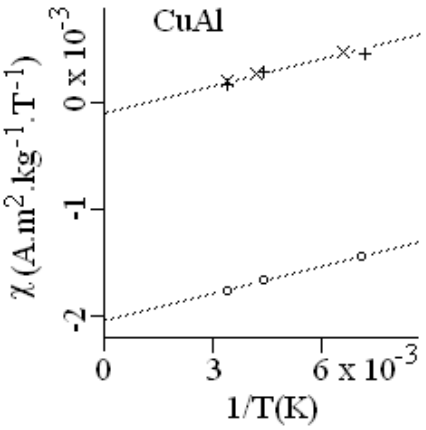


*Fig.51.1 reports on the susceptibility of three copper aluminium powder samples (12.3 weight % Al). + indicates the sample as pressed. The two others, were heat treated for one hour in hydrogen, X at 300 °C and* O *at 400 °C.*

In the early days of the construction of our susceptibility apparatus we were eager to find a material with susceptibility zero. In theory, such material would be favourable for constructing the balance pan, no field induced force and a pan heavy enough to stretch the suspension wires, good for positioning. One of our attempts was a profound mixture of aluminium and copper powder. The basic idea

was to compensate the diamagnetism of copper with the paramagnetism of aluminium. The intention exposed naivety, being not aware off the presence of a substantial ferromagnetic component in most commercial metals.

We studied three sample platelets of the pressed mixture of 14 g aluminium with 100 g copper powder. Two samples were heat treated under a hydrogen atmosphere. Sintering the powder aimed a mechanical stronger material. The hydrogen prevented the oxidation of the compound.

From the point of view of zero susceptibility balance pan the experiment was a failure. The samples were contaminated by a ferromagnetic component. The degree of contamination was different for the three samples.

From the point of view of the additivity law of Wiedemann the situation is less dramatic. Although our experiment is no paragon of precision, the measured susceptibilities can be analysed in agreement with the additivity law when we accept the possible presence of reasonable uncertainties on all data.

We got our samples by friendly turn. We have no feeling how precise the composition of the mixture was. Neither have we an idea about the impurity level of the composing materials. Calculating the susceptibility of the powder mixture we used for the powders the susceptibility values mentioned in literature for the solid metals. For the susceptibilities we took no uncertainties in account.

Analysing our measuring data, we corrected the experimental susceptibilities for ferromagnetism. Fig.51.1 reports on the corrected data. The resulting susceptibility at room temperature is much lower than the absolute value of the susceptibility of each of the components. The diamagnetism of the copper largely compensates the paramagnetism of aluminium indicating the additivity law holds. However, the room temperature mass susceptibility of the mixture was calculated for being negligible compared to the value obtained by the experiment. The observation expresses the precision of the experiment on the aspect of the additivity law is limited.

The correction for ferromagnetism seems to be good as indicated by the mutual agreement between the resulting susceptibilities for the sample as pressed and the sample heat treated at 300 °C. The

statement implies we assume the mutual agreement indicates the heat treatment at 300 °C did not alter noticeably the sample.

The resulting susceptibility is temperature dependent. The linearity of the susceptibility versus reciprocal temperature points towards the presence of Brillouin centres as possible impurities. However, when pure aluminium metal is present the temperature dependence of its susceptibility accounts for about 20% of the temperature dependence of the susceptibility of the mixture. We found in literature indications the same kind of temperature dependence may hold for pure copper. Therefore only part of the slope of the linear reciprocal temperature dependence can be attributed to Brillouin impurities. Correcting for the impurity effect partly reduces our experimental susceptibility value we yet corrected for ferromagnetism. The underlying susceptibility of the pure mixture one can explain by reasonable small deviations from the used parameter values.

The additivity law of Wiedemann can be looked on as an extrapolation of the additivity technique we used discussing the ionic susceptibility. A macroscopic effect is the sum for all entities of the effect of each entity. The statement holds as long as each single entity keeps its own peculiarity. We consider here each powder grain as an entity in the mixture. Fig.51.1 reports on a typical case in which the physical property of the single entities does not remain constant. The heat treatment at 400 °C changed the intrinsic susceptibility of our CuAl sample.

The magnetic susceptibility of the 400 °C heat treated copper aluminium powder sample is diamagnetic. The diamagnetism is about the susceptibility calculated from the Klemm data for the mixture of $Al^{3+}$ and $Cu^{1+}$ ions. The coincidence indicates that the susceptibility component which should be attributed to the valence electrons is strongly reduced.

We are again confronted with a restriction inherent on the magnetic susceptibility. The susceptibility result does not yield a model. The imagination of the analyser together with new information can point to a certain model. Knowing from literature that the Hume-Rothery-γ-phase of an Al-Cu-alloy is strongly diamagnetic we assume the diamagnetic susceptibility of valence electrons trapped in orbitals approximately compensates the paramagnetism of the valence electrons retained in the conduction band of our mixture. The change

in susceptibility indicates a change in the solid state of the sample material.

## 52 Peierls distortion

We found indication for a Peierls distortion in the static magnetic susceptibilities measured on a single crystal of the mixed-valence platinum compound, $K_2Pt(CN)_4Br_{0.3}.nH_2O$. Deltour from ULB (B) [52] procured us with some ferromagnetism free single crystals. Fig.52.1 reports on the susceptibility in the temperature domain of interest.

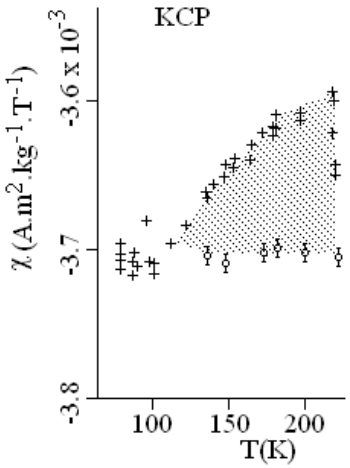


*Fig.52.1 reports on the susceptibilities measured, from lower to higher temperature, on a single $K_2Pt(CN)_4Br_{0.3}.nH_2O$ crystal. Crosses report on values measured at the indicated temperature. The marks* O *are measured at liquid nitrogen temperature after the sample reached the indicated temperature.*

The component of the magnetic susceptibility, the dotted region in Fig.52.1 between the + and O marks, we attribute to Pauli paramagnetism. We relate it to the magnetism of conducting electrons.

In $K_2Pt(CN)_4Br_{0.3}.nH_2O$ the platinum atoms form linear chains. Although the crystal on the whole is three-dimensional the chains can be considered, at room temperature, as "quasi one-dimensional metallic" electric conductors. Below 100 K the material is electrically insulating.

The importance of the investigation lies in the correlation of the relative ease with which one dimensional (1-D) systems can be handled theoretically and the possibility to detect experimentally the calculated effects. Peierls showed that theoretically in the one-particle

approximation the 1-D metallic state becomes unstable. The linear electron system should transform spontaneously into an insulator. In our perception of the susceptibility data the thermal agitation keeps the material in the conducting energetically higher state. At reduced thermal activity, the material turns into the insulating ground state.

Our knowledge of the Pauli-paramagnetic contribution is not very precise. The quantitative analysis leans on the assumption the underlying diamagnetism of the sample remains temperature independent. However it is an assumption as a susceptibility measurement yields only one value, the total susceptibility. It does not differentiate between the para- en dia-magnetic contributions. In Fig.52.1 the O marks all relate to measurements carried out at liquid nitrogen temperature. The constancy of the susceptibility only indicates the physical state of the sample at low temperature remained the same while the sample temperature rose up to the temperature indicated by the O mark.

The disappearance of the Pauli-paramagnetism at about 100 K we perceive as the magnetic counter part of the metallic-insulator transition.

At variance, I am in the dark for which effect the apparent paramagnetic susceptibility component decrease at 220 K expresses. The temperature coincides with the onset water escaping “violently” from the crystal into the vacuum.

For being able to measure the data in Fig.52.1 we were obliged to cool the water contenting crystal down to somewhat below 220 K in a moist atmosphere and afterwards pump off the air and switch over to He at reduced pressure. The He, free from impurity gases, prevents condensation on the sample. In such an atmosphere, the water-vapour pressure is extremely low. In a dry atmosphere a single crystal at room temperature loses its metallic copper glare and becomes black. The water diffuses smoothly out. The diffusion process is reversible. In a moist atmosphere the water diffuses in the crystal. Below 220 K, water molecules remain solidly trapped in the crystal.

## 53 Free radicals

A tendency exists to call any molecule possessing an odd number of electrons a “free radical”. Times ago I hoped for a free radical as reference material. The vitreous Gadolinium Meta-phosphate showed some drawbacks. The centres interacted magnetically by the Weiss field. In the diluted Lanthanum-Gadolinium system, in which the Weiss-field can be neglected, the Gd concentration is not precisely known. I hoped that one could do better by taking a sample of one kind of large molecules each with one single unpaired electron. Taking one kind of molecules would be favourable for the precision on the concentration of the unpaired electrons. The largeness of the molecule should reduce the concentration of centres beyond a noticeable Weiss effect. I hoped the remainder of the large molecule could be magnetically inert avoiding the unpaired electron to interact with its neighbour by exchange coupling. Fig.53.1 reports on the susceptibilities of two solvent-free 2,2-diphenyl-1-picryl-hydrazyl (DPPH) samples procured by Grobet KUL B [53].

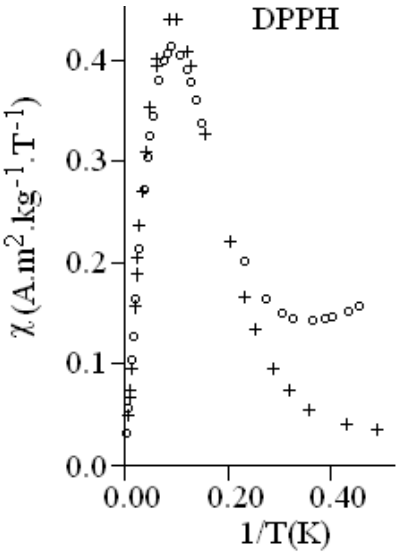


*Fig.53.1 reports on the susceptibilities of two solvent-free 2,2-diphenyl-1-picryl-hydrazyl (DPPH) samples. The + marks indicates values taken on a powder sample. The O marks indicate data taken on a more crystallized needle.*

Fig.53.1 indicates DPPH is not useful as a susceptibility reference material. At first, it does not relate simply to the Brillouin function. Moreover, it seems very difficult to get pure free-radical samples.

The paramagnetism above 150 K relates well to a Brillouin function. The susceptibility reduction in the lower temperature region we perceive as due to electron pairing of neighbouring free radicals.

Here again, the model states a lower thermal agitation results in a higher concentration of pairs.

In the needle, the susceptibility below 2.7 K increases with reciprocal temperature. The pairing with lowering temperature is not anymore going on. Isolated Brillouin centres may be stabilized by diamagnetic molecules.

Preparing free radicals it is difficult to avoid the oxidized form, the hydrazine, in which no unpaired electron occurs. Fig.53.1 indicates in the needle more hydrazine molecules replace free radicals. The indication leans on the fact that in the higher temperature region the paramagnetism in the needle is less than in the powder sample. Moreover, in the very low temperature, more diamagnetic hydrazine molecules may stabilize more unpaired electrons, insulating these from other unpaired electrons.

The magnetic susceptibility of the needle, measured at a temperature about 4.3 K, was isotropic within the experimental accuracy.

In a DPPH sample in which the free radicals were separated by deuterated benzene the paramagnetism related much better to the Brillouin function for single unpaired electrons. However, at room temperature the sample is not stable, the benzene slowly diffusing out.

## 54 Magnetic susceptibility and the chemical bond

Let us return to the polyatomic compounds with no resultant electron spin. Interpreting the underlying diamagnetic mole susceptibility of our $La_{1-x}Gd_x(PO_3)_3$ glass sample we used the ionic values based on a compilation by Klemm. The agreement leans on the minor importance we could attach to the interaction existing between the entities.

The influence of the chemical bonds can not be ignored anymore at the interpretation of the magnetic susceptibility of diamagnetic organic molecules. Pascal developed empirically an incremental (additivity) system in which appeared also terms depending on particular structure elements. He published his system in a period the atomic theory outgrew the state of being a handy terminology for a

hypothetical model. It was in a time much before quantum mechanics were developed and earlier than the compilation work of Klemm appeared in literature.

Since then, many researchers worked on “variants of the same theme” improving the system. Van Vleck [54a] stated that Pascal’s results must be regarded as distinct evidence favouring quantum mechanics. Haberditzl [54b] developed a half empirical incremental system. The susceptibility increments, due to core electrons and to electrons in free electron pairs, are quantum mechanically calculated. He argued the magneto-chemical method for studying magnetic compounds approaches better the physical meaning. The empirical formal scheme of Pascal and his school, which assumes that the carbon atoms possess an unchanging diamagnetic increment, independent of the type of the C-C bond, lacks such physical significance. Haberditzl states that in many cases the calculated values are more precise than the empirical ones. However, for the chemical bonds he could not without empirical susceptibility contributions.

In our work we also were confronted with the problem of a chemical bond related susceptibility contribution. I perceived an anisotropy of the magnetic susceptibility, measured on single crystals of $K_2Pt(CN)_4Br_{0.3}.nH_2O$, as due to a chemical bond. Fig.54.1 shows measured susceptibility data plotted versus the angle indicated by the position pointer of the electromagnet.

Our analysing result, given by the dotted line in Fig.54.1, fits rather precisely the data. Calculated in relation to the maximum susceptibility difference, the relative standard deviation of the measured data from the fitting function is a quarter percent. Mathematicians will argue that you always can precisely fit data when you introduce enough functions. In the present case the fitting equation contains only tree terms: a constant one, a linear angle dependent one and a symmetrical bell shaped angular dependent one. In our perception, all three have a physical meaning.

The angular independent constant term in our fitting expression refers to an average diamagnetic susceptibility. The angular depending terms relate to the susceptibility modulation about the average. Attributing the whole modulation to a genuine susceptibility effect is an extreme case which goes against the physical structure. An equally strong argument does not exist against the other extreme case which assigns the whole modulation to a mere consequence of measuring

errors. The internal consistency of more anisotropy measurements indicates the anisotropies are reproducible to ten percent.

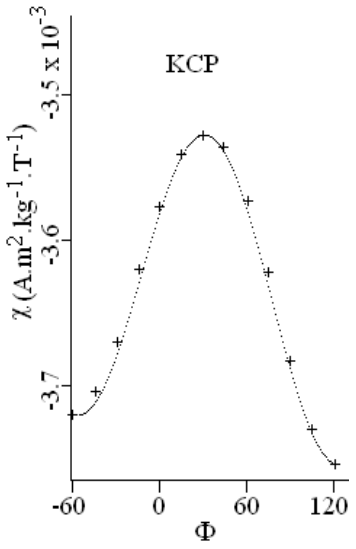


*Fig.54.1 shows the angular dependence of the diamagnetic susceptibility of single crystals of the mixed-valence platinum compound $K_2Pt(CN)_4Br_{0.3}.nH_2O$, measured at a temperature about 130 K.*

The time we measured the KCP crystals I did not found any information on the magnetic anisotropy of the triple CN bond, neither empirical neither quantum mechanical. My knowledge on quantum mechanics is too passive to tackle the problem. My interpretation leans on qualitative arguments. We discuss a model based on the structure of the material, the essence of which is given in Fig.54.2. The structure element, drawn in Fig.54.2, lies in the plane described by the direction of the magnetic field on rotating the electromagnet.

The platinum atoms form a one-dimensional electric conductive chain. Perpendicular to the chain each Pt has four CN molecules. Only the CN groups lying in the same plane are drawn.

At different angles the field sees a different aspect of the structure. Due to the symmetry of the structure the field sees the same configuration when the electromagnet rotated over half a turn. From the structural point of view, measuring at different angles over a range of 180 degrees is sufficient for determining the susceptibility. From this structural point of view, the difference in susceptibility values between the angle Φ -60 and +120 can not be due to a difference in susceptibility of KCP.

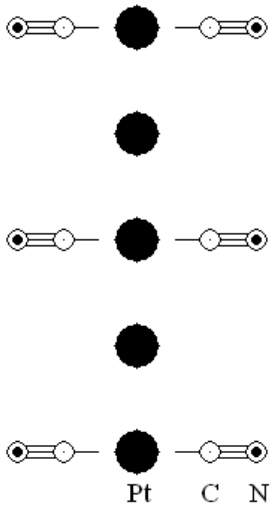


*Fig.54.2 outlines the basic elements we need for understanding the structure symmetry of $K_2Pt(CN)_4Br_{0.3}.nH_2O$, related to the susceptibility. The platinum atoms form a one-dimensional electric conductive row. Perpendicular to the row each Pt has four CN molecules. Only those lying in the same plane are drawn.*

The apparent difference in susceptibility is due to an apparatus related deviation of the local field and gradient from the values used at the calculations of the susceptibility. The balance pan does not remain in the same position on lowering the temperature in the cryostat. Fig.13.2. shows it. The sample therefore is not always exactly positioned on the axis of rotation of the electromagnet. The magnetic induction field and gradient are not cylindrically symmetric around the axis of rotation of the electromagnet. The values of the local field and gradient at the sample deviate from their values at the rotation axis.

The relative difference between the susceptibilities at the angles Φ -60 and the Φ +120 is about one percent. It does not mean that the field and gradient differed by the same relative amount. The largest part of the difference is due to the diamagnetic susceptibility of the balance pan which, in the calculations, is only corrected for by a constant angle independent value related to the field and gradient at the rotating axis.

In our analysis of the susceptibility data we approached the correction by a linear function of the position angle. The line is fitted to bring the measured susceptibility value of angle 120 to that of angle -60. Such approach implies the interpretation our measuring data for angles in between to be sample susceptibility related.

The second angular dependent function we used to fit the dotted line to the experimental data, in Fig.54.1, is symmetrically bell shaped. In this fitting is the maximum relative difference in susceptibility 6 percent. The maximal diamagnetic susceptibility is measured when the field is perpendicular to the one-dimensional Pt chains. This direction coincides with the triple bond direction of CN molecules. The coincidence is the reason why we related the susceptibility anisotropy with the chemical bond.

The symmetrically bell shaped function is the angular unfolding of the elliptically symmetric susceptibility when the sample rotates about an axis perpendicular to the one-dimensional Pt chains. In three dimensions we describe the susceptibility of KCP by an oblate spheroid with its rotational symmetric semi-axis along the Pt chains.

The average mol-susceptibility of $K_2Pt(CN)_4Br_{0.3}.nH_2O$ compares rather well with the Klemm addition value ($-16.5x10^{-4}$ $A.m^2.mol^{-1}.T^{-1}$). For the comparison, we built KCP up by ions. The ions, K(1+), CN(1-), Br(1-) OH(1-) and H(1+) all appear as such in Klemm's compilation table. For Pt(2.3+) we interpolated between Klemm's Pt(2+) and Pt(3+) values. The absolute value of our result is only by 6% lower than the Klemm value. The overall agreement of the diamagnetic susceptibility indicates KCP is a polyatomic compound with no resultant spin.

In the Klemm approach is the susceptibility increment for the $CN^-$ molecular ion an average value ($-1.8x10^{-4}$). The analysis of our anisotropy indicates the magnetic mole susceptibility of the cyanide molecular ion in a field directed along the CN connecting direction is 40% more diamagnetic than the average. In a direction which is perpendicular to the connecting direction, it is 20% less.

Our model is rather simple. In fact, KCP is much more complex. E.g. we did not consider the water molecule although it neither is spherically symmetric. We have no idea about its orientation, so we neglect the possible effect. We again are confronted with the restriction inherent to our susceptibility measurements. The result does not yield a model.

## 55 Van Vleck susceptibility

The diamagnetic susceptibility of a Lithium-Fluoride crystal we approximated as built up simply by the addition of the diamagnetism of the ions. Each ion is an entity on its own. Each entity of the same kind contributes to the same amount. The interaction between the entities is of minor importance. The ions have no resultant electron spin. Field free, the ions have no magnetic moment. Putting on the field induces a diamagnetic moment. The moment is attributed to persistent currents in the ions. The susceptibility for creating moment is field and temperature independent. The interpretation of the diamagnetism leans on quantum mechanics. In this system the diamagnetism relates to electrons in their orbitals. Each orbital relates with energy. There are lots of orbitals of which only those of lowest energy are filled. When the energy of orbitals is sufficiently different the orbitals do not mix. This is, in short, the basis on which our discussion on the Van Vleck susceptibility leans.

The quantum mechanical susceptibility expression of Van Vleck is the sum of two terms, a diamagnetic and a paramagnetic one. Dorfman [55] formulated the experimental susceptibilities in his context as $\chi = \chi_d + \chi_p$. A measured susceptibility value can mathematically be equalized by an infinite number of such contributing pairs. However, we are in search for that pair which has a physical meaning.

Dorfman knew some polyatomic systems exhibit anisotropic susceptibility. The anisotropy was for him a direct result of the Van Vleck paramagnetism. Dorfman perceived the Van Vleck equation as a perturbation calculation. In such calculations relatively small effects are accounted for by relatively small correction terms. Dorfman considered the main diamagnetic term as due to spherically symmetric entities. He followed Van Vleck who, in his paragraph on “molecules without a resultant spin”, used for the diamagnetic term of the susceptibility the expression related to spherically symmetric entities.

For an experimentalist the calculation of the diamagnetic Van Vleck term is a rather difficult task. Dorfman circumvented the difficulty. He used for his $\chi_d$ value the $\chi_d$ value calculated by Kirkwood. Kirkwood derived quantum mechanically for radial symmetrical systems, the experimentally measured static electric polarizability is proportional to the square of the difficult to calculate

part of the diamagnetic Van Vleck term. Kirkwood related the diamagnetic Van Vleck term to the electric polarizability. The combination resulted in expressing the Van Vleck diamagnetism to be proportional to the square root of the product, polarizability times the number of electrons involved in the system. Dorfman showed that in a number of cases the experimental susceptibility minus the Kirkwood diamagnetism practically equals zero. The agreement between experimental and Kirkwood diamagnetism indirectly indicates, for spherically symmetric ions the underlying quantum mechanical theory describes well the experiment. In the cases where the Kirkwood diamagnetism was different from the experimental one, the experimental one was often less diamagnetic. This observation stimulated Dorfman to attribute the difference to a paramagnetic Van Vleck term.

We situate the Dorfman model treating the magnesium oxide case. Fig.55.1 reports on our experimental quasi static susceptibility values measured on an MgO single crystal. We analysed the susceptibilities as being composed of two contributions, a temperature and field independent diamagnetism and Brillouin related paramagnetism.

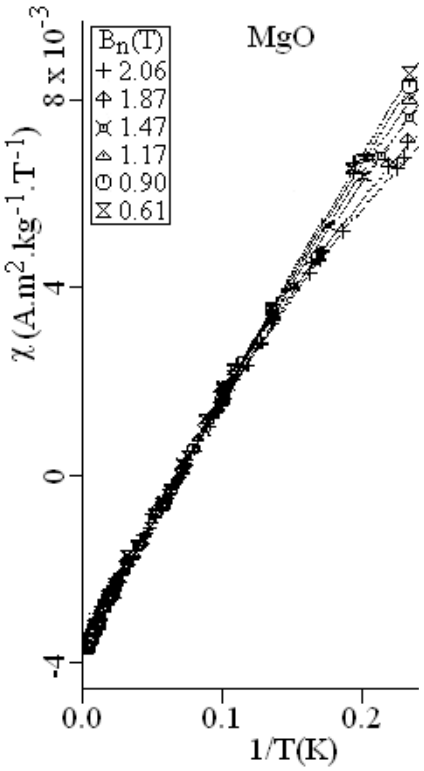


*Fig.55.1 shows the static magnetic susceptibility of a single crystal of MgO at different temperatures and magnetic induction fields. The susceptibility has two components, a temperature and field independent diamagnetism and Brillouin related paramagnetism. The former is attributed to MgO while the latter to iron impurity.*

What is our experimental value for the mole susceptibility of MgO? From Fig.55.1, by extrapolation to reciprocal temperature zero, we deduced the mass susceptibility. We then transposed the mass- into the mole susceptibility. The result is -1.52, expressed in ten to the minus four ampere square meter. What is the Klemm expectation value? The addition of the $Mg^{2+}$ and the $O^{2-}$ term results in -1.5. The agreement is exceptionally good for this kind of comparisons.

What figures Dorfman used for the mole susceptibility? He used for the Kirkwood diamagnetism -1.84 and for the experimental value of the diamagnetism -1.02. He interprets the difference +0.82 being the Van Vleck paramagnetic contribution to the susceptibility. Our experimental data, strengthened by the Klemm result, indicates the magnitude of the experimental mole susceptibility of MgO used by Dorfman is too low.

It seems the sample Dorfman referred to was not pure. At the time Dorfman published his book, some refractory materials were not available without ferromagnetic impurities. Later in 1978 Ed. Sonder from ORNL USA procured us with some, for that time, very pure single crystals. We did not observe ferromagnetism in those samples. The fan-wise low temperature pattern put its stamp upon the kind of susceptibility. The paramagnetism relates with Brillouin centres. The fan spread points to iron ions being the paramagnetic centres. Because iron occurs in two ionic states, two and three plus, the analysis of the paramagnetism is more complex than in the Gadolinium case. Although there remain uncertainties on the precise iron concentration, the paramagnetism indicates only about one in fourteen thousand Mg ions being replaced by an iron. From a chemical point of view the samples were very pure.

Although the susceptibility of the MgO samples is expressed in two terms which both have a physical meaning, nobody will perceive here the paramagnetic term as a Van Vleck term. We consider the system as rather trivial. The diamagnetic term is attributed to pure MgO while the paramagnetic term to iron impurity. The latter relates with Brillouin centres which have, in the ground state, electron spins.

In the Dorfman approach our experimental diamagnetic susceptibility value, which remained after correction for the paramagnetic impurity effect, is considered as built up of two terms. When the larger diamagnetic term is approximated by the Kirkwood diamagnetism a paramagnetic correction term is needed to explain our

experimental diamagnetic susceptibility value. Using our data the correction term is much smaller than the term reported by Dorfman. However, the smallness of the correction term is not an argument against the Dorfman interpretation, attributing the correction term to Van Vleck paramagnetism.

## 56 Increments

The empirical incremental susceptibility system evolved since Pascal. Haberditzl attributed susceptibility increments to parts of atoms, to cores and to bonds. The increment implies physical independency of the subatomic entity in the molecule. It suggests the persistent currents only flow in a limited region. The Meissner-Ochsenfeld model fits such request. The experimental increments given, the moment allows calculating the radii of the superconducting region being of the order of a few pico-meter. Such approach is at variance with the Dorfman approach. Dorfman, in his paragraph "susceptibilities of covalent bonds" in "Diamagnetism and the chemical bond", attributes to the triple bond in the CN(1-) molecular ion two values: a larger diamagnetic (Kirkwood like) one and a smaller paramagnetic (Van Vleck-type) one. The Meissner-Ochsenfeld model sustains only a diamagnetic term.

Let us look for the consequences of an increment. The increments on its own do not explain anisotropy. For fixing the idea we consider a cyanide molecular ion ($CN^-$). The elder valence-bond structure formulation considers three groups of valence electrons in the molecular ion. In the middle between the carbon and the nitrogen nuclei form the three electron pairs the triple bond. On the outsides of the molecule each of the two free electron pairs is considered as a group. The centres of gravity of each electron group all are in line with the carbon-nitrogen connecting direction. The main contribution to the magnetic susceptibility of the cyanide ion relates with the valence electrons. Interpreting the main contribution as the sum of three increments tacitly implies physical independency of the three electron groups referred to. It means you consider each electron group as an entity on its own. Putting on an applied magnetic induction field all three entities will respond independently from the others, becoming diamagnetic to an amount given by the increment. In such case it makes no difference whether or not the ion axis is in line with the direction of the field. In other words, in my perception dividing the

susceptibility in three independent increments can not explain the anisotropy.

One could try to save aspects of the model allowing physical interaction between the incremental entities. In the two-term perturbation calculation one can consider the larger diamagnetic term as a kind of magnetic polarization of a major entity. The smaller paramagnetic term then expresses the magnetic polarization of minor entities by the magnetic moment of the main polarized entity. When one considers the incremental entity as a dipole, the Weiss field generated by the triple bond moment is way out to small to induce a perceptible effect on the moment of the free electron pair dipoles. Moreover, the model drives the anisotropy in the wrong direction. In my perception, in search for an explanation of the anisotropy of the magnetic susceptibility physically independent increments will not help.

Concluding, you need physical interaction between the electron groups for explaining the anisotropy. The conclusion also implies that the Meissner-Ochsenfeld model does not apply here. The persistent currents in the ion are not able to completely shield certain regions of the molecular ion from the applied field.

## 57 An anisotropic diamagnetic susceptibility

Half a century of interest in magnetism modulated my perception of the magnetic susceptibility. We discuss now, in the later option, the diamagnetism of the cyanide molecular ion.

For explaining the susceptibility contribution of highly localized atomic core electrons we still use the incremental model. The carbon as well as the nitrogen atom has two electrons in the lower energy orbital, the K shell. We estimate their susceptibility contribution taking the Klemm value for respectively carbon four plus and nitrogen five plus. Each of them contributes relatively about half a percent to the averaged diamagnetic susceptibility of the $CN^-$ molecular ion. Even when this approximation is not very precise it will not harm further discussion because the relative smallness of the susceptibility contribution.

At variance with the highly localized core electrons, the ten valence electrons spread over the molecule in the molecular orbitals. We briefly discuss my perception of the quantum mechanical origin of the molecular orbitals.

Quantum mechanics gave a physical interpretation to the table of Mendeljev. It explains why carbon has four and nitrogen five valence electrons. The carbon and nitrogen valence electrons occur in the second atomic shell. The shell contains two kinds of electron density distribution atomic orbitals, the s and the p. The s orbital is spherical symmetrical. A p orbital is radial symmetric about one of the coordination axes. The energy related with the s-orbital is somewhat less than that related with the p-orbital [57a]. There exist three p-orbitals, orthogonal to each other, in the shell. In the free atoms, the three p-orbitals are equivalent.

It is difficult to picture an orbital as the electron density is not sharply limited by a surface. The electron density dies out the farther the considered location is away from the nuclei. To get nevertheless some feeling for the symmetry it is common use to draw a boundary surface. The surface embraces 90 percent of all electron density. Fig.57.1 outlines two examples.

For making a cyanide molecule a carbon atom combines with a nitrogen atom. The proximity of a second nuclear charge modulates the electron density distributions. By hybridization the atomic orbitals are going over into molecular orbitals.

For reason of simplicity we consider the model with limited possible combinations. We take in account only interactions between the same orbitals of both atoms. Only four interactions take place, s-s, $p_x$-$p_x$, $p_y$-$p_y$ and $p_z$-$p_z$. The combination of two such atomic orbitals results in two molecular orbitals, a bonding and an anti-bonding one. In the bonding one the larger part of the electron density is located in a region between the two nuclei. In the anti-bonding orbital a larger part of the electron density lies outside the two nuclei.

The molecular orbitals derived from the s-s and $p_z$-$p_z$ hybridizations are radial symmetric about the nuclei connecting direction, when the latter is chosen to be the z-axis. The molecular orbitals derived by the hybridization of $p_x$-$p_x$ or $p_y$-$p_y$ on their own are not radial symmetric about the z-axis. However, keeping in mind the orbitals are not sharply limited in space, the smooth electron density

distribution of the sum of both is practically radial-symmetrically distributed about the carbon-nitrogen connecting axis.

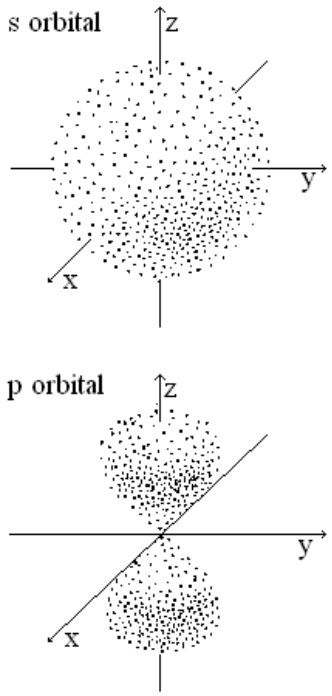


*Fig.57.1 Four atomic orbitals build up the shell concerning the valence electrons in carbon and nitrogen. One is spherical symmetrical, called s orbital. A $p_z$ orbital is radial symmetric about the z-coordination axis. There exist three orbitals of p type, $p_x$, $p_y$ and $p_z$, all perpendicular to each other. The figures are taken from "Electrons and the chemical bonding", by H.B.Gray, W.A.Benjamin Inc. Publ. 1965.*

The nine valence electrons (4+5) fill up the molecular orbitals starting with the lowest energetic one. At first two electrons populate (Pauli Exclusion Principle) the bonding orbital coming from the s-s interaction. Then two stay in the anti-bonding MO. Then five electrons occupy the bonding orbitals derived from the p-p interactions. The CN molecule fills up the latter molecular orbital picking up an electron from the nearby Pt atom, resulting in a cyanide molecular ion. The three p-p derived bonding orbitals filled refer to the triple bond.

The $CN^-$ ion has no resultant electron spin. We have not to deal with a strongly paramagnetic Brillouin centre. Magnetically seen, each ion is an entity on its own. As $F^-$ in LiF is $CN^-$ kept in the KCP lattice by ionic bonding. Covalent bonding keeps the carbon and the nitrogen together. At variance with $F^-$ the $CN^-$ ion is not spherical symmetric. Wikipedia cyanide data results in our Fig.57.2.

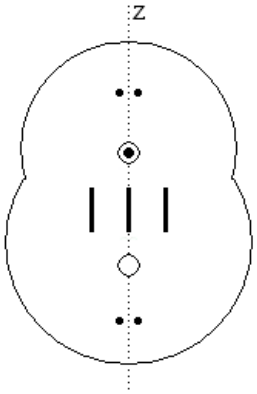


*Fig.57.2 is an artist conception of the cyanide molecular ion. The z-axis of our coordination set passes trough the nuclei. The open larger circle refers to the carbon nucleus, the one with the dot to the nitrogen nucleus.*

The contour in Fig.57.2 outlines the boundary surface in a plane in which the nuclei lie. Inside, figures the valence bond structure formulation of the cyanide molecular ion. The open larger circle refers to the carbon nucleus, the one with the dot to the nitrogen. The three bars in between the two nuclei refer to the triple bond. The outer dots stay for free electron pairs. Compared to the quantum mechanical approach is the structural formula a crude way to express the larger electron density situates in between the nuclei.

The model responds to the quest we formulated in the former paragraph wherein we argued the valence electrons all are in close contact with each other. However, the spread over the whole molecule does not imply the charge density to be homogeneous. Fig.57.2 indicates the charge density will be higher in a region between the two nuclei. The model agrees with the fist part of the statement “The presence of triple bonds concentrates electronic charge in the bond and decreases the magnitude of the diamagnetic contribution”. This statement Goudenough expressed yet in 1963 in the paragraph “molecules” in “Magnetism and the chemical bond”. The second part of the statement leans on the incremental susceptibility system comparing different chemical molecules. In the statement the decrease concerns a spatially averaged susceptibility value. We concentrate now on the orientation dependent susceptibility of one single molecular ion.

At first, we consider the susceptibility measured the magnetic induction field parallel to the carbon-nitrogen connecting direction. The omission of the x- and y-directions in the coordination set expresses there is no preferential direction for them. The CN- molecular ion is considered as an entity on its own, free to rotate about

the z-axis. The possibility to circle around allows “the Maxwell law”, on changing the applied field, to introduce persistent circular currents flowing in plains perpendicular to the carbon-nitrogen connecting direction. The diamagnetic susceptibility is largest in this direction. The relative magnitude agrees with the common expectation a radial symmetry being in favour with diamagnetism. The model is in line with the common perception. We slightly will modulate the picture, based on the following discussion.

The susceptibility measured the field perpendicular to the molecular ion rotational symmetry axis is less diamagnetic. We have to adapt the model for explaining the anisotropy. As the susceptibility does not yield a model we have to involve our imagination and all information we can get to propose one. The usefulness of that model will be judged later by history.

In search for a solution to the problem we return to our old recipe. We simulate the electron density cloud around the carbon and nitrogen nuclei by the contour. The rotational symmetry axis of the boundary surface lies along the carbon nitrogen connecting direction. The boundary surface embraces ninety per cent of all electron density. The rotational symmetry allows explaining the diamagnetism which is measured with the magnetic induction field along the symmetry axis, by the rotation of the molecular orbital. However, steric hindrance prevents the molecular orbital to rotate about an axis perpendicular to the carbon nitrogen connecting direction. We adapt the model introducing a super fluid charge density stream inside the molecular orbital. We expose our arguments.

We simplify further. In the simulation we relate the magnetic moment to the cross section of the contour. We know the magnetic moment is the product of the area of the cross section times the electric current flowing on the border of the cross section. The surface of the cross section at the plane which is perpendicular to the rotational symmetry axis is smaller than the surface of the cross section at the plane along the rotational symmetry axis. Experimentally, the induced magnetic moment in the former situation is larger than that in the latter configuration. Both statements are compatible with each other when the current in the former case is larger than in the latter case. Then the question rises what reduces the current intensity relatively in the latter case?

We consider at first the case of higher current intensity. Fig.57.2 indicates the positions of the centres of gravity of the charge densities in the valence structural approach. In the molecular orbital approximation the charge densities are more smeared out. The result is radial symmetric. A super fluid charge density stream flows inside the molecular orbital. The radial symmetry of the charge density in the molecular orbital expresses a homogeneous local fluid stream potentiality along the circular current circuit. As there is no locally reduced charge density along the circuit the relatively high intensity electric current is free to flow over the whole ring.

The current contour circuit in the mid-plane along the carbon nitrogen connecting direction passes through regions of lower charge densities beyond the two nuclei as the electronic charge is more concentrated in the region in between. The local fluid stream potentiality along the circuit is not homogeneous. In the simulation the location with reduced charge density, with lower current carrying potentiality, limits the current intensity over the whole circuit.

When the intensity is limited by the lowest charge density on its path the model implies the charge densities are not disturbed by the super fluid stream. Why the non spherical symmetric super fluid charge density stream leaves the region of reduced charge density unperturbed? The answer is the restoration of the local charge density is much faster than its perturbation. We estimated roughly the dimensions of the boundary surface on the basis of the triple bond length. The magnetic moment divided by the circuit surface results in the current intensity which is of the order of a small fraction of a micro ampere. The latter result yields, for the electric charges, a drift velocity of the order of a few meters per second. The information on charge density changes, by the Coulomb repulsion between the electrons, travels around about hundred million times faster.

The charge density distribution in the molecular ion, as defined by the molecular orbitals, practically has not to change on applying a magnetic field on the ion. Gray in his book [57b] “Electrons and chemical bonding” allocates to the CN- molecular ion a ground-state in which all spins are paired. In the ground-state the ion has no resultant electron spin. This is exactly the kind of entity which we discuss in the Van Vleck susceptibility. We leave the framework of the charge building undisturbed allowing a super-fluid to flow. The introduction of the internal flow in the ion results only in a diamagnetic effect caused by the applied field. We do not need

currents flowing in an opposite sense. In principle, we do not need a paramagnetic Van Vleck term. Introducing such a term is an expression of the inability to find a formulation for calculating the diamagnetism.

For finding a model for calculating the diamagnetic Van Vleck term of the molecular ion, the internal energy may be of interest. We take the product of the diamagnetic moment of the ion times the used applied field as measure for the energy involved in the super fluid circuit. Even with the highest magnetic induction field we used, this energy is a billion times smaller than the energy involved in the triple bond (Gray). In my perception, the high ratio makes it practically impossible to express, in a direct numerical calculation, the difference between the state of the ion before and after putting on the applied field. The stiffness of the charge distribution allows thinking of the possibility to use a kind of Born-Oppenheimer approximation, the separation of the variables. At first, you calculate the charge density distribution in the ion. You take it as a constant and store the data. You then try to find in the data indications for possible paths for the super fluid circuits.

## 58 The paramagnetic Van Vleck term

The quantum mechanical susceptibility expression of Van Vleck for a polyatomic molecule without a resultant spin has two terms, a diamagnetic and a paramagnetic one. Van Vleck mentioned the diamagnetic term is the larger in the commonest cases. A more interesting but less common situation arises when the paramagnetic term predominates. He further admitted substance having a feeble temperature independent paramagnetism will be difficult to measure. He nevertheless was confident some materials would fit his system. Between the candidates figured vanadium pentoxide.

My first contact with $V_2O_5$ single crystals dates from June 1968. Nagels SCK/CEN (B) procured us with a sample. The single crystal cleaves very easily. In practice we got only a thin platelet. Fig.58.1 reports on our magnetic susceptibilities measured in 1968 at room temperature on a single crystal.

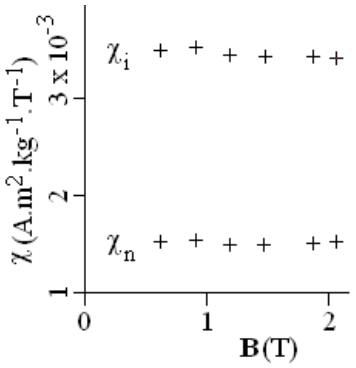


*Fig.58.1 reports on $V_2O_5$ susceptibilities measured in 1968 at room temperature on a single crystal. The field direction normal to the plane of cleavage yields $\chi_n$ while $\chi_i$ refers to in-plane field direction.*

The susceptibilities measured the direction of the applied field parallel to the cleavage plane are referred to by $\chi_i$ (in plane). When the direction of the field is normal to the cleavage plane the susceptibilities are referred to by $\chi_n$.

The pattern reveals anisotropy. The susceptibility is weakly paramagnetic. Not shown it's rather temperature independency down to the lowest temperature (63 K) we could reach at that time. The data do not have the precision we got later. Khan reported in 1968 comparable data.

Vennik and Clauws UG (B) procured us, in 1978, with some other single crystals of $V_2O_5$. In that time we knew better our apparatus. On these samples we measured the $\chi_i$ values more precisely down to 2 K. The result revealed about 4% anisotropy. The three-dimensional body representing the susceptibility is ellipsoid.

The $\chi_i$ susceptibilities, measured on the Vennik-Clauws samples and averaged in relation to the $\chi_i$ anisotropy, have a small ferromagnetic component. The correction for the contaminant contribution resulted in a room temperature susceptibility which is 3% lower than our 1968 result which was measured on a different sample. The susceptibilities, corrected for ferromagnetism, plot versus reciprocal temperature shows a Brillouin function related pattern. At room temperature Brillouin centres contribute to the susceptibility for 12%. Concluding, the underlying temperature and field independent $\chi_i$ susceptibility is 15% lower than the room temperature value, deduced from Fig.58.1.

In the analysis of our data we neglect, for reason of clarity, the relatively small $\chi_i$ anisotropy. We approximate the susceptibility representation by a spheroid. It simplifies the analysis by reducing the number of mass susceptibilities to two. Their values multiplied by the molecular weight of $V_2O_5$ yields two mole susceptibility values.

Each of the two experimental susceptibilities can be considered as built up by two components, a diamagnetic and a paramagnetic one.

For analysing the data, we assume the paramagnetic contribution being the same for both experimental values, reducing the number of independent parameters to three. Three unknowns ask for a third equation to solve the problem. We put the average diamagnetic mole susceptibility equal to the Klemm expectation value. The set of equations solved, the paramagnetic susceptibility contribution $\chi_p$ is +11.05 expressed in ten to the minus four ampere square meter. The diamagnetic susceptibility component measured with the magnetic induction field normal to the cleavage plane is $\chi_{dn}$ = -9.2 (in the same units). It is by 36% more diamagnetic than -6.8, the Klemm value. The diamagnetic susceptibility component measured with the magnetic induction field direction in the cleavage plane is $\chi_{di}$ = -5.6 (in the same units). It is by 18% less diamagnetic than the Klemm value.

The diamagnetism of the $V_2O_5$ crystal shows similarity with the diamagnetism of the CN- molecular ion. In both cases the diamagnetism is anisotropic. In the diatomic CN- case we related the lower diamagnetic susceptibility with a region of smaller electron density the super fluid circuit crosses. We could do so because we had a rough idea of the spatial electron density distribution in the ion. In the more complex $V_2O_5$ we have no knowledge of the electron density distribution. We look for an indication considering the mechanical anisotropy of the crystal. The easiness of cleaving the material indicates the crystal is more resistant to a uniaxial tension with its direction in the cleavage plane than with its direction normal to that plane. In an oversimplified model we consider a one atomic layer parallel to the cleavage plane. On both surfaces of the layer there is a cleavage plane. At these planes the bond-strength keeping the atomic layers together is relatively weak. We attribute the weakness to a local lower electron density. In the atomic layer the bond is relatively stronger, indicating a relatively larger electron density inside the atomic layer.

An applied field, with its direction normal to the cleavage plane, generates persistent currents in circuits inside the atomic layer. The larger electron density allows a larger persistent current to flow. An applied field, with its direction parallel to the cleavage plane, generates persistent currents in circuits being perpendicular to the field direction. The circuits cross regions of lower electron density on the outsides of the atomic layer near the cleavage planes. The lower electron density region limits the persistent current intensity.

As in the CN- case, in the $V_2O_5$ crystal there is no need for a no-nonsense physical paramagnetic circuit for explaining the diamagnetic persistent currents. One should look expressing the diamagnetism by a pure diamagnetic term.

The analysis of the susceptibilities of the $V_2O_5$ crystal result, besides in a pure diamagnetic term, in a feeble temperature independent paramagnetic term. Formerly, the response of $V_2O_5$ to an applied magnetic induction field meets the requirements of Van Vleck susceptibility.

The Van Vleck model physically attributes the paramagnetism to exited electrons which populate rather empty more energetic orbitals. In literature you find models in which the applied field causes the exited electrons. Philosophically spoken you can justify the field is acting on a wave function. Quantitative energy considerations, however, indicate this process is negligibly small for fields we apply in our susceptibility measurements.

As in the Brillouin function, we compare the energy involved in the diamagnetic persistent moment to the energy involved in the thermal agitation. The energy involved in the diamagnetic moment, at our maximum measuring magnetic field, is equivalent to an average thermal agitation related with a temperature maximum 0.3 milli Kelvin. The result is orders in magnitude lower than our lowest measuring temperature.

The energy equivalence indicates that, at our measurements, the creation of unpaired electrons by the applied field is negligibly small compared to the creation by the measuring temperatures. We attributed the paramagnetism to unpaired electrons which, by thermal activation, populate rather empty more energetic orbitals.

Such concept rises the question what Van Vleck meant by “without resultant spin”? At zero magnetic induction field the presence of unpaired electrons does not show up as thermal agitation result in spatial homogenisation of the magnetic moment orientation of unpaired electrons. In my perception, the resultant spin-moment is zero but not the resultant spin. $V_2O_5$ is only without resultant spin at zero Kelvin, where lack of thermal agitation result in no excited electrons.

The “thermal activation” model resembles more the model explaining the Pauli-paramagnetism. However, our $V_2O_5$ crystal was an electric insulator. The susceptibility contribution therefore does not relate with conduction electrons but with unpaired electrons in molecular orbital. At higher temperatures, the thermal agitation excites more electrons. However it also reduces the average moment of each electron. In a first approximation, the effect of a higher number of unpaired electrons is compensated by the reduction of the average moment per electron, explaining the feeble temperature independent paramagnetism. An applied field does not create unpaired electrons but only reorients the moments of existing unpaired electrons. It is the polarisation of existing unpaired electrons that results in a macroscopic magnetic moment of the sample.

In literature, discussing the Van Vleck paramagnetism, you find models in which the applied field excites electrons into an orbital which energy difference with the ground state is much smaller than the average thermal agitation. Such model is considered as the other asymptotic Van Vleck case in which the induced paramagnetism is strongly temperature dependent. Increasing the temperature does not change much the excited electron concentration. Only temperature dependency shows up.

In my perception the two Van Vleck premises are practically incompatible. On the one hand you ask for a polyatomic system which has no resultant electron spin. On the other hand you consider a system in which the electrons are easily thermally excited. The excited electrons are unpaired, they have spin. Once more, the applied field does not create unpaired electrons but only reorients the moments of existing excited electrons.

**59 Bi-radicals?**

In a $K_2Pt(CN)_4Br_{0.3}.nH_2O$ single crystal, cooled in the way described before, we interpret the magnetic susceptibility, at a temperature where the Pauli-paramagnetism vanished, as being the proper susceptibility of the sample material. Before heating the single crystal under vacuum, the as grown $K_2Pt(CN)_4Br_{0.3}.nH_2O$ is diamagnetic. We interpret KCP is a material without a "resultant spin". The energy level of the lowest excited state is high compared to the ground state energy. The number of electrons excited by thermal agitation is negligibly small. The thermal agitation is low. In the crystal no diffusion occurs. The material is a solid with a rigid structure. We consider the susceptibility at 80 K as a reference for the state of the solid sample material.

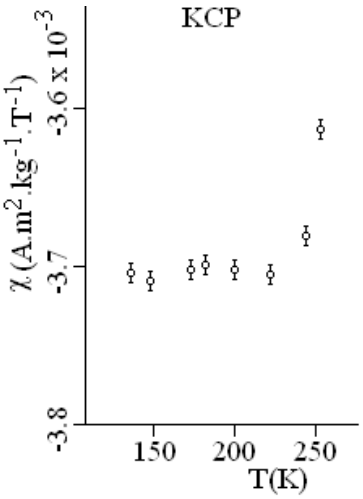


*Fig.59.1 reports on susceptibilities measured at about 80 K on a single $K_2Pt(CN)_4Br_{0.3}.nH_2O$ crystal. The temperatures indicated are those reached by the sample before the susceptibility had been measured. In between measurements, the sample heated slowly up from lower to higher temperature.*

After the crystal slowly warmed up to certain temperature, we checked the susceptibility at about 80 K. After the sample temperatures arose above 220 K, the 80 K susceptibility was changed, indicating that something happened to the solid state of the material. Fig.59.1 reports on the 80 K susceptibility change. An additional Curie-type paramagnetic susceptibility component appeared after the sample reached temperatures at which water escaped "violently" from the crystal.

In search for an explanation of the experimental observations we consider the CN- molecular ion. We start with the CN- molecular ion in the ground state as discussed before. It has a triple bond as outlined

in Fig.57.2. On warming up the sample, at 220 K water starts moving in a still rather rigid sample lattice. The displaced water puts the lattice under tension by Coulomb repulsion. The thermal agitation is to low for allowing the lattice to relax the tensions. Tension pushes on the triple bond. The question rises whether, driven by the tension, the reversed process from the hybridization of two atomic orbitals into one molecular orbital is going on? Two single electrons in two not sufficiently overlapping atomic orbitals?

## 60 Antiferromagnetism

We measured quasi static magnetic susceptibilities on a single crystal of $K_2CoF_4$. Legrand SCK/CEN B [60] studied the magnetic structure of $K_2NiF_4$ type compounds by means of neutron diffraction. In this context he procured us with the sample in 1965. Fig.60.1 reports on our magnetic susceptibilities.

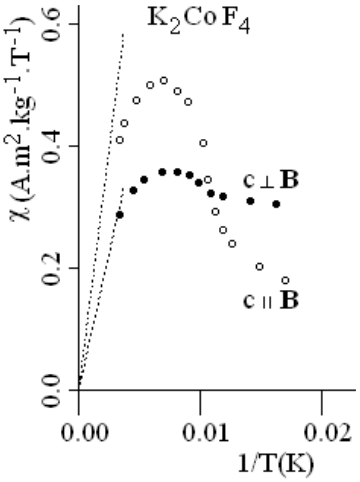


*Fig.60.1 reports on the magnetic susceptibilities measured in 1965 on a $K_2CoF_4$ single crystal. All measurements have been carried out at a magnetic induction field 1.7 T between room temperature and 60 K.*

The crystal is paramagnetic and strongly anisotropic. The susceptibility versus reciprocal temperature pattern shows characteristic features of antiferromagnets. We consider the maxima as the transition temperature, the Néel temperature. The Néel temperature separates two temperature regions. In the higher region the susceptibility increases with lowering temperature. It approaches a Curie-Weiss law related evolution. Below the Néel temperature the susceptibility does not increases anymore with lowering temperature.

Measured with the magnetic induction field parallel to the c-axis, the susceptibility decreases strongly with decreasing temperature.

Above the Néel transition temperature the cobalt two plus ion can be approached as a Brillouin centre. However, the situation is more complex than in the earlier discussed gadolinium three plus ion case. In the gadolinium the 4f-orbitals were half filled, resulting in a spin-only value for the magnetic moment of the Brillouin centre. In the $Co^{2+}$ ion seven electrons fill more than half the ten available states of the 3d-orbitals. The magnetic moment of the Brillouin centre is not only due to the spins but contains also an orbital contribution.

The orbital contribution does not show up in all cases. The orbital has a three dimensional structure which stiffness is mainly based on electron density distributions. In certain cases steric hindrance obstructs the reorientation of the magnetic moment by the applied magnetic induction field. In such case the orbital moments is said to be quenched. The well or not contributing to the susceptibility by the orbital strongly depends on the symmetry of the structure.

The dotted lines in Fig.60.1 indicate the theoretical Brillouin related susceptibilities calculated for a magnetically isolated centre with constant moment. The lower dotted line relates to the spin only value of the cobalt ion, the higher one indicates the maximum expectation value taking in account the possible orbital contribution.

Our apparatus was not adapted for measuring susceptibilities at temperatures above room temperature. The room temperature data indicate some susceptibilities are more paramagnetic than their spin only expectation value. Orbital moments need to be taken in account.

Due to the limitations of our apparatus we were not able to check whether above room temperature the susceptibility follows approximately the Curie-Weiss law as expected. The maxima at about 140 K indicate a rather large Weiss field reduces the applied magnetic induction field at the $Co^{2+}$ centre. In the antiferromagnetic case is the main Weiss field contribution not due to a long range dipole-dipole interacting. The field at the ion mainly is due to exchange coupling which can be considered basically as a short range interaction. However, the three dimensional chained mail coupling can extend over the whole crystal. The exchange interaction is anisotropic.

The strong susceptibility decrease with lowering temperature indicates, in the temperature region below the Néel temperature, the magnetic moments of the cobalt ions aligned anti-parallel along the c-axis. Neutron diffraction patterns indicate below 110 K the electron spins align in a three dimensional regular pattern. The ordering shows some similarity with the relative magnetization following a Weiss model, reported in Fig.30.1. The lower the temperature is, the higher the ordering is. However, in the antiferromagnetic preferential direction, the higher the ordering is the lower the resultant magnetic moment is. It is the main result of the negative coupling between adjacent moments.

In polycrystalline antiferromagnetic samples with no preferential orientation the averaged susceptibility also shows a maximum. It explains the slightly protruding susceptibility values measured in the stainless steel 304 data, at the left in Fig.41.1.

## 61 Nuclear moments

The Klemm compilation table reports for the mole susceptibility of the hydrogen positive ion ‘zero’. Klemm neglected the nuclear magnetic moment because compared to the magnetic moment of a single unpaired electron the nuclear moment is about three orders in magnitude smaller. The nuclear moment is difficult to measure with the aid of quasi static magnetic susceptibility techniques.

The NBS reference material aluminium brought me in 1973 in contact with the question of nuclear magnetism. For temperatures below 25 K the quasi static magnetic susceptibility of pure aluminium approximately obeys the Curie law. Down to 4 K the relative susceptibility increases about 1%. Although the Curie constant is somewhat too high as compared to the nuclear expectation value, we attribute the susceptibility contribution to nuclear magnetism.

As far I’m aware off, in a quasi static system the susceptibility contribution of nuclear magnetism was never of practical use. At variance, ‘Nuclear Magnetic Resonance’ techniques realised a wonderful explosion of possibilities. To start with, you need nuclei which have a magnetic moment, a property called spin. Following quantum mechanics the moments take discrete states in a static magnetic induction field. Up till now we recognise the situation as

similar to our electron related gadolinium ion case. In the ‘resonance’ technique however you do not measure the static total resultant magnetic moment. In stead, using electromagnetic radiation of the proper energy you excite the moment to a higher state. When the excited nuclei relax in a suitable time-period and you can catch the photon emitted at the relaxation you possesses the basic ingredients you need for the resonance techniques.

The subtle interplay between nuclear magnetic resonance techniques, today data processing systems and superconducting coils for the applied magnetic induction field allows specific custom-built systems. Well known are the ‘MRI’, the magnetic resonance imaging, computer designed brain pictures.

Pascal, about hundred years ago, was able using static magnetic susceptibility measurements to make structural analysis of simple organic molecules. Since then three-dimensional pictures of complex medical drugs appear on the computer-screen as the result of nuclear magnetic resonance techniques. The dynamic susceptibility techniques outgrow the quasi static magnetic susceptibility measuring domain I worked in for more than a quarter of a century.

## 62 References

[1] An apparatus for the precise measurement of magnetic susceptibilities of solids; A. Van den Bosch; Plenum press, Vacuum Microbalance Techniques 5 77 (1966)

[2a] Over statische magnetische susceptibiliteiten van supergeleidende schijfjes; A. Van den Bosch; VITO.95/MAT/040 (1995)

[2b] On the magnetic behaviour of superconducting lead discs; A. Van den Bosch and J. Vansummeren; Thermochimica Acta 152, 19 (1989)

[3] Classical electricity and magnetism, W.K.H.Panofsky and M.Phillips, 2nd edit. Addison-Wesley Publ. Co. 1964

[13] On sample positioning at low temperatures; A. Van den Bosch and J. Vansummeren; Thermochimica Acta, 29 225 (1979)

[14] On the precision of a susceptibility apparatus as deduced from measurements on superconducting vanadium; A. Van den Bosch and J. Vansummeren; Thermochimica Acta, 82, 51 (1984)

[21] On the precision of a magnetic susceptibility apparatus as deduced from the formulation of data measured on $La_{1-x}Gd_x(PO_3)_3$ glass, A Van den Bosch, Physicalia Mag. 27(2005)3 pp 245-264.

[22] A cryostat for the measurement of the static magnetic susceptibility in the temperature range 3 - 300 K; J. Vansummeren and A. Van den Bosch; Progress in Vacuum Microbalance Techniques, 2, 147 (1973), Edit.S.C.Bevan, S.J.Gregg and N.D.Parkyns, Publ. Heyden & Son.

[24] Modern Magnetism, L.F.Bates, 3th edit Cambridge at the university press 1951

[37] Experience with a data processing system for magnetic susceptibility measurements; A. Van den Bosch; Progress in Vacuum Microbalance Techniques 3, 361 (1975) Edit. C.Eyraud and M.Escoubes, Publ. Heyden.

[42] Static magnetic susceptibility measurements on NBS-SRM aluminium; A. Van den Bosch; Progress in Vacuum Microbalance Techniques 3, 398 (1975) Edit. C.Eyraud and M.Escoubes, Publ. Heyden.

[45] Magnetochemistry, P.W.Selwood, $2^{nd}$ edit. Interscience Publishers, Inc. 1956.

[46] Theorie des electrons, L. Rosenfeld, Hermann & Cie edit. Paris 1951.

[48] On the magnetic moment induced in thin superconducting discs; A. Van den Bosch; Supercond. Sci. Technol. 11, 9-12 (1998)

[49] Magnetism of radiation-damaged LiF; A. Van den Bosch; J. Phys. Chem. Solids 25 1293 (1964)

[50] Magnetism and the chemical bond, J.B.Goodenough, Interscience Publ. 1963

[51] Magnetische susceptibiliteitsmetingen aan gesinterd aluminium-koper-poeder; A. Van den Bosch; Bull. BNV V 1 35 (1966)

[52] Magnetic susceptibility measurements on K(2)Pt(CN)(4)Br(0.3).nH(2)O single crystals; A. Van den Bosch, J. Vansummeren and R. Deltour; Thermochimica Acta 24 251 (1978)

[53] Magnetic interaction and spin diffusion in solventfree DPPH; J. Burg, P. Grobet, A. Van den Bosch and J. Vansummeren; Sol. state comm. 43 785 (1982)

[54a] The theory of electric and magnetic susceptibilities, J.H.Van Vleck, 1st edit. 1932, Oxford University Press

[54b] Magnetochemie, W.Haberditzl, Pergamon Press 1968

[55] Diamagnetism and the chemical bond, Ya.G.Dorfman, Edward Arnold Publ.Ltd 1965

[57a] The electron-repulsion theory of the chemical bond, W.F.Luder, Reinhold Publishing Corporation, 1967

[57b] Electrons and the chemical bonding, H.B.Gray, W.A.Benjamin Inc. Publ. 1965

[60] Magnetic measurements on compounds with K(2)NiF(4)structure; E. Legrand and A. Van den Bosch; Solid state communications 7 1191 (1969)

Subject index